BioMed Research International

# Bone and Tooth Regeneration in Maxillofacial Region

Guest Editors: Kazuhisa Bessho, Joo L. Ong, Norbert R. Kübler, and John G. Clement

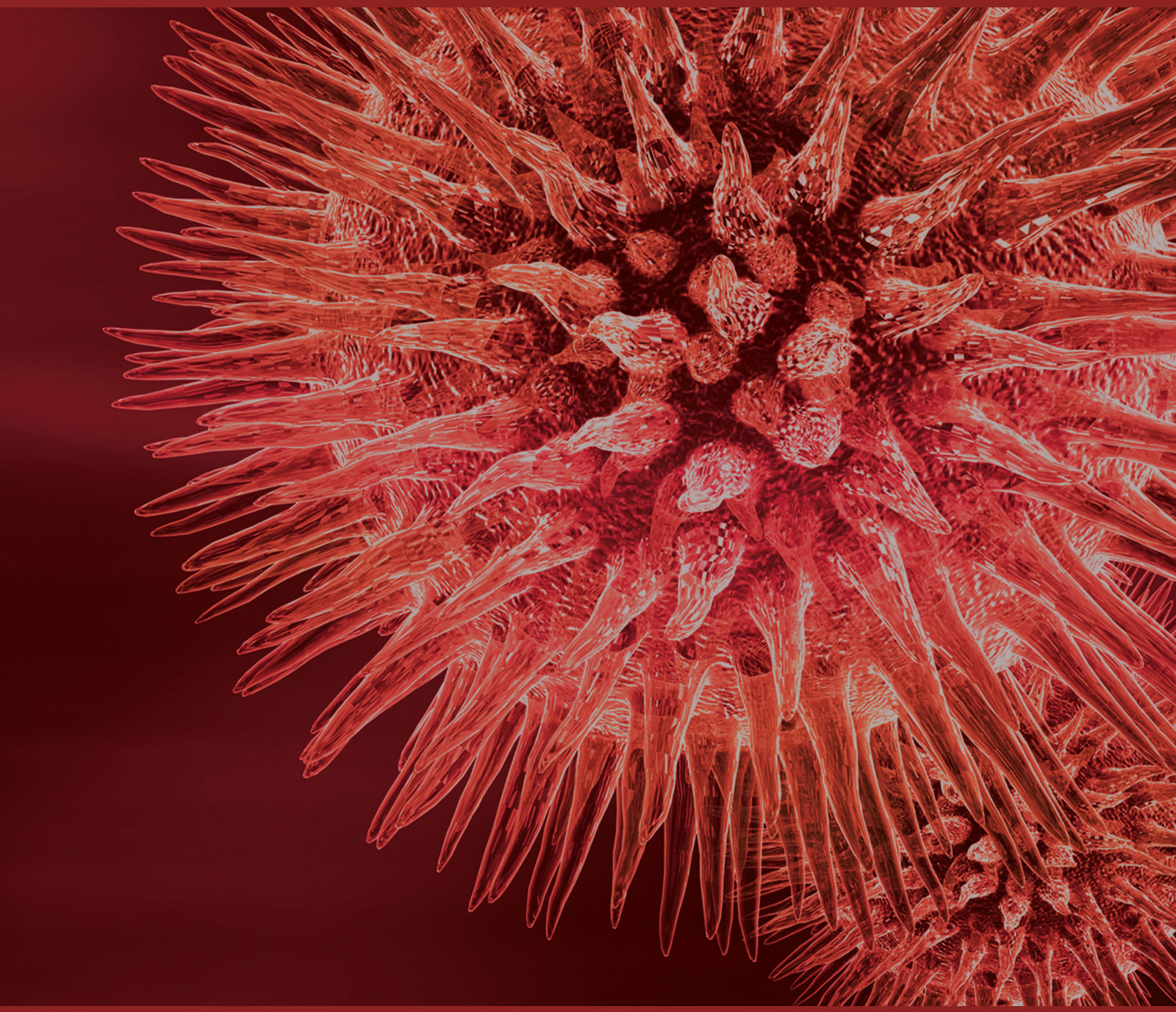

# Bone and Tooth Regeneration in Maxillofacial Region

BioMed Research International

# Bone and Tooth Regeneration in Maxillofacial Region

Guest Editors: Kazuhisa Bessho, Joo L. Ong, Norbert R. Kübler, and John G. Clement

# Contents

Hindawi Publishing Corporation
BioMed Research International
Volume 2015, Article ID 934525, 1 page
http://dx.doi.org/10.1155/2015/934525

*Editorial*

# Bone and Tooth Regeneration in Maxillofacial Region

**Kazuhisa Bessho,[1] Joo L. Ong,[2] Norbert R. Kübler,[3] and John G. Clement[4]**

[1]*Department of Oral and Maxillofacial Surgery, Graduate School of Medicine, Kyoto University, Kyoto 606-8507, Japan*
[2]*USAA Foundation, College of Engineering, The University of Texas at San Antonio, San Antonio, TX 78249, USA*
[3]*Department of Oral and Maxillofacial Surgery, Center of Operative Medicine II, Heinrich Heine University, 40225 Düsseldorf, Germany*
[4]*Forensic Odontology, Melbourne Dental School, The University of Melbourne, Carlton, VIC 3053, Australia*

Correspondence should be addressed to Kazuhisa Bessho; bes@kuhp.kyoto-u.ac.jp

Received 6 August 2015; Accepted 6 August 2015



Autogenous graft is the preferred material of choice due to its excellent clinical outcome and thus has been the gold standard for hard tissue reconstruction, especially for small defects. However, there are drawbacks to the use of autogenous graft materials and these drawbacks include the need for a second surgical site to harvest healthy donor tissues, the limited amount of donor tissues that can be harvested for large defects, and the increased possibility for tissue morbidity, infection, and pain at the second surgical site. Although it is more plentiful to obtain allografts, there is a risk of disease transmission from donor sites when using allogenic grafts for treatment in the clinics. With the advent in biomaterials research, various other sources of graft materials have shown promise for clinical use. As such, the ability of clinicians to evaluate, to understand, and to use other sources of graft materials is a key for successful reconstructions as well as tissue regenerations. This special issue represents a small cross section of some of the graft materials that are currently being investigated for clinical applications. Ranging from synthetic biomaterials to the use of stem cells, these papers also represent the diverse and multidisciplinary approaches that can be adapted for both maxillofacial and orthopedics reconstructions as well as tissue regenerations.

*Kazuhisa Bessho*
*Joo L. Ong*
*Norbert R. Kübler*
*John G. Clement*

Hindawi Publishing Corporation
BioMed Research International
Volume 2015, Article ID 659542, 10 pages
http://dx.doi.org/10.1155/2015/659542

*Research Article*

# Endothelial Progenitor Cell Fraction Contained in Bone Marrow-Derived Mesenchymal Stem Cell Populations Impairs Osteogenic Differentiation

**Fabian Duttenhoefer,[1,2] Rafael Lara de Freitas,[1,3] Markus Loibl,[1,4] Gido Bittermann,[2] R. Geoff Richards,[1] Mauro Alini,[1] and Sophie Verrier[1]**

[1]*AO Research Institute Davos, Davos Platz, Switzerland*
[2]*Department of Oral and Maxillofacial Surgery, Albert Ludwigs University, Freiburg, Germany*
[3]*Medical School of Ribeirão Preto, University of São Paulo, São Paulo, Brazil*
[4]*Department of Trauma Surgery, University Medical Center Regensburg, Germany*

Correspondence should be addressed to Sophie Verrier; sophie.verrier@aofoundation.org

Received 27 March 2015; Accepted 28 July 2015

Academic Editor: Joo L. Ong



In bone tissue engineering (TE) endothelial cell-osteoblast cocultures are known to induce synergies of cell differentiation and activity. Bone marrow mononucleated cells (BMCs) are a rich source of mesenchymal stem cells (MSCs) able to develop an osteogenic phenotype. Endothelial progenitor cells (EPCs) are also present within BMC. In this study we investigate the effect of EPCs present in the BMC population on MSCs osteogenic differentiation. Human BMCs were isolated and separated into two populations. The MSC population was selected through plastic adhesion capacity. EPCs ($CD34^+$ and $CD133^+$) were removed from the BMC population and the resulting population was named depleted MSCs. Both populations were cultured over 28 days in osteogenic medium ($Dex^+$) or medium containing platelet lysate (PL). MSC population grew faster than depleted MSCs in both media, and PL containing medium accelerated the proliferation for both populations. Cell differentiation was much higher in $Dex^+$ medium in both cases. Real-time RT-PCR revealed upregulation of osteogenic marker genes in depleted MSCs. Higher values of ALP activity and matrix mineralization analyses confirmed these results. Our study advocates that absence of EPCs in the MSC population enables higher osteogenic gene expression and matrix mineralization and therefore may lead to advanced bone neoformation necessary for TE constructs.

## 1. Introduction

Bone is a complex and highly vascularized tissue involving several cell types. Bone development, maintenance, and repair have been shown to be closely dependent on the presence of blood vessels that promote natural bone healing [1, 2]. However, in certain medical conditions, leading to large bone defects (e.g., tumor excision and high impact fractures), the natural repair capacity fails. In particular, in the field of oral and maxillofacial surgery, where comparatively small but anatomically complex bones are affected, reconstruction in terms of an esthetic and functional outcome is often difficult to achieve [3]. To treat defects such as osteoporosis and bisphosphonate-related osteonecrosis of the jaw (BRONJ), cancellous and cortical autologous bone grafts are the gold standard [4]. However, apart from limited bone availability and many times second surgery site complications such as donor side morbidity, possible fracturing of the donor bone may occur [5].

To overcome the various drawbacks of the autologous bone grafts, alternative treatments have been envisaged. Notably, tissue engineering approaches are aiming to reconstruct the missing tissue using cell-based strategies in association with a biomaterial. Bone marrow is a natural and easily available source of stem cells. Bone marrow aspirates are considered to be the most favorable source of mesenchymal stem cells (MSCs) to promote new bone formation [6]. In previous clinical studies, conducted by the authors, successful

long-term survival rates of dental implants in MSC-based regenerated bone were shown [7]. In a randomized split-mouth study, MSCs in combination with a bone substitute material showed high implant survival rates similar to those obtained with autologous bone grafts [8].

Large vertical or even critical sized bone defects remain a clinical challenge and the hypothesis that MSCs alone may respond to the local microenvironment of bony defects and thereby promote craniofacial defect regeneration is still at the centre of debate [9].

To date, no specific MSC markers have been identified [10, 11]. Typically, MSCs are enriched from the bone marrow mononucleated cells (BMC) *via* selection of the plastic adherent fibroblastoid cell fraction [12]. Under appropriate experimental conditions, MSCs show a high proliferation rate *in vitro* [6] and can differentiate into bone, cartilage, adipose tissue, and hematopoietic-supportive stromal cells [13]. Recruitment, proliferation, and differentiation of MSCs into mature osteoblasts are regulated by many factors including cytokines, systemic hormones, growth factors, and other regulators [14]. These factors are released to some extent by the osteoblastic cells themselves but also by cells that are part of the tightly connected vascular system, such as endothelial cells [15, 16] or pericytes [17, 18]. It is widely accepted that there is communication between endothelial cells and osteoblastic cells in order to coordinate the formation of blood vessel as well as the differentiation of bone forming cells to regulate bone turnover. Several studies report interactions between osteoblasts or MSCs and endothelial cells. They demonstrated the formation of microvessel-like structures and cell to cell communication through gap junctions [19, 20]. On the other hand, a notable variety of results have been gathered on the influence of endothelial cells on osteoblastic differentiation [21, 22]. This conflicting evidence might be due to the disparity of cell types, cell origin, and experimental set-ups. Most of these studies are using MSCs isolated from BMC fraction by their adherence ability to cell culture plastic. However, amongst the heterogeneous population of BMC, some hematopoietic stem cells also bear the ability to adhere to plastic [23]. In particular CD34 and CD133 positive cell fractions ($CD34^+$, $CD133^+$) have been identified and are known to give rise to endothelial cells *in vitro* [19, 24]. Postnatal regeneration and neoformation of vessels result from migration and differentiation of lineage committed progenitor cells [25, 26]. This process has been identified as the key mechanism to heal injury in most tissues [27] as, for example, in bone healing [17].

The aim of our study was to investigate the influence of $CD34^+$ and $CD133^+$ EPCs, contained in the full heterogeneous BMC population, on the osteogenic potential of MSCs. For this purpose, the osteogenic potential of the complete BMC population (called MSC postamplification) was compared with bone marrow samples that have been depleted from all $CD34^+$ and $CD133^+$ cells (called depleted MSCs). Osteogenic differentiation was induced using either a classical osteogenic medium (containing dexamethasone) or medium containing autologous growth factors (PL) that was shown to promote MSCs differentiation [19, 28].

## 2. Materials and Methods

*2.1. Cell Culture Media.* Iscove's Modified Dulbecco's Medium (IMDM), Fetal Calf Serum (FSC), Nonessential Amino Acids (NEAA), and antibiotics (PenStrep, PS) were purchased from Gibco/Invitrogen Life Technologies (Zug, Switzerland). Basic Fibroblast Growth Factor (bFGF) was purchased from R&D Biosystems (Minneapolis, MN, USA), and ascorbic acid, $\beta$-glycerophosphate, and dexamethasone were purchased from Sigma-Aldrich (Hamburg, Germany):

Basic medium: IMDM, 100 U/mL PenStrep (IMDM-PS), 10% FCS, 1% NEAA, and bFGF (5 ng/mL).

Osteogenic medium: IMDM-PS, 10% FCS, 0.1 mM ascorbic acid, 10 nM dexamethasone, and 10 mM $\beta$-glycerophosphate.

PL medium: IMDM-PS, 5% FCS, and 5% PL growth factors.

*2.2. Bone Marrow.* Human bone marrow (BM) samples (20 mL) were obtained from patients undergoing routine orthopaedic surgery upon informed consent and according to Inselspital Bern (Switzerland) ethical commission's guideline (KEK Bern 126/03).

Bone marrow aspirates were obtained from 5 donors (44 to 83 years old, with an average age of 62 years: 4 males and 1 female) in CPDA-containing Sarstedt S-Monovettes (Sarstedt, Nümbrecht, Germany) and processed within 24 hours after harvesting [29].

*2.3. Cell Populations*

*Bone Marrow Mononucleated Cells (BMCs).* BMCs were isolated from bone marrow aspirates as previously reported [30]. After homogenization, BM aspirates were diluted 1 : 4 with IMDM containing 5% (v/v) FCS and mononucleated cells were separated on a Histopaque-1077 (Sigma-Aldrich) density gradient. Samples were centrifuged at 800 g for 20 minutes. The low-density mononucleated cell interphase was collected and washed twice in 5 mL of IMDM containing 10% FCS, followed by centrifugation at 400 g for 15 minutes. Subsequently, BMCs were further processed for cell selection.

*Mesenchymal Stem Cells (MSCs).* MSCs were further isolated from total BMC through their plastic adhesion capacity. $16 \times 10^6$ cells were seeded in 300 $cm^2$ cell culture flask in presence of basic medium and let to adhere for 4 days as described before [29]. After 4 days, nonadherent cells were removed and fresh medium was added. After the first cell amplification step (first passage), cells were called MSCs.

*Endothelial Progenitor Cells (EPCs).* EPCs were selected from the BMCs population by MiniMAC Magnetic Microbead System (Miltenyi Biotec) using CD34 and CD133 specific antibodies according to manufacturer's instructions. Selected CD34 and CD133 positive cells ($CD34^+$ and $CD133^+$) were frozen for further experiments.

*EPC-Depleted BMCs (Depleted MSCs) [31].* After removal of $CD34^+$ cells and $CD133^+$ cells from the BMCs samples (see "Endothelial Progenitor Cells (EPCs)" section), the resulting cell population was named depleted MSCs.

*2.4. Platelet Lysate Preparation.* Platelet Lysate growth factors (PL) and Platelet Rich Plasma (PRP) were prepared from platelet concentrates, as described earlier [19, 32]. Platelet bags were obtained from the blood bank of Kantonsspital Graubünden in Chur in accordance with the current ethical laws of Switzerland. The platelet bags contain a standardized platelet density (5 times higher than normal), obtained through blood apheresis. We further increased the platelet density by a centrifugation at 2000 g for 7 minutes, followed by resuspension of the pellet in half of the original platelet-bag volume. Phosphate buffered saline (PBS) was used for the PL preparations, while original plasma was used for the PRP preparations to obtain a final concentration 10 times higher than normal blood (2.5 million (±10%) platelets/$\mu$L). As expected, the concentrations we obtained were about 10 times higher than the range measured in blood plasma (data not shown). In order to avoid two levels of interindividual variations (bone marrow donors *versus* platelet donors), PL and PRP samples were pooled from three different platelet concentrates and randomly matched [33, 34].

*2.5. Cell Expansion.* Cells (MSCs and depleted MSCs) were seeded at the density of $0.9 \times 10^6$ mononucleated cells per 300 $cm^2$ T-flask (Techno Plastic Products AG, Trasadingen, Switzerland) in basic media [35]. Medium was changed every 3 days, and cells were subcultured 1 : 4. Cells in passages 2–4 were subsequently used. MSCs and depleted MSCs were further cultured in the exact same conditions.

*2.6. Cell Differentiation.* MSCs or depleted MSCs were seeded at the density of $10'000$ cells/$cm^2$ in 24-well plates in triplicate for each donor and each analysis. Cells were cultured for 28 days in osteogenic medium and PL medium as described above [36].

*2.7. Cell Growth (DNA Quantification Assay).* Cell growth was determined as described by Labarca and Paigen [37] after 1, 7, 14, 21, and 28 days of culture in either osteogenic medium or PL medium. Briefly, DNA was quantified by measuring the binding of Hoechst 33258 (Polysciences Inc., 09460) to the DNA helix after cells overnight digestion at 56°C in a proteinase K solution (0.5 mg/mL in 3.36 mg/mL disodium-EDTA-PBS). After appropriate dilution of the samples in Dulbecco's phosphate buffered saline (DPBS) containing 0.1% (v/v) H33258, the bound fluorescence was measured using a PE HTS 7000 Bio Assay Reader at 360 nm excitation and 465 nm emission wavelength.

*2.8. Gene Expression Analysis*

*RNA Isolation and Reverse Transcription.* Total RNA was extracted from cells monolayers at different time points (days 1, 7, 14, 21, and 28) using TRI-Reagent (MRC Inc., TR-118) according to the manufacturer's instructions (Molecular Research Center, Cincinnati, Ohio). cDNA was synthetized from 1 $\mu$g of total RNA using TaqMan reverse transcription reagents (Applied Biosystems, Foster City, CA) with random hexamer primers.

*Real-Time Polymerase Chain Reaction (PCR).* Real-Time Polymerase Chain Reaction (PCR) was performed on a 7500 Real-Time PCR System (Applied Biosystems). Genes of interest were detected using specific oligonucleotide primers and TaqMan probes (Microsynth, Balgach, Switzerland) or Assays-on-Demand (Applied Biosystems) as specified in Table 1. Eukaryotic 18S (Applied Biosystems) was used as a housekeeping gene. PCR conditions were 95°C for 10 min, followed by 42 cycles of amplification at 95°C for 15 sec and 60°C for 1 min using the GeneAmp 5700 Sequence Detection System (Applied Biosystems). Gene expression was analysed according to the $^{\Delta\Delta}$CT method, with expression normalized to the corresponding reference (specified on each graph) at the same time point.

*2.9. ALP Activity Assay.* Samples for ALP activity measurement were harvested on days 1, 7, 14, 21, and 28. After medium removal and a washing step with PBS, 1 mL of 0.1% Triton-X in 10 mM Tris-HCl (pH 7.4) was added to the cell monolayers and incubated for 4 h at 4°C on a gyratory shaker [38]. ALP activity was assessed by measuring the p-nitrophenol production during 15 min incubation at 37°C with p-nitrophenyl phosphate as substrate (Sigma Kit number 104) on a Perkin Elmer Bio Assay Reader HTS 7000.

*2.10. $^{45}Ca^{2+}$ Incorporation Assay.* Matrix mineralization was estimated by the incorporation of $^{45}Ca^{2+}$ into the extracellular matrix. 1.25 $\mu$Ci/mL isotope (Amersham CES3, Amersham, UK) was diluted in pure IMDM, added to each well, and incubated at 37°C o/n [38]. After medium removal and 3 washes in PBS, 0.5 mL of 70% formic acid was added to each well and incubated at 65°C for 1 h. The formic acid solution was transferred to a scintillation tube containing 3.5 mL of scintillation liquid (OptiPhase HiSafe'3, Perkin Elmer, Waltham, MA, USA) and the radioactivity was measured after 28 days of culture using a Wallac 1414 WinSpectral Liquid Scintillation Counter (Perkin Elmer).

*2.11. Statistical Analyses.* Statistical analyses were performed using the software package SPSS. Data were tested for normal distribution using Shapiro-Wilk test. Consequently, data were analyzed using a general linear model with repeated measures. $p$ values were corrected by Bonferroni's method. All experiments were done using 5 different donors and in triplicate for each donor. Significant values were defined as $^{*}p < 0.05$ and $^{**}p < 0.01$.

## 3. Results

*3.1. Cell Growth.* Cell growth was assessed by DNA quantification. MSC and depleted MSC populations were seeded into tissue culture plastic wells and cultured in presence of PL- or dexamethasone-containing medium. As shown in Figure 1

Table 1: Genes of interest were detected by Polymerase Chain Reaction (PCR) using specific oligonucleotide primers, TaqMan probes, or Assays-on-Demand. Eukaryotic 18S was used as a housekeeping gene.

| Microsynth (target gene sequence (5′ → 3′)) | Applied Biosystems |
|---|---|
| Bone marker genes | |
| Collagen I$\alpha$1 | |
| Forw CCC TGG AAA GAA TGG AGA TGA T | |
| Rev ACT GAA ACC TCT GTG TCC CTT CA | |
| Probe CGG GCA ATC CTC GAG CAC CCT | |
| Osteonectin | |
| Forw ATC TTC CCT GTA CAC TGG CAG TTC | Bone marker genes |
| Rev CTC GGT GTG GGA GAG GTA CC | ALP: Hs00758162_m1 |
| Probe CAG CTG GAC CAG CAC CCC ATT GAC | |
| BMP-2 | Endothelial marker genes |
| Forw AAC ACT GTG CGC AGC TTC C | PECAM-I: HS01065282_m1 |
| Rev CTC CGG GTT GTT TTC CCA C | vWF: Hs00169795_m1 |
| Probe CCA TGA AGA ATC TTT GGA AGA ACT ACC AGA AAC TG | TEK: Hs00176096_m1 |
| Osteopontin | Flt1: Hs00176573_m1 |
| Forw CTC AGG CCA GTT GCA GCC | KDR: Hs00176676_m1 |
| Rev CAA AAG CAA ATC ACT GCA ATT CTC | HOX9: Hs00365956_m1 |
| Probe AAA CGC CGA CCA AGG AAA ACT CAC TAC C | |
| Runx2 | Housekeeping gene |
| Forw AGC AAG GTT CAA CGA TCT GAG AT | 18s: 4319413E |
| Rev TTT GTG AAG ACG GTT ATG GTC AA | |
| Probe TGA AAC TCT TGC CTC GTC CAC TCC G | |
| BSP II | |
| Forw TGC CTT GAG CCT GCT TCC | |
| Rev GCA AAA TTA AAG CAG TCT TCA TTT TG | |
| Probe CTC CAG GAC TGC CAG AGG AAG CAA TCA | |

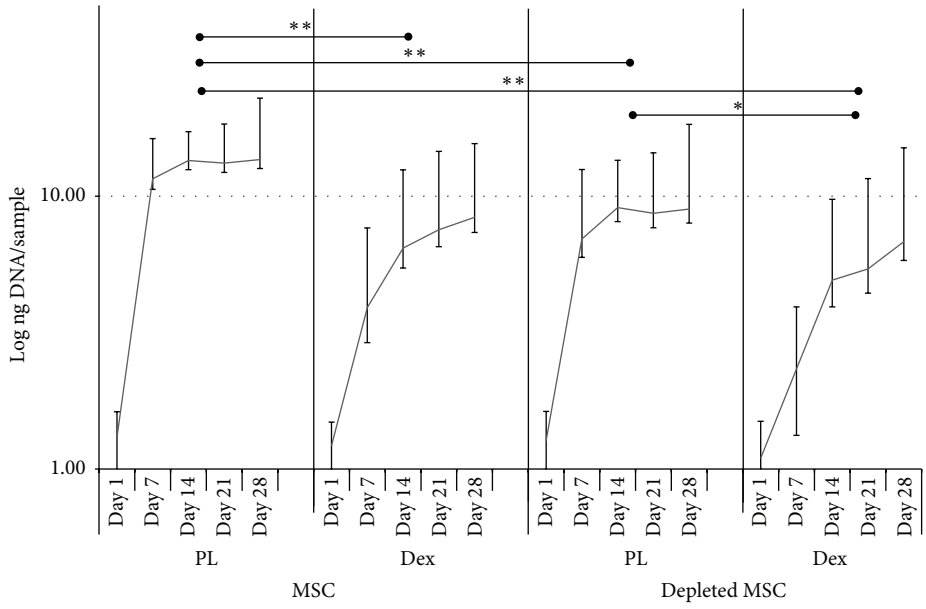


Figure 1: Cell proliferation. MSCs or depleted MSCs were cultured in presence of medium containing Dex or PL. DNA quantification was performed at different time points over a period of 28 days.

(note the logarithmic scale of the $y$-axis), both cell populations showed a typical cell growth profile, starting with an exponential growth phase, reaching a plateau of proliferation. In both cell populations, this plateau was reached around day 14 when cells were cultured in medium containing dexamethasone. In the presence of PL, cells grew significantly faster for both cell populations ($p < 0.01$ for MSC and $p < 0.05$ for depleted MSC) than in dexamethasone-containing medium. In PL medium, the MSCs population showed a significantly higher cell proliferation rate when compared to the depleted MSCs in the same conditions ($p < 0.01$) (Figure 1).

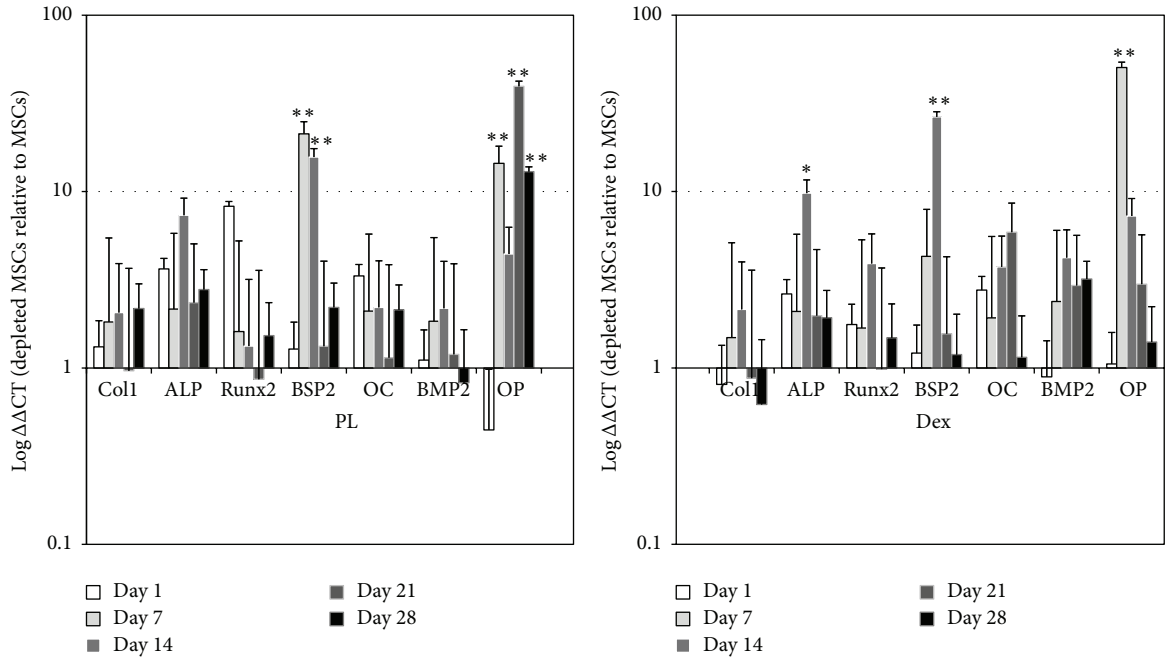


Figure 2: Osteogenic gene expression analysis. Osteoblastic marker genes were analyzed by real-time RT-PCR on the two cell populations. Results are expressed in expression of fold changes in depleted MSC relative to MSC.

*3.2. Osteogenic Gene Expression.* In addition to cell proliferation, the osteogenic differentiation of depleted MSCs and MSCs was looked at. Cells were cultured in either PL-containing medium or dexamethasone-containing medium during the course of 28 days. RNA samples were extracted at different time points of culture, and real-time RT-PCR was performed for osteogenic marker genes. Results are presented as relative gene expression in depleted MSCs relative to MSCs ($^{\Delta\Delta}$CT). When depleted MSCs were cultured in PL medium, all studied osteoblastic genes were upregulated in comparison to the MSC population cultured in the same condition. This finding was consistently observed at each time point (Figure 2). In addition, the same trend of upregulation was observed for all genes when cells were cultured in classical osteogenic medium (Dex$^+$). Most of the genes were significantly highly expressed in depleted MSCs compared to MSCs in both media (PL and Dex). Of particular interest was the significant upregulation of Bone Sialoprotein 2 (BSP2) and Osteopontin (OP) in both media ($p < 0.01$) and ALP in presence of dexamethasone ($p < 0.05$). Gene expression is reported as log fold regulation in the depleted MSC population relative to the MSC population at the same time point in Figure 2.

*3.3. ALP Activity.* Looking at the ALP activity (Figure 3), both cell populations (MSCs and depleted MSCs) showed a low peak of alkaline phosphatase activity by day 7 in presence of PL medium, with a significantly higher peak for depleted MSC compared to MSC. On the contrary, a high peak of alkaline phosphatase activity was obtained in Dex$^+$ medium for both cell populations. This activity level was significantly higher in depleted MSCs when compared to MSCs ($p < 0.01$ for the overall time points).

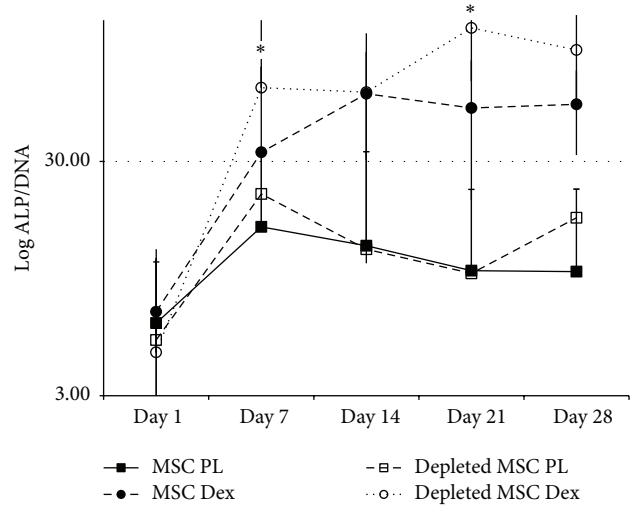


Figure 3: ALP activity of cells cultured in presence of Dex$^+$ showed a highly significant level compared to PL medium ($p < 0.01$) in parallel; ALP level of activity was more elevated in depleted MSCs compared to MSCs ($p < 0.05$). ALP activity values were corrected to cell numbers (ALP/DNA).

*3.4. $^{45}Ca^{2+}$ Incorporation.* Matrix mineralization was followed by $^{45}Ca^{2+}$ incorporation (Figure 4). Depleted MSCs and MSCs populations were cultured during 28 days in presence of either PL-containing medium or classical osteogenic medium (Dex) (Figure 4). Interestingly, depleted MSCs cultured in PL medium showed a high incorporation of $^{45}Ca^{2+}$ in comparison to MSCs after 28 days of cell culture. The presence of dexamethasone in osteogenic medium resulted in a further increase of calcium incorporation in both depleted MSCs and MSCs (both $p < 0.01$). Matrix mineralization

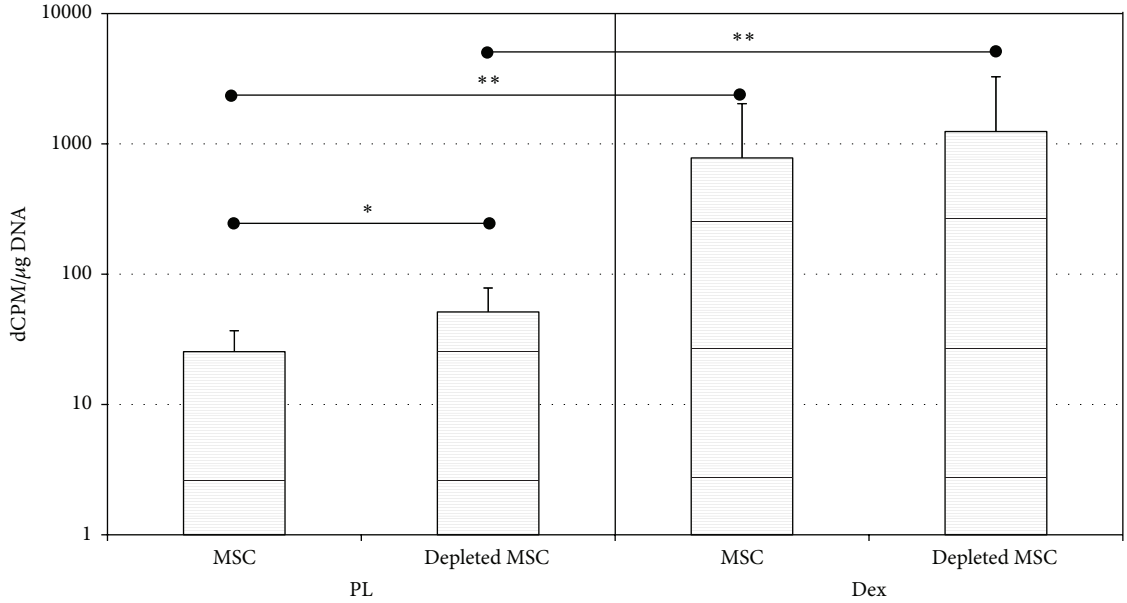


FIGURE 4: $^{45}Ca^{2+}$ was measured after 28 days of culture in PL or $Dex^{+}$ medium. Results are presented in dCPM related to cell number. Matrix mineralization was found higher in presence of $Dex^{+}$ ($p < 0.01$) compared to PL, while depleted MSCs showed better ability to mineralize their matrix compared to MSCs ($p < 0.05$ in PL).

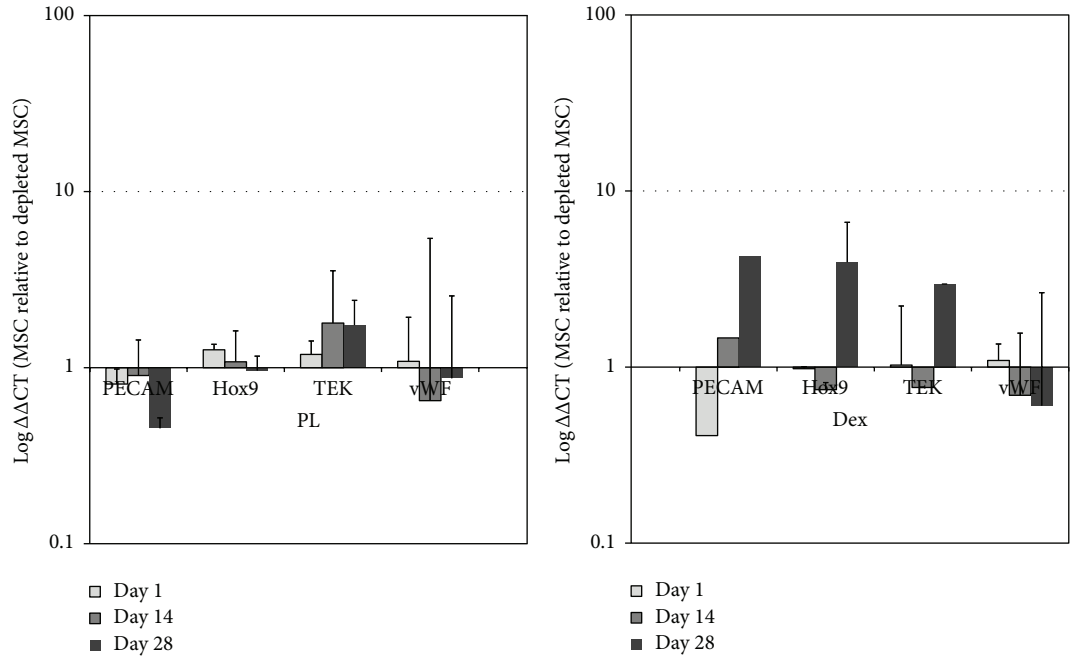


FIGURE 5: Endothelial marker genes analysis in depleted MSCs and MSCs after 28 days of culture was performed by real-time RT-PCR. No significant differences in gene expression pattern could be observed between MSC and depleted MSC populations. The results are expressed in log fold changes in MSCs relative to depleted MSCs ($^{\Delta\Delta}CT$).

obtained by the use of depleted MSCs was higher than that for MSCs in PL medium ($p < 0.05$) and appears to be higher in osteogenic medium (missing statistical significance).

*3.5. EPC Population Contained in Full MSC.* To follow the prevalence of the EPC fractions contained in the MSC population, we performed gene expression analysis for endothelial specific marker genes over a period of 28 days (Figure 5). The genes expression in MSCs is reported as fold changes of the gene expression relative to the same genes in depleted MSCs. Values are shown in logarithmic scale. As seen in Figure 5, no significant changes in gene expression pattern were obtained for MSC compared to the depleted MSC population, showing that the EPCs present in the MSCs population did not differentiate towards a mature endothelial cell phenotype. The same trend of results was obtained in both culture media (PL and Dex).

## 4. Discussion

In the present study, we investigated the influence of the naturally coresident endothelial progenitor cells in bone marrow on the proliferation and osteogenic differentiation of MSCs. MSCs (selected through their plastic adhesion ability) were compared to EPC-depleted BMC population (depleted MSCs). These two cell populations were cultured in presence of classical osteogenic medium (containing $\beta$-glycerophosphate, ascorbic acid, and dexamethasone) or in presence of medium (containing $\beta$-glycerophosphate, ascorbic acid, and PL). During 28 days of cell culture in either of these media, we followed cell proliferation, cell osteogenic differentiation, alkaline phosphatase activity, and matrix mineralization. We found that the osteogenic potential of the EPC-depleted cell population was higher than that for MSC. On the opposite side, the MSC population grew significantly faster than the depleted MSCs population in the presence of PL medium when compared to the $Dex^+$ medium.

MSCs were first described by Friedenstein et al. [28] and are characterized by the ability to differentiate *in vitro* into the three mesenchymal lineages, that is, cartilage, fat, and, in our case, bone [13]. The classical osteogenic differentiation of human MSCs [35] requires incubation of cell monolayers with ascorbic acid, $\beta$-glycerophosphate, and dexamethasone (added to medium containing FCS), resulting in increased alkaline phosphatase activity followed by calcium deposition.

Intense investigations on MSC selection have been performed. The most common method consists in the MSCs selection through their ability to adhere to cell culture plastic, followed by serial passaging to reduce the presence of remaining hematopoietic cells. The use of monoclonal antibodies in order to preselect MSCs with the use of surface marker such as CD90 and CD105 (i.e., positive selection) [39, 40] is also deeply investigated. On the contrary, a negative selection approach can also be used. In this case, other cell types, such as hematopoietic cells, usually removed [41] through different adhesion properties can be sorted from the BMC pool using CD34 and CD133 specific antibodies.

Hematopoietic stem cells gained increasing attention for their potential use in regenerative medicine and tissue engineering, essentially the $CD34^+$ and $CD133^+$ endothelial progenitor cells [42, 43]. Stem cell niches have been described so far for a number of tissue types such as the hair follicle, intestine, and the bone marrow [44, 45]. The two distinct niches of hematopoietic stem cells (HSCs) in bone marrow are the endosteal niche with HSC in close contact with osteoblasts and the perivascular niche where HSCs are found close to the sinusoids. This conformation might serve as a good example for the complexity of the niche functional concept [45]. In the endosteal niche signaling events between osteoblasts and HSCs play a crucial role in maintenance and activation of stem cells [46]. There is increasing evidence to indicate that MSC populations are heterogeneous with coexisting subsets having varying potency. This applies to bone marrow MSCs as well as those from other tissues [47].

Taking niche signaling processes into account, a variety of studies were conducted during the past decade looking at the influence of endothelial cell coculture with osteoblastic cells and/or MSC. And even if the effects described concerning the osteogenic differentiation of MSC are relatively divergent [20, 48], the positive effect of this coculture on MSCs and osteoblastic cells proliferation is quite consistent [22, 49]. However, in all these studies, endothelial cells (EC) (mainly HUVEC) were added to the MSC population. In our case, no endothelial cells were added to the cultures. Instead, endothelial progenitor cells were left in their natural niche microenvironment containing MSCs and compared with BMCs that were depleted from their natural EPC content (depleted MSCs).

In previous investigations, PL showed positive effects on endothelial progenitor cell proliferation [32] and on gene expression of pericyte markers in MSCs and depleted MSCs [31]. In contrast, in the present work, no significant differences were depicted between MSCs and depleted MSCs endothelial specific gene expression when cultured in either PL or osteogenic medium. Nevertheless, the overall osteogenic gene expression as well as matrix mineralization potential of the depleted MSC population was higher than for MSCs. In the present investigation, EPCs remained in their niche environment along with MSCs and therefore provided them with a specific microenvironment protecting the stemness characteristics of MSCs [50]. In the depleted MSCs population, on the other hand, the remaining MSCs may have lost such protective paracrine and direct cell contact mechanisms and could therefore be more susceptible to osteogenic differentiation. Similar mechanisms were described previously, where the cross talk of bone marrow-derived EPCs (BM-EPC) and MSCs through paracrine and direct cell contact mechanisms could modulate the angiogenic response [51].

In synopsis with the present data, it is tempting to speculate that the degree of differentiation and therefore the maturity of EPCs could play an important role in their influence on MSCs osteogenic differentiation. This is supported by the study of Loibl et al. 2014 that indicates EPC differentiation into mature EC by direct cell-cell contact with MSCs [31]. Furthermore, there is evidence that the presence of PL induced cell growth of EPC in EPC-MSC coculture supports a pericyte-like differentiation of MSCs in both MSC and EPC-depleted MSC populations [29, 31]. Moreover, it was shown that the addition of MSC promotes stable neovascularization in EPC-derived tube formation *in vivo* [52]. Still, the ideal ratio of EPC for early neovascularization is controversially debated in the literature. Previous *in vitro* experiments from our group found the ratio of 50/50 of MSC and EPC ideal [29]. These results were corroborated *in vivo*, where the highest number of vessels in the center of scaffolds, implanted subcutaneously in nude mice, was found in 50% MSC + 50% EPC proportion [53]. On the contrary, Fu et al., 2015, concluded that the ratio of 75% EPC + 25% MSC in modified calcium polyphosphate constructs showed the highest expression of osteogenic and angiogenic markers, whereas the degree of EPC maturation still remains unclear [54].

A limitation of this work certainly could be the average age of the bone marrow donors (62 years). Siegel et al. [55] showed the influence of gender and/or age (and age-related

medication intake) on several MSCs characteristics such as time of doubling population, while no correlation was found between donor's age or gender and the expression level of some stemness related genes (e.g., Oct4 or Nanog). In another study, using MSCs from late adult patients' bone marrow (52 to 92 years old), Leskelä et al. [56] suggested that the osteogenic differentiation potential does not decrease with age. Likewise, Dexheimer et al. reported the influence of the cell proliferation status rather than the age or gender of the patient on the multilineage differentiation potential of MSCs [57]. In a study published by Herrmann et al. [58], no correlation was observed between age or gender and the percentage of CD133/CD34 double positive EPCs present in bone marrow samples from patients with an average age of 63 years. In this present work, we compared the differentiation potential of MSCs with their corresponding depleted MSCs (same donor) and could demonstrate the effect of EPCs on the MSCs growth and differentiation.

In detail, our results indicate that absence of EPCs in MSC population enables higher osteogenic gene expression and matrix mineralization and therefore may lead to earlier new bone formation. Nevertheless, the application of cells in bone tissue engineered constructs demands the support of a functional blood supply. Therefore our results may lead to novel approaches in cell seeding to develop vascularized bone tissue engineered scaffolds, such as selective, prioritized, or time dependent seeding of different cell types. Still, further investigations on the mechanisms by which $CD34^+/CD133^+$ EPC influence MSC osteogenic differentiation as well as the influence of EPC maturation in this process are necessary.

## Conflict of Interests

The authors declare that there is no conflict of interests regarding the publication of this paper.

## Authors' Contribution

Fabian Duttenhoefer and Rafael Lara de Freitas contributed equally to this work.

## Acknowledgment

The authors thank AOER/AO Foundation for funding.

## References

[1] S. Fuchs, A. Hofmann, and C. J. Kirkpatrick, "Microvessel-like structures from outgrowth endothelial cells from human peripheral blood in 2-dimensional and 3-dimensional co-cultures with osteoblastic lineage cells," *Tissue Engineering*, vol. 13, no. 10, pp. 2577–2588, 2007.

[2] J. M. Kanczler and R. O. C. Oreffo, "Osteogenesis and angiogenesis: the potential for engineering bone," *European Cells and Materials*, vol. 15, pp. 100–114, 2008.

[3] J. P. Schmitz and J. O. Hollinger, "The critical size defect as an experimental model for craniomandibulofacial nonunions," *Clinical Orthopaedics and Related Research*, vol. 205, pp. 299–308, 1986.

[4] D. C. Tong, K. Rioux, M. Drangsholt, and O. R. Beirne, "A review of survival rates for implants placed in grafted maxillary sinuses using meta-analysis," *International Journal of Oral and Maxillofacial Implants*, vol. 13, no. 2, pp. 175–182, 1998.

[5] J. C. Beirne, H. J. Barry, F. A. Brady, and V. B. Morris, "Donor site morbidity of the anterior iliac crest following cancellous bone harvest," *International Journal of Oral and Maxillofacial Surgery*, vol. 25, no. 4, pp. 268–271, 1996.

[6] P. Niemeyer, K. Fechner, S. Milz et al., "Comparison of mesenchymal stem cells from bone marrow and adipose tissue for bone regeneration in a critical size defect of the sheep tibia and the influence of platelet-rich plasma," *Biomaterials*, vol. 31, no. 13, pp. 3572–3579, 2010.

[7] F. Duttenhoefer, S. F. Hieber, A. Stricker, R. Schmelzeisen, R. Gutwald, and S. Sauerbier, "Follow-up of implant survival comparing ficoll and bone marrow aspirate concentrate methods for hard tissue regeneration with mesenchymal stem cells in humans," *BioResearch Open Access*, vol. 3, no. 2, pp. 75–76, 2014.

[8] D. Rickert, A. Vissink, W. J. Slot, S. Sauerbier, H. J. A. Meijer, and G. M. Raghoebar, "Maxillary sinus floor elevation surgery with BioOss mixed with a bone marrow concentrate or autogenous bone: test of principle on implant survival and clinical performance," *International Journal of Oral and Maxillofacial Surgery*, vol. 43, no. 2, pp. 243–247, 2014.

[9] Y. Yang, B. Hallgrimsson, and E. E. Putnins, "Craniofacial defect regeneration using engineered bone marrow mesenchymal stromal cells," *Journal of Biomedical Materials Research*, vol. 99, no. 1, pp. 74–85, 2011.

[10] A. I. Caplan and D. Correa, "The MSC: an injury drugstore," *Cell Stem Cell*, vol. 9, no. 1, pp. 11–15, 2011.

[11] P. Bianco, P. G. Robey, and P. J. Simmons, "Mesenchymal stem cells: revisiting history, concepts, and assays," *Cell Stem Cell*, vol. 2, no. 4, pp. 313–319, 2008.

[12] M. F. Pittenger, "Mesenchymal stem cells from adult bone marrow," *Methods in Molecular Biology*, vol. 449, pp. 27–44, 2008.

[13] M. F. Pittenger, A. M. Mackay, S. C. Beck et al., "Multilineage potential of adult human mesenchymal stem cells," *Science*, vol. 284, no. 5411, pp. 143–147, 1999.

[14] J. B. Lian and G. S. Stein, "Development of the osteoblast phenotype: molecular mechanisms mediating osteoblast growth and differentiation," *The Iowa Orthopaedic Journal*, vol. 15, pp. 118–140, 1995.

[15] O. M. Tepper, J. M. Capla, R. D. Galiano et al., "Adult vasculogenesis occurs through in situ recruitment, proliferation, and tubulization of circulating bone marrow-derived cells," *Blood*, vol. 105, no. 3, pp. 1068–1077, 2005.

[16] J. Street, M. Bao, L. DeGuzman et al., "Vascular endothelial growth factor stimulates bone repair by promoting angiogenesis and bone turnover," *Proceedings of the National Academy of Sciences of the United States of America*, vol. 99, no. 15, pp. 9656–9661, 2002.

[17] T. Matsumoto, A. Kawamoto, R. Kuroda et al., "Therapeutic potential of vasculogenesis and osteogenesis promoted by peripheral blood CD34-positive cells for functional bone healing," *The American Journal of Pathology*, vol. 169, no. 4, pp. 1440–1457, 2006.

[18] A. R. Jones, C. C. Clark, and C. T. Brighton, "Microvessel endothelial cells and pericytes increase proliferation and repress osteoblast phenotypic markers in rat calvarial bone cell cultures," *Journal of Orthopaedic Research*, vol. 13, no. 4, pp. 553–561, 1995.

[19] S. Verrier, T. R. Meury, L. Kupcsik, P. Heini, T. Stoll, and M. Alini, "Platelet-released supernatant induces osteoblastic differentiation of human mesenchymal stem cells: potential role of BMP-2," *European Cells and Materials*, vol. 20, pp. 403–414, 2010.

[20] F. Villars, B. Guillotin, T. Amédée et al., "Effect of HUVEC on human osteoprogenitor cell differentiation needs heterotypic gap junction communication," *The American Journal of Physiology—Cell Physiology*, vol. 282, no. 4, pp. C775–C785, 2002.

[21] G. Bianchi, A. Banfi, M. Mastrogiacomo et al., "Ex vivo enrichment of mesenchymal cell progenitors by fibroblast growth factor 2," *Experimental Cell Research*, vol. 287, no. 1, pp. 98–105, 2003.

[22] Y. Xue, Z. Xing, S. Hellem, K. Arvidson, and K. Mustafa, "Endothelial cells influence the osteogenic potential of bone marrow stromal cells," *BioMedical Engineering OnLine*, vol. 8, no. 1, article 34, 2009.

[23] M. Y. Gordon, N. Levičar, M. Pai et al., "Characterization and clinical application of human $CD34^+$ stem/progenitor cell populations mobilized into the blood by granulocyte colony-stimulating factor," *Stem Cells*, vol. 24, no. 7, pp. 1822–1830, 2006.

[24] T. Asahara, H. Masuda, T. Takahashi et al., "Bone marrow origin of endothelial progenitor cells responsible for postnatal vasculogenesis in physiological and pathological neovascularization," *Circulation Research*, vol. 85, no. 3, pp. 221–228, 1999.

[25] P. Zammaretti and A. H. Zisch, "Adult 'endothelial progenitor cells': renewing vasculature," *International Journal of Biochemistry and Cell Biology*, vol. 37, no. 3, pp. 493–503, 2005.

[26] R. Khurana and M. Simons, "Endothelial progenitor cells: precursors for angiogenesis," *Seminars in Thoracic and Cardiovascular Surgery*, vol. 15, no. 3, pp. 250–258, 2003.

[27] O. M. Tepper, B. A. Sealove, T. Murayama, and T. Asahara, "Newly emerging concepts in blood vessel growth: recent discovery of endothelial progenitor cells and their function in tissue regeneration," *Journal of Investigative Medicine*, vol. 51, no. 6, pp. 353–359, 2003.

[28] A. J. Friedenstein, R. K. Chailakhyan, N. V. Latsinik, A. F. Panasyuk, and I. V. Keiliss-Borok, "Stromal cells responsible for transferring the microenvironment of the hemopoietic tissues. Cloning in vitro and retransplantation in vivo," *Transplantation*, vol. 17, no. 4, pp. 331–340, 1974.

[29] F. Duttenhoefer, R. L. de Freitas, T. Meury et al., "3D scaffolds co-seeded with human endothelial progenitor and mesenchymal stem cells: evidence of prevascularisation within 7 days," *European Cells & Materials*, vol. 26, pp. 49–65, 2013.

[30] S. P. Bruder, N. Jaiswal, and S. E. Haynesworth, "Growth kinetics, self-renewal, and the osteogenic potential of purified human mesenchymal stem cells during extensive subcultivation and following cryopreservation," *Journal of Cellular Biochemistry*, vol. 64, no. 2, pp. 278–294, 1997.

[31] M. Loibl, A. Binder, M. Herrmann et al., "Direct cell-cell contact between mesenchymal stem cells and endothelial progenitor cells induces a pericyte-like phenotype *in vitro*," *BioMed Research International*, vol. 2014, Article ID 395781, 10 pages, 2014.

[32] S. Lippross, M. Loibl, S. Hoppe et al., "Platelet released growth factors boost expansion of bone marrow derived $CD34^+$ and $CD133^+$ endothelial progenitor cells for autologous grafting," *Platelets*, vol. 22, no. 6, pp. 422–432, 2011.

[33] M. Herrmann, A. Binder, U. Menzel, S. Zeiter, M. Alini, and S. Verrier, "CD34/CD133 enriched bone marrow progenitor cells promote neovascularization of tissue engineered constructs *in vivo*," *Stem Cell Research*, vol. 13, no. 3, pp. 465–477, 2014.

[34] A. Lubkowska, B. Dolegowska, and G. Banfi, "Growth factor content in PRP and their applicability in medicine," *Journal of Biological Regulators and Homeostatic Agents*, vol. 26, no. 2, supplement 1, pp. 3S–22S, 2012.

[35] N. Jaiswal, S. E. Haynesworth, A. I. Caplan, and S. P. Bruder, "Osteogenic differentiation of purified, culture-expanded human mesenchymal stem cells in vitro," *Journal of Cellular Biochemistry*, vol. 64, no. 2, pp. 295–312, 1997.

[36] E. Lucarelli, A. Beccheroni, D. Donati et al., "Platelet-derived growth factors enhance proliferation of human stromal stem cells," *Biomaterials*, vol. 24, no. 18, pp. 3095–3100, 2003.

[37] C. Labarca and K. Paigen, "A simple, rapid, and sensitive DNA assay procedure," *Analytical Biochemistry*, vol. 102, no. 2, pp. 344–352, 1980.

[38] M. Alini, D. Carey, S. Hirata, M. D. Grynpas, I. Pidoux, and A. R. Poole, "Cellular and matrix changes before and at the time of calcification in the growth plate studied in vitro: arrest of type X collagen synthesis and net loss of collagen when calcification is initiated," *Journal of Bone and Mineral Research*, vol. 9, no. 7, pp. 1077–1087, 1994.

[39] D. Campioni, F. Lanza, S. Moretti et al., "Functional and immunophenotypic characteristics of isolated $CD105^+$ and $fibroblast^+$ stromal cells from AML: implications for their plasticity along endothelial lineage," *Cytotherapy*, vol. 5, no. 1, pp. 66–79, 2003.

[40] E. Flores-Figueroa, R. M. Arana-Trejo, G. Gutiérrez-Espíndola, A. Pérez-Cabrera, and H. Mayani, "Mesenchymal stem cells in myelodysplastic syndromes: phenotypic and cytogenetic characterization," *Leukemia Research*, vol. 29, no. 2, pp. 215–224, 2005.

[41] M. Baddoo, K. Hill, R. Wilkinson et al., "Characterization of mesenchymal stem cells isolated from murine bone marrow by negative selection," *Journal of Cellular Biochemistry*, vol. 89, no. 6, pp. 1235–1249, 2003.

[42] M. Y. Gordon, "Stem cells for regenerative medicine—biological attributes and clinical application," *Experimental Hematology*, vol. 36, no. 6, pp. 726–732, 2008.

[43] A. Kawamoto, T. Asahara, and D. W. Losordo, "Transplantation of endothelial progenitor cells for therapeutic neovascularization," *Cardiovascular Radiation Medicine*, vol. 3, no. 3-4, pp. 221–225, 2002.

[44] E. Fuchs, T. Tumbar, and G. Guasch, "Socializing with the neighbors: stem cells and their niche," *Cell*, vol. 116, no. 6, pp. 769–778, 2004.

[45] T. A. Mitsiadis, O. Barrandon, A. Rochat, Y. Barrandon, and C. De Bari, "Stem cell niches in mammals," *Experimental Cell Research*, vol. 313, no. 16, pp. 3377–3385, 2007.

[46] M. J. Kiel and S. J. Morrison, "Uncertainty in the niches that maintain haematopoietic stem cells," *Nature Reviews Immunology*, vol. 8, no. 4, pp. 290–301, 2008.

[47] C. C. I. Lee, J. E. Christensen, M. C. Yoder, and A. F. Tarantal, "Clonal analysis and hierarchy of human bone marrow mesenchymal stem and progenitor cells," *Experimental Hematology*, vol. 38, no. 1, pp. 46–54, 2010.

[48] T. Meury, S. Verrier, and M. Alini, "Human endothelial cells inhibit BMSC differentiation into mature osteoblasts in vitro by interfering with osterix expression," *Journal of Cellular Biochemistry*, vol. 98, no. 4, pp. 992–1006, 2006.

[49] S. J. Bidarra, C. C. Barrias, M. A. Barbosa, R. Soares, J. Amédée, and P. L. Granja, "Phenotypic and proliferative modulation of human mesenchymal stem cells via crosstalk with endothelial cells," *Stem Cell Research*, vol. 7, no. 3, pp. 186–197, 2011.

[50] D. T. Scadden, "The stem-cell niche as an entity of action," *Nature*, vol. 441, no. 7097, pp. 1075–1079, 2006.

[51] A. Aguirre, J. A. Planell, and E. Engel, "Dynamics of bone marrow-derived endothelial progenitor cell/mesenchymal stem cell interaction in co-culture and its implications in angiogenesis," *Biochemical and Biophysical Research Communications*, vol. 400, no. 2, pp. 284–291, 2010.

[52] N. E. Fedorovich, R. T. Haverslag, W. J. A. Dhert, and J. Alblas, "The role of endothelial progenitor cells in prevascularized bone tissue engineering: development of heterogeneous constructs," *Tissue Engineering, Part A*, vol. 16, no. 7, pp. 2355–2367, 2010.

[53] J. S. Hermann, D. Buser, R. K. Schenk, and D. L. Cochran, "Crestal bone changes around titanium implants. A histometric evaluation of unloaded non-submerged and submerged implants in the canine mandible," *Journal of Periodontology*, vol. 71, no. 9, pp. 1412–1424, 2000.

[54] W.-L. Fu, Z. Xiang, F.-G. Huang et al., "Coculture of peripheral blood-derived mesenchymal stem cells and endothelial progenitor cells on strontium-doped calcium polyphosphate scaffolds to generate vascularized engineered bone," *Tissue Engineering Part A*, vol. 21, no. 5-6, pp. 948–959, 2015.

[55] G. Siegel, T. Kluba, U. Hermanutz-Klein, K. Bieback, H. Northoff, and R. Schäfer, "Phenotype, donor age and gender affect function of human bone marrow-derived mesenchymal stromal cells," *BMC Medicine*, vol. 11, no. 1, article 146, 2013.

[56] H. V. Leskelä, J. Risteli, S. Niskanen, J. Koivunen, K. K. Ivaska, and P. Lehenkari, "Osteoblast recruitment from stem cells does not decrease by age at late adulthood," *Biochemical and Biophysical Research Communications*, vol. 311, no. 4, pp. 1008–1013, 2003.

[57] V. Dexheimer, S. Mueller, F. Braatz, and W. Richter, "Reduced reactivation from dormancy but maintained lineage choice of human mesenchymal stem cells with donor age," *PLoS ONE*, vol. 6, no. 8, Article ID e22980, 2011.

[58] M. Herrmann, A. Binder, U. Menzel, S. Zeiter, M. Alini, and S. Verrier, "CD34/CD133 enriched bone marrow progenitor cells promote neovascularization of tissue engineered constructs in vivo," *Stem Cell Research*, vol. 13, no. 3, pp. 465–477, 2014.

Hindawi Publishing Corporation
BioMed Research International
Volume 2015, Article ID 621481, 7 pages
http://dx.doi.org/10.1155/2015/621481

*Research Article*

# Are Biodegradable Osteosyntheses Still an Option for Midface Trauma? Longitudinal Evaluation of Three Different PLA-Based Materials

**Andreas Kolk,[1] Robert Köhnke,[2,3] Christoph H. Saely,[4] and Oliver Ploder[3,5]**

[1]*Department of Oral- and Craniomaxillofacial Surgery, Klinikum Rechts der Isar der Technischen Universität München, Ismaninger Strasse 22, 81675 Munich, Germany*
[2]*Department for Oral- and Maxillofacial Surgery, University Medical Center Hamburg-Eppendorf, Martinistrasse 52, 20246 Hamburg, Germany*
[3]*Department of Oral- and Maxillofacial Surgery, Academic Teaching Hospital Feldkirch, Carinagasse 47, 6800 Feldkirch, Austria*
[4]*Department of Medicine and Cardiology, VIVIT Research, Academic Teaching Hospital, Carinagasse 47, 6800 Feldkirch, Austria*
[5]*Department of Craniomaxillofacial and Oral Surgery, Medical University Vienna, Vienna General Hospital, Waehringer Guertel 18-20, 1090 Vienna, Austria*

Correspondence should be addressed to Andreas Kolk; kolk@mkg.med.tum.de

Received 26 March 2015; Accepted 16 June 2015

Academic Editor: Joo L. Ong



The aim was to evaluate three different biodegradable polylactic acid- (PLA-) based osteosynthesis materials (OM). These OM (BioSorb, LactoSorb, and Delta) were used in 64 patients of whom 55 (85.9%) had fractures of the zygoma, five (7.8%) in the LeFort II level, two of the frontal bone (3.1%), and two of the maxillary sinus wall (3.1%). In addition to routine follow-up (FU) at 3, 6, and 12 months (m) (T1, T2, and T3) all patients were finally evaluated at a mean FU after 14.1 m for minor (e.g., nerve disturbances, swelling, and pain) and major (e.g., infections and occlusal disturbances) complications. Out of all 64 patients 38 presented with complications; of these 28 were minor (43.8%) and 10 major (15.6%) resulting in an overall rate of 59.4%. Differences in minor complications regarding sensibility disturbance at T1 and T3 were statistically significant ($P = 0.04$). Differences between the OM were not statistically significant. Apart from sufficient mechanical stability for clinical use of all tested OM complications mostly involved pain and swelling probably mainly related to the initial bulk reaction attributable to the drop of pH value during the degradation process. This paper includes a review of the current aspects of biodegradable OM.

## 1. Introduction

In maxillofacial trauma, osteosynthesis materials (OM) manufactured from titanium have been routinely used for many years [1, 2]. Such bone plates are biocompatible and provide adequate stability. Several potential problems with these systems can occur including palpability, temperature sensitivity, infection, interference with radiographic imaging [3, 4] and radiation therapy, and the necessity of removal especially in the young growing face after 3–6 months (m) [5]. Additionally, scar tissue covering these plates and locoregional lymph nodes can contain titanium particles [6]. In a recent publication, titanium plates have even been seen as a risk factor for the development of the bisphosphonate-related osteonecrosis of the jaw [7]. In order to avoid these problems, biodegradable synthetic semicrystalline polymers that are mainly polylactic acid- (PLA-) based have been developed for use as OM in maxillofacial trauma [8, 9]. Since their first descriptions in the 1970s and mainly within the last 20 years, biodegradable OM have been investigated and shown to achieve adequate strength, rigidity, and biocompatibility [10–14]. Initially, synthetic polymers of lactic (PLA) and glycolic (PGA) acid were considered to be biocompatible and rigid [15], with PLA also serving as a device for controlled drug delivery in addition to its use as an OM [16, 17]. Because of various problems with OM based only on PGA,

and because of the early loss of stability attributable to fast degradation [18], further developments have concentrated more on the high-molecular-weight biodegradable polymer PLA, a combination of two different stereoisomeric forms such as poly-L-lactide (PLLA) and poly-D-lactide (PDLA), or a combination of PLA and PGA. The last-mentioned form is characterized by an inferior degradation rate attributable to lower crystallinity and minor resistance against hydrolysis. To combine properties, copolymers of PLA are joined in different ratios of PLLA and PDLA.

Thus, many different materials with diverse compositions of PLA for various applications in the field of oral and maxillofacial surgery are available on the market and are used in the treatment of fractures of the frontal bone and midface [19, 20]. Although many of these materials are widespread, no evidence has been presented for their indication and localization, or whether they can serve as an alternative to titanium-based OM. Most problems with biodegradable OM are related to the duration of the degradation process with a consecutive change of the local tissue environment caused by foreign body reaction and tissue shrinking mainly within weeks, but also up to many months after implantation.

The vast majority of clinical studies have compared the outcome of the use of biodegradable materials with titanium in the treatment of midface fractures [21–24]. The results of the latter studies have shown no differences between biodegradable and titanium fixation regarding short-term outcome. Little long-term data are available concerning comparisons of various biodegradable materials in clinical applications [21, 25]. Therefore, the aim of this study has been to evaluate the use of three different biodegradable OM in the treatment of midface trauma and to analyze their long-term clinical outcome.

## 2. Patients and Methods

Over a period of 45 months, 64 patients (50 men and 14 women, mean age (±SD) 30.2 ± 15.4 years, ranging from 6 to 80 years) with fractures of the midfacial skeleton were enrolled in the study and, after randomization, were treated at the University Hospital of Cranio-Maxillofacial and Oral Surgery of the Medical University Vienna with three different biodegradable OM as an alternative to the classic titanium OM: BioSorb (copolymer with PLLA/PDLA (ratio 70 : 30), Bionx Implants Linvatec Corp., Largo, FL, USA) (BS), LactoSorb (amorphic copolymer with PLLA/PGA (ratio 82 : 18), Walter Lorenz Surgical, Inc., Jacksonville, FL, USA) (LS), and Delta (terpolymer with PLLA/PDLA/PGA (ratio 85 : 5 : 10), Stryker Leibinger Micro Corp., Freiburg, Germany) (DS).

In contrast to the two other OM (LS/DS), BS plates on the basis of a self-reinforced poly (L-/DL-) (70 : 30) lactic acid copolymer can be adapted to the bony contour (Figure 1) at room temperature without any heating. To obtain a preferably homogeneous collective, patients were selectively filtered for this study. Subjects with previous surgery or systemic diseases, such as diabetes or osteoporosis, were excluded. After choosing biodegradable OM as an alternative to titanium, all patients gave their written informed consent for the surgical procedure and research purposes at the time of initial presentation. The local hospital ethic committee approved the study. Three, six, and twelve m after trauma (time points T1, T2, and T3), patients took part in routine follow-up (FU) with clinical and radiological examination (conventional X-rays or CT scans) by one investigator using a standardized FU protocol. Preoperative data were taken from the charts of each patient. All findings (temporary and permanent symptoms) that occurred during any part of the observation period were recorded and categorized as minor (e.g., swelling, pain, or nerve disturbance) or major (infection, occlusal disturbance, need of revision surgery, or hypertrophic scar) complications (Table 1). Parameters such as swelling and redness were recorded with yes/no answers. Pain was documented on a visual analog scale (VAS > 0) from 0 to 10. All the last-mentioned parameters were classified as minor complications if they were still observed at investigation date T1–T3. Potential dysfunctions (an-, hyp-, and paraesthesia) of the trigeminal nerve branches were tested on both sides at the forehead, cheek, nose, and lip area by using the touch-detection-threshold at T1–T3. Further postoperative findings such as infections were recorded. Maximum mouth opening and occlusal conditions (centric occlusion, lateral excursions, and occlusal disturbance) were analyzed in cases of occlusal involvement of the central midface (Table 1). At the end of the study after a mean (±SD) of 14.1 ± 0.8 m a final clinical examination took place in addition to the previous FU at T3.

Descriptive statistics for quantitative variables are given as means ± standard deviation and, where appropriate, as medians and ranges. All data were analyzed with the "Statistical Package for the Social Sciences" (SPSS for windows, release 14.0.0 2011; SPSS Inc.). All $P$ values given are

Table 1: Categories of potential complications.

| Minor complications | Major complications |
|---|---|
| Swelling* | Infection |
| Redness* | Malocclusion |
| Pain* | Revision surgery |
| Sensitivity disturbance | Ectropion |
| | Hypertrophic scar |

*Recorded if still observed at the final clinical investigation date (mean final FU after 14.1 m).

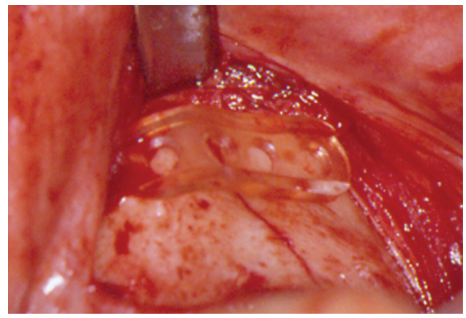

Figure 1: Intraoperative view. Adaption of biodegradable OM in the zygoma region.

Table 2: Distribution of fracture localization and applied OM ($N$ = 64).

| Localization | Number | Material | | |
|---|---|---|---|---|
| | | BS | LS | DS |
| Frontal bone | 2 | 2 (1.5) | | |
| Midface | | | | |
| Le Fort II | 5 | 5 (2.0) | | |
| Zygoma | 55 | 27 (1.5) | 12 (1.5) | 16 (1.7) |
| Max. sinus wall | 2 | 2 (1.5) | | |
| Total | 64 | 36 | 12 | 16 |

OM with plate thickness behind the number (mm); BS: Biosorb; LS: LactoSorb; DS: Delta.

unadjusted, two-sided, and subject to a significance level of $P < 0.05$.

## 3. Results

In 64 patients, the fractures were treated with three different biodegradable OM (BS, LS, and DS); 55 patients (85.9%) had zygoma fractures, five patients (7.8%) had fractures in the LeFort II level, two of the frontal bone (3.1%), and two of the maxillary sinus wall (3.1%) (Table 2). Thirty-six patients (56.2%) were treated with BS, 12 patients (18.8%) were treated with LS, and in 16 cases (25%) DS was used. Fracture localization, the number of cases in each area, and the OM used are shown in detail in Table 2. The mean time interval (±SD) between trauma and operation was 3.9 ± 4.8 days. Patients were divided into two groups regarding the time duration to fracture reduction: one group was operated up to day 4 after injury and the other between 5 and 9 days after trauma. The difference between the two groups was not statistically significant. The mean final clinical FU (±SD) was after 14.1 ± 0.8 m (ranging from 12.4 to 22 m). All fractures showed stable healing without any signs of redislocation until T1. None of the patients required any revision surgery or other additional procedures.

Out of the total collective ($N$ = 64) 38 patients presented with problems, of these 28 (43.8%) had minor and 10 (15.6%) major complications resulting in an overall complication rate of 59.4%. Whereas differences regarding sensory disturbance between T1 and T3 were statistically significant ($P$ = 0.04), the variances in the outcome between the materials were statistically not significant (Tables 3 and 4). Twelve months postoperatively (T3), 37 patients (57.8%) experienced pain in the plate region (VAS > 0): out of the latter subgroup, 28 patients belonged to group BS (77.8%), two to group LS (16.7%), and seven to group DS (43.8%). The difference between the materials was not statistically significant. At the final clinical investigation date (mean 14.1 m postoperatively), pain (VAS > 0, mean ± SD, 3.05 ± 1.31) was still present and was considered as quality-of-life-limiting complaints in 19 patients of group BS, one of group LS, and 6 of subgroup DS. Differences between the materials were statistically marginally significant ($P$ = 0.05).

In 18 patients treated with BS (50.0%), in three patients of group LS (25.0%), and in five patients with DS (31.3%), swelling was still evident at the final clinical evaluation time point (after mean 14.1 m). The differences between the materials were statistically not significant. The presence of nerve disturbance and its different degrees of severity or quality, the fracture localization, and the applied OM subgroup are displayed in Tables 3 and 4.

## 4. Discussion

The use of titanium plates and screws for the treatment of facial fractures is well documented and accepted as the treatment of choice [1, 2]. In order to avoid implant-related problems with these materials, for example, palpable and prominent plates or thermal sensitivity followed by a second operation for removal, biodegradable OM were invented for the treatment of facial fractures more than 40 years ago [10, 12, 26–30]. Additionally, these materials are used for craniofacial and reconstructive facial surgery [23, 30, 31]. Nevertheless, only a few studies have compared outcome with regard to the localization and different material compositions of the OM [22, 24, 25, 32]. The complication rate in these investigations varies between 0.0% and 22.8% [22, 24, 31, 32]. Eppley et al. have reported their experience and success with L-/DL-lactide (70/30) for the fixation of maxillofacial trauma, including fractures of the central midface, zygoma, and orbital rim and floor [23]; they observed no implant-related complications (e.g., infection, erythema, fracture instability, or relapse) up to one year after fixation. Enislidis et al. have recorded 22.8% of minor complications by using BioSorb (BS) for the fixation of zygoma fractures [24]. In contrast to the current literature and an analysis of the latter, we have obtained a much higher complication rate of 59.4%, independent of the material. This can be explained by the long-term FU and the extensive listing of various clinical symptoms, including swelling, being categorized as major or minor complications. Furthermore, the evaluation of swelling and pain have been categorized with yes or no answers and assigned to minor complications, for example, each patient presenting with swelling (yes or no answers) or pain (VAS > 0 equals pain). The majority of minor complications are related to pain and swelling. At T3 even 37/64 patients (57.8%) and even at the final FU 26 of 64 patients (40.6%) still exhibited pain and swelling in the plate region. The high number of these symptoms can probably be explained by implant-related foreign body reaction (Figure 2) caused by the material-associated degradation process and the thickness of the plates (Figure 1) in general with local tissue trauma. Bioresorbable polymers are mainly high-molecular-weight aliphatic polyesters with repeating units of $\alpha$-hydroxy acid (HO- CHR-COOH) derivatives manufactured by ring-opening polymerization [33]. The absorption of these polymers begins with depolymerization through the acid hydrolysis of their ester bonds. The local pH value drops followed by a change in osmotic pressure. Toxic responses result [34] in concomitant damage of macrophages and fibroblasts [35], and osteoblasts are affected [36]. The resulting chronic inflammatory response by the body leads to acid hydrolytic degradation [37–39]. The material is probably metabolized by macrophages via the citric acid cycle and converted into $CO_2$

Table 3: Fracture localization and distribution and quality of nerve disturbance ($N = 64$).

| FU | Localization | Norm (%) | Hyp (%) | Par (%) | An (%) | MD (%) | $P$ |
|---|---|---|---|---|---|---|---|
| T1 | Upper jaw | 11 (17.2) | 43 (67.2) | 7 (10.9) | 3 (4.7) | 0 | |
| T2 | Upper jaw | 35 (54.7) | 26 (40.6) | 2 (3.1) | 1 (1.6) | 0 | |
| T3 | Upper jaw | 50 (78.1) | 8 (12.5) | 4 (6.3) | 1 (1.6) | 1 (1.6) | 0.045* |

FU: Follow-up time point in months (m), (T1 = 3 m, T2 = 6 m, T3 = 12 m); Norm: normal; Hyp: hypaesthesia; Par: paraesthsia; An: anaesthesia; MD: missing data. Apart from T1 versus T3, no statistical significance was seen between the FU time points, level of significance * ($P < 0.05$).

Table 4: Nerve disturbance depending on FU and OM ($N = 64$).

| FU | OM | Norm | Hyp | Par | An | MD | $P$ |
|---|---|---|---|---|---|---|---|
| T1 | BS | 5 (13.9%) | 25 (69.4%) | 3 (8.3%) | 3 (8.3%) | 0 | — |
| | LS | 2 (16.7%) | 10 (83.3%) | 0 | 0 | 0 | — |
| | DS | 4 (25.0%) | 8 (50.0%) | 4 (25.0%) | 0 | 0 | — |
| T2 | BS | 14 (38.9%) | 14 (38.9%) | 2 (5.6%) | 1 (2.8%) | 5 (13.9%) | — |
| | LS | 9 (75.0%) | 3 (25.0%) | 0 | 0 | 0 | — |
| | DS | 11 (68.8%) | 3 (18.8%) | 2 (12.5%) | 0 | 0 | — |
| T3 | BS | 23 (63.9%) | 5 (13.9%) | 2 (5.6%) | 1 (2.8%) | 5 (13.9%) | — |
| | LS | 10 (83.3%) | 2 (16.7%) | 0 | 0 | 0 | — |
| | DS | 12 (75.0%) | 2 (12.5%) | 2 (12.5%) | 0 | 0 | — |

FU: FU time point (T1 = 3 m, T2 = 6 m, and T3 = 12 m); Norm: normal; Hyp: hypaesthesia; Par: paraesthesia; An: anaesthesia; MD: Missing Data. $P$: the difference between the materials was not statistically significant.

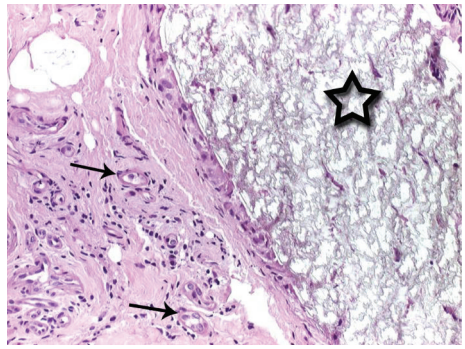

Figure 2: Histologic evaluation of a biodegradable material (asterix). Surrounding foreign body reaction with giant-cell-formation (arrows).

and $H_2O$ via bulk hydrolysis; it is also metabolized by the liver (a two-phase degradation process) [40, 41].

The resorption time of the metabolized components ranges between 6 and 18 months and can even occur up to 60 months [42, 43]. Generally, degradation characteristics depend on many factors of the material itself and the local tissue environment including the copolymer ratio, micro- and molecular structure, processing conditions, implant shape and thickness, and implantation site including vascularization. Initial biodegradable systems involved high-molecular-weight polylactic acid polymers, but unfortunate foreign body reactions occurred and were attributed to their long resorption period [44, 45]. BS, for example, is a copolymer formed by combining L-lactide and DL-lactide (70 : 30) to provide optimal strength and acceptable spatiotemporal degradation characteristics. It retains approximately 68% of its initial bending strength after 8 weeks, approximately 30% after 6 months, and has a total resorption time of 24 months [32]. The copolymer compositions and thus the degradation behavior of LS + DS differ slightly from that of BS. Despite their possible differences in stability during the fracture healing process and in the local tissue environment attributable to the different rates in the pH value decrease, only minor differences concerning the clinical outcome were apparent between BS, LS, and DS. BS exhibited slightly more long-term swelling and pain, as their overall degradation time span was longer than those of LS and DS. In the literature, some serious nonspecific foreign body reactions have been reported as being caused by high-molecular PLLA implants [44, 46, 47]. The PLLA remnants are surrounded by a fibrotic capsule and have been detected intracellularly. Even after 5.7 years, unabsorbed PLLA particles are present in the specimens [44, 46, 47].

Another important aspect is the ability of the implantation site to dissolve and remove metabolized materials. Good vascularization leads to faster removal and prevents the accumulation of degradation products causing acidity of the tissue [48, 49].

After the first week of implantation, a rapid decline in strength of PLLA occurs, which might lead to premature failure [50]. A 50% loss of strength by two weeks after implantation and a total loss of strength and consistency after 6 weeks limit the reliable clinical use of this material [50].

In an experimental study, four biodegradable materials (LactoSorb, Inion CPS 1.5 baby, Delta, and RFS) were evaluated, and their stability was tested *in vitro* via microrigidity [51]. LactoSorb and Inion CPS 1.5 baby were the weakest implants after three months. After a year, Delta and RFS were still rigid [51]. Biodegradable materials are composed of various combinations of poly($\alpha$-hydroxypolyesters), such as polylactic acid (PLA) and polyglycolic acid (PGA), and therefore show diverse intensities of inflammatory reaction because of their variable degradation rates [30, 52, 53]. Intraoperative warming of most OM (not BS) is needed in order to adapt the shape of the biodegradable material to the anatomical implantation site. Bergsma et al. speculate that this manipulation accelerates the degradation progress [49]. Furthermore, crystallinity leads to a slower absorption rate and is known to cause greater tissue reaction than with more easily absorbed components [48]. In future, polymethylmethacrylate bone cement bonding and degradable magnesium alloy implants [54, 55] might alternatively be used for the treatment of facial trauma, especially in the non-load-bearing region of the frontal and calvaria bone [56].

In our study, we have found a large number of complications such as pain, swelling, infections, and nerve disturbances. Most of the documented problems are related to the implantation site and not to the materials. However, we assume that the degradation process of the implants is another important reason for the high number of minor complications. Because of the inevitable drop of the local pH-value, short- and long-term effects occur as the osmotic pressure is increased, so that the implant cavity is expanded or sterile fluid accumulates.

The shrinking of the periosteum, pain, and sensory disturbance, sometimes over many months, are probably the most important negative consequences for the patient. Buffering systems such as the incorporation of basic salts [57] and other modifications might reduce these unpleasant side effects and might therefore help to broaden the range of applications of these OM in the field of facial trauma and reconstruction and to increase patient acceptance. Many factors influence the physicochemical behavior and, consecutively, the degradation process of PLA [17]. Whereas low stress, high crystallinity, and orientation can reduce the degradation rate [58]; high temperature [59] and acidity [60] tend to induce the opposite.

However, further investigations with modified copolymer compositions, buffering systems, and biodegradable OM with more tissue-compatible physicochemical characteristics thus need to be carried out and analyzed.

In conclusion, the current study and the literature provide evidence that the use of biodegradable OM in the treatment of fractures of the midface and particularly in load-bearing applications such as the mandible is still not an alternative to the classic titanium OM and should therefore be reserved for specific indications. Moreover, long-term effects generated by the degradation process and its products have to be critically observed. Developments such as degradable magnesium alloy implants [54] might show stability comparable with titanium, might be an alternative to the latter, and might replace classic biodegradable OM.

## Abbreviations

FU: Follow-up
m: Months
OM: Osteosynthesis material
PLA: Polylactic acid
PGA: Polyglycolic acid
PDLA: Poly-D-Lactic Acid
PLLA: Poly-L-Lactic Acid
T: Time point.

## Conflict of Interests

The authors declare that there is no conflict of interests regarding the publication of this paper.

## Authors' Contribution

Andreas Kolk and Robert Köhnke contributed equally to this work.

## References

[1] D. G. Bowers Jr. and J. B. Lynch, "Management of facial fractures," *Southern Medical Journal*, vol. 70, no. 8, pp. 910–918, 1977.

[2] R. Schmelzeisen, T. McIff, and B. Rahn, "Further development of titanium miniplate fixation for mandibular fractures. Experience gained and questions raised from a prospective clinical pilot study with 2.0 mm fixation plates," *Journal of Cranio-Maxillofacial Surgery*, vol. 20, no. 6, pp. 251–256, 1992.

[3] T. G. S. Fiala, R. A. Novelline, and M. J. Yaremchuk, "Comparison of CT imaging artifacts from craniomaxillofacial internal fixation devices," *Plastic and Reconstructive Surgery*, vol. 92, no. 7, pp. 1227–1232, 1993.

[4] E. Wiener, C. Pautke, T. M. Link, A. Neff, and A. Kolk, "Comparison of 16-slice MSCT and MRI in the assessment of squamous cell carcinoma of the oral cavity," *European Journal of Radiology*, vol. 58, no. 1, pp. 113–118, 2006.

[5] J. C. Yu, S. P. Bartlett, D. S. Goldberg et al., "An experimental study of the effects of craniofacial growth on the long-term positional stability of microfixation," *The Journal of Craniofacial Surgery*, vol. 7, no. 1, pp. 64–68, 1996.

[6] C. P. Case, V. G. Langkamer, C. James et al., "Widespread dissemination of metal debris from implants," *The Journal of Bone & Joint Surgery—British Volume*, vol. 76, no. 5, pp. 701–712, 1994.

[7] E. N. Siniscalchi, L. Catalfamo, A. Allegra, C. Musolino, and F. S. De Ponte, "Titanium miniplates: a new risk factor for the development of the bisphosphonate-related osteonecrosis of the jaw," *Journal of Craniofacial Surgery*, vol. 24, no. 1, pp. e1–e2, 2013.

[8] A. U. Daniels, M. K. Chang, and K. P. Andriano, "Mechanical properties of biodegradable polymers and composites proposed for internal fixation of bone," *Journal of Applied Biomaterials*, vol. 1, no. 1, pp. 57–78, 1990.

[9] W. H. Harris, B. J. L. Moyen, E. L. Thrasher II et al., "Differential response to electrical stimulation: a distinction between induced osteogenesis in intact tibiae and the effect on fresh fracture defects in radii," *Clinical Orthopaedics and Related Research*, vol. 124, pp. 31–40, 1977.

[10] R. K. Kulkarni, E. G. Moore, A. F. Hegyeli, and F. Leonard, "Biodegradable poly(lactic acid) polymers," *Journal of Biomedical Materials Research*, vol. 5, no. 3, pp. 169–181, 1971.

[11] L. K. Cheung, L. K. Chow, and W. K. Chiu, "A randomized controlled trial of resorbable versus titanium fixation for orthognathic surgery," *Oral Surgery, Oral Medicine, Oral Pathology, Oral Radiology and Endodontology*, vol. 98, no. 4, pp. 386–397, 2004.

[12] R. K. Kulkarni, K. C. Pani, C. Neuman, and F. Leonard, "Polylactic acid for surgical implants," *Archives of Surgery*, vol. 93, no. 5, pp. 839–843, 1966.

[13] K. L. Gerlach, "Resorbable polymers as osteosynthesis material," *Mund Kiefer Gesichtschir*, vol. 4, supplement 1, pp. S91–S102, 2000.

[14] K. L. Gerlach, "In-vivo and clinical evaluations of poly(L-lactide) plates and screws for use in maxillofacial traumatology," *Clinical Materials*, vol. 13, no. 1–4, pp. 21–28, 1993.

[15] S. J. Gourlay, R. M. Rice, A. F. Hegyeli et al., "Biocompatibility testing of polymers: in vivo implantation studies," *Journal of Biomedical Materials Research*, vol. 12, no. 2, pp. 219–232, 1978.

[16] A. Kolk, C. Haczek, C. Koch et al., "A strategy to establish a gene-activated matrix on titanium using gene vectors protected in a polylactide coating," *Biomaterials*, vol. 32, no. 28, pp. 6850–6859, 2011.

[17] A. Kolk, J. Handschel, W. Drescher et al., "Current trends and future perspectives of bone substitute materials—from space holders to innovative biomaterials," *Journal of Cranio-Maxillofacial Surgery*, vol. 40, no. 8, pp. 706–718, 2012.

[18] J. Vasenius, S. Vainionpää, K. Vihtonen et al., "Comparison of *in vitro* hydrolysis, subcutaneous and intramedullary implantation to evaluate the strength retention of absorbable osteosynthesis implants," *Biomaterials*, vol. 11, no. 7, pp. 501–504, 1990.

[19] J. A. Goldstein, F. A. Quereshy, and A. R. Cohen, "Early experience with biodegradable fixation for congenital pediatric craniofacial surgery," *Journal of Craniofacial Surgery*, vol. 8, no. 2, pp. 110–115, 1997.

[20] K. D. Kiely, K. S. Wendfeldt, B. E. Johnson, B. S. Haskell, and R. C. Edwards, "One-year postoperative stability of LeFort I osteotomies with biodegradable fixation: a retrospective analysis of skeletal relapse," *American Journal of Orthodontics and Dentofacial Orthopedics*, vol. 130, no. 3, pp. 310–316, 2006.

[21] G. Wittwer, W. L. Adeyemo, M. Voracek et al., "An evaluation of the clinical application of three different biodegradable osteosynthesis materials for the fixation of zygomatic fractures," *Oral Surgery, Oral Medicine, Oral Pathology, Oral Radiology and Endodontology*, vol. 100, no. 6, pp. 656–660, 2005.

[22] G. Wittwer, W. L. Adeyemo, K. Yerit et al., "Complications after zygoma fracture fixation: Is there a difference between biodegradable materials and how do they compare with titanium osteosynthesis?" *Oral Surgery, Oral Medicine, Oral Pathology, Oral Radiology and Endodontology*, vol. 101, no. 4, pp. 419–425, 2006.

[23] B. L. Eppley, C. D. Prevel, A. M. Sadove, and D. Sarver, "Resorbable bone fixation: its potential role in craniomaxillofacial trauma," *Journal of Cranio-Maxillofacial Trauma*, vol. 2, no. 1, pp. 56–60, 1996.

[24] G. Enislidis, G. Lagogiannis, G. Wittwer, C. Glaser, and R. Ewers, "Fixation of zygomatic fractures with a biodegradable copolymer osteosynthesis system: short- and long-term results," *International Journal of Oral & Maxillofacial Surgery*, vol. 34, no. 1, pp. 19–26, 2005.

[25] L. Yang, M. Xu, X. Jin et al., "Complications of absorbable fixation in maxillofacial surgery: a meta-analysis," *PLoS ONE*, vol. 8, no. 6, Article ID e67449, 2013.

[26] D. E. Cutright, E. E. Hunsuck, and J. D. Beasley, "Fracture reduction using a biodegradable material, polylactic acid," *Journal of Oral Surgery*, vol. 29, no. 6, pp. 393–397, 1971.

[27] B. L. Schmidt, D. H. Perrott, D. Mahan, and G. Kearns, "The removal of plates and screws after Le Fort I osteotomy," *Journal of Oral and Maxillofacial Surgery*, vol. 56, no. 2, pp. 184–188, 1998.

[28] B. R. Simon, S. L.-Y. Woo, M. McCarty, S. Lee, and W. H. Akeson, "Parametric study of bone remodeling beneath internal fixation plates of varying stiffness," *Journal of Bioengineering*, vol. 2, no. 6, pp. 543–556, 1978.

[29] J. S. Orringer, V. Barcelona, and S. R. Buchman, "Reasons for removal of rigid internal fixation devices in craniofacial surgery," *Journal of Craniofacial Surgery*, vol. 9, no. 1, pp. 40–44, 1998.

[30] P. Schumann, D. Lindhorst, M. E. H. Wagner, A. Schramm, N.-C. Gellrich, and M. Rücker, "Perspectives on resorbable osteosynthesis materials in craniomaxillofacial surgery," *Pathobiology*, vol. 80, no. 4, pp. 211–217, 2013.

[31] B. L. Eppley and A. M. Sadove, "Effects of resorbable fixation on craniofacial skeletal growth: a pilot experimental study," *The Journal of Craniofacial Surgery*, vol. 3, no. 4, pp. 190–196, 1992.

[32] R. B. Bell and C. S. Kindsfater, "The use of biodegradable plates and screws to stabilize facial fractures," *Journal of Oral and Maxillofacial Surgery*, vol. 64, no. 1, pp. 31–39, 2006.

[33] P. U. Rokkanen, "Absorbable materials in orthopaedic surgery," *Annals of Medicine*, vol. 23, no. 2, pp. 109–115, 1991.

[34] A. A. Ignatius and L. E. Claes, "In vitro biocompatibility of bioresorbable polymers: poly(L, DL-lactide) and poly(L-lactide-co-glycolide)," *Biomaterials*, vol. 17, no. 8, pp. 831–839, 1996.

[35] B. Saad, G. Ciardelli, S. Matter et al., "Characterization of the cell response of cultured macrophages and fibroblasts to particles of short-chain poly[(R)-3-hydroxybutyric acid]," *Journal of Biomedical Materials Research*, vol. 30, no. 4, pp. 429–439, 1996.

[36] M. C. Wake, P. D. Gerecht, L. Lu, and A. G. Mikos, "Effects of biodegradable polymer particles on rat marrow-derived stromal osteoblasts *in vitro*," *Biomaterials*, vol. 19, no. 14, pp. 1255–1268, 1998.

[37] H. Pihlajamäki, J. Kinnunen, and O. Böstman, "In vivo monitoring of the degradation process of bioresorbable polymeric implants using magnetic resonance imaging," *Biomaterials*, vol. 18, no. 19, pp. 1311–1315, 1997.

[38] R. A. Miller, J. M. Brady, and D. E. Cutright, "Degradation rates of oral resorbable implants (polylactates and polyglycolates): rate modification with changes in PLA/PGA copolymer ratios," *Journal of Biomedical Materials Research*, vol. 11, no. 5, pp. 711–719, 1977.

[39] D. E. Cutright, B. Perez, J. D. Beasley III, W. J. Larson, and W. R. Posey, "Degradation rates of polymers and copolymers of polylactic and polyglycolic acids," *Oral Surgery, Oral Medicine, Oral Pathology*, vol. 37, no. 1, pp. 142–152, 1974.

[40] W. S. Pietrzak, "Principles of development and use of absorbable internal fixation," *Tissue Engineering*, vol. 6, no. 4, pp. 425–433, 2000.

[41] W. S. Pietrzak, D. R. Sarver, and M. L. Verstynen, "Bioabsorbable polymer science for the practicing surgeon," *Journal of Craniofacial Surgery*, vol. 8, no. 2, pp. 87–91, 1997.

[42] M. J. Imola, D. D. Hamlar, W. Shao, K. Chowdhury, and S. Tatum, "Resorbable plate fixation in pediatric craniofacial surgery: long-term outcome," *Archives of Facial Plastic Surgery*, vol. 3, no. 2, pp. 79–90, 2001.

[43] J. Wiltfang, H.-A. Merten, S. Schultze-Mosgau, U. Schrell, D. Wénzel, and P. Keßler, "Biodegradable miniplates (LactoSorb): long-term results in infant minipigs and clinical results," *Journal of Craniofacial Surgery*, vol. 11, no. 3, pp. 239–243, 2000.

[44] E. J. Bergsma, F. R. Rozema, R. R. M. Bos, and W. C. de Bruijn, "Foreign body reactions to resorbable poly(L-lactide) bone plates and screws used for the fixation of unstable zygomatic fractures," *Journal of Oral and Maxillofacial Surgery*, vol. 51, no. 6, pp. 666–670, 1993.

[45] R. R. M. Bos, G. Boering, F. R. Rozema, and J. W. Leenslag, "Resorbable poly(L-lactide) plates and screws for the fixation of zygomatic fractures," *Journal of Oral and Maxillofacial Surgery*, vol. 45, no. 9, pp. 751–753, 1987.

[46] J. E. Bergsma, W. C. de Bruijn, F. R. Rozema, R. R. M. Bos, and G. Boering, "Late degradation tissue response to poly(L-lactide) bone plates and screws," *Biomaterials*, vol. 16, no. 1, pp. 25–31, 1995.

[47] R. R. M. Bos, F. B. Rozema, G. Boering et al., "Degradation of and tissue reaction to biodegradable poly(L-lactide) for use as internal fixation of fractures: a study in rats," *Biomaterials*, vol. 12, no. 1, pp. 32–36, 1991.

[48] P. Laine, R. Kontio, C. Lindqvist, and R. Suuronen, "Are there any complications with bioabsorbable fixation devices? A 10 year review in orthognathic surgery," *International Journal of Oral and Maxillofacial Surgery*, vol. 33, no. 3, pp. 240–244, 2004.

[49] J. E. Bergsma, F. R. Rozema, R. R. M. Bos, G. Boering, W. C. de Bruijn, and A. J. Pennings, "*In vivo* degradation and biocompatibility study of *in vitro* pre-degraded as-polymerized polylactide particles," *Biomaterials*, vol. 16, no. 4, pp. 267–274, 1995.

[50] P. Tormala, J. Vasenius, S. Vainionpaa, J. Laiho, T. Pohjonen, and P. Rokkanen, "Ultra-high-strength absorbable self-reinforced polyglycolide (SR-PGA) composite rods for internal fixation of bone fractures: in vitro and in vivo study," *Journal of Biomedical Materials Research*, vol. 25, no. 1, pp. 1–22, 1991.

[51] J. Düchting, *Chemische und mechanische Eigenschaften bioresorbierbarer Osteosyntheseplatten nach in-vitro Degradation [M.S. thesis]*, Department of Maxillofacial and Facial Plastic Surgery, University of Rostock, Rostock, Germany, 2008.

[52] J. C. Posnick and R. L. Ruiz, "Treacher Collins syndrome: current evaluation, treatment, and future directions," *Cleft Palate-Craniofacial Journal*, vol. 37, no. 5, p. 434, 2000.

[53] J. C. Posnick and R. L. Ruiz, "The craniofacial dysostosis syndromes: current surgical thinking and future directions," *Cleft Palate-Craniofacial Journal*, vol. 37, no. 5, p. 433, 2000.

[54] Y. Li, C. Wen, D. Mushahary et al., "Mg-Zr-Sr alloys as biodegradable implant materials," *Acta Biomaterialia*, vol. 8, no. 8, pp. 3177–3188, 2012.

[55] R. Smeets, K. Endres, G. Stockbrink et al., "The innovative application of a novel bone adhesive for facial fracture osteosynthesis—in vitro and in vivo results," *Journal of Biomedical Materials Research A*, vol. 101, no. 7, pp. 2058–2066, 2013.

[56] C. A. Landes and A. Ballon, "Indications and limitations in resorbable P(L70/30DL)LA osteosyntheses of displaced mandibular fractures in 4.5-year follow-up," *Plastic and Reconstructive Surgery*, vol. 117, no. 2, pp. 577–587, 2006.

[57] C. M. Agrawal and K. A. Athanasiou, "Technique to control pH in vicinity of biodegrading PLA-PGA implants," *Journal of Biomedical Materials Research*, vol. 38, no. 2, pp. 105–114, 1997.

[58] R. M. Felfel, I. Ahmed, A. J. Parsons, P. Haque, G. S. Walker, and C. D. Rudd, "Investigation of crystallinity, molecular weight change, and mechanical properties of PLA/PBG bioresorbable composites as bone fracture fixation plates," *Journal of Biomaterials Applications*, vol. 26, no. 7, pp. 765–789, 2012.

[59] N. A. Weir, F. J. Buchanan, J. F. Orr, D. F. Farrar, and G. R. Dickson, "Degradation of poly-L-lactide. Part 2: increased temperature accelerated degradation," *Proceedings of the Institution of Mechanical Engineers, Part H: Journal of Engineering in Medicine*, vol. 218, no. 5, pp. 321–330, 2004.

[60] Y. Shikinami and M. Okuno, "Bioresorbable devices made of forged composites of hydroxyapatite (HA) particles and poly-L-lactide (PLLA): part I. Basic characteristics," *Biomaterials*, vol. 20, no. 9, pp. 859–877, 1999.

Hindawi Publishing Corporation
BioMed Research International
Volume 2015, Article ID 324014, 15 pages
http://dx.doi.org/10.1155/2015/324014

*Research Article*

# Amniotic Mesenchymal Stem Cells Can Enhance Angiogenic Capacity via MMPs *In Vitro* and *In Vivo*

**Fei Jiang,[1,2] Jie Ma,[1,2] Yi Liang,[1,2] Yuming Niu,[3] Ning Chen,[1,2] and Ming Shen[1,2]**

[1] *Jiangsu Key Laboratory of Oral Diseases, Nanjing Medical University, No. 140, Han Zhong Road, Nanjing, Jiangsu 210029, China*
[2] *Department of Dental Implant, Affiliated Hospital of Stomatology, Nanjing Medical University, No. 140, Han Zhong Road, Nanjing, Jiangsu 210029, China*
[3] *Department of Stomatology, Taihe Hospital, Hubei University of Medicine, No. 32, Renmingnan Road, Shiyan, Hubei 442000, China*

Correspondence should be addressed to Ning Chen; cn_njmu@163.com and Ming Shen; mingshen85@yahoo.com

Received 5 October 2014; Revised 18 December 2014; Accepted 22 December 2014

Academic Editor: Kazuhisa Bessho



The aim of this study was to evaluate the angiogenic capacity and proteolytic mechanism of coculture using human amniotic mesenchymal stem cells (hAMSCs) with human umbilical vein endothelial cells (HUVECs) *in vivo* and *in vitro* by comparing to those of coculture using bone marrow mesenchymal stem cells with HUVEC. For the *in vivo* experiment, cells (HUVEC-monoculture, HUVEC-hAMSC coculture, and HUVEC-BMMSC coculture) were seeded in fibrin gels and injected subcutaneously in nude mice. The samples were collected on days 7 and 14 and histologically analyzed by H&E and CD31 staining. CD31-positive staining percentage and vessel-like structure (VLS) density were evaluated as quantitative parameters for angiogenesis. The increases of CD31-positive staining area and VLS density in both HUVEC-hAMSC group and HUVEC-BMMSC group were found between two time points, while obvious decline of those was observed in HUVEC-only group. For the *in vitro* experiment, we utilized the same 3D culture model to investigate the proteolytic mechanism related to capillary formation. Intensive vascular networks formed by HUVECs were associated with hAMSCs or BMMSCs and related to MMP2 and MMP9. In conclusion, hAMSCs shared similar capacity and proteolytic mechanism with BMMSCs on neovascularization.

## 1. Introduction

Bone defects remain a major clinical problem in patients' functional reconstruction and remodeling appearance. Bone tissue engineering and regenerative medicine based on stem cells combined with tissue-engineered scaffolds and cytokines have shown a promising potential in regenerating bone defects [1]. Bone is a vital organism that needs blood for material exchange to maintain normal metabolism. Typically, bone is supplied with an intraosseous vasculature with osteocytes at a distance of maximum 100 $\mu$m from an intact capillary [2]. However, only cells at the surface of cell-loaded grafts *in vivo* can obtain sufficient blood and nutrient supply to maintain their metabolism and function within a distance of 100–200 $\mu$m to the nearest capillaries while cells in the core of the grafts may die [3, 4]. Thus, angiogenesis is a key factor in regeneration medicine.

Therapeutic angiogenesis has been developed as a possible means to treat ischemic diseases via the delivery of proangiogenic molecules to promote neovascularization and tissue repair [5]. Although some strategies have been established to sustain delivery of proangiogenic factors or genes from biodegradable scaffolds [6, 7] and mimic the process of natural vessel development in some degree [8], vascularization *in vivo* triggered by complex proangiogenic signal network still cannot fully reappear by offering combinations of multiple factors. Cell-based therapies have also been explored to more completely mimic the cascade of signals needed to promote the formation of stable neovasculature [9]. A variety of cell types have been shown to form new capillary networks and/or induce collateral blood vessel development after implantation *in vivo* [10–12] and *in vitro* [13]. Their findings were consistent that codelivery of endothelial cells (ECs) and a secondary mesenchymal cell type (e.g., BMMSCs [14–16], AdSCs

[17, 18], NHLFs [19], and SMCs [20]) produces the necessary cues to induce tubular sprouting of ECs and stromal cell differentiation toward a pericytic phenotype [21].

The application of mesenchymal stem cells (MSCs) has drawn considerable research interest in bone tissue engineering and regenerative medicine relies on their characteristics of self-renewal and multidirectional differentiation. It has been established that MSCs could be isolated from several tissues, including bone marrow, peripheral blood, and adipose tissue [22]. Although MSCs obtained from these tissues show promising prospect, their application also shows some limitations, where the procedures required to obtain the above tissues are invasive, the number of MSCs obtained is low, and the potential to proliferate and differentiate diminishes as the donor's age increases [23]. Human term placenta has recently attracted wide attention as a valuable source of stem/progenitor cells. It is routinely discarded postpartum as biological waste and is easy to gain without invasive procedures and its use is free of ethical concerns [24].

It had been reported that amniotic membrane-derived mesenchymal stem cells (AMSCs) have potential of osteogenic, adipogenic, chondrogenic, and myogenic differentiation. In addition, Alviano et al. found AMSCs could differentiate into ECs by exposure to VEGF in angiogenic experiments [25]. AMSCs have the higher angiogenic and chemotactic properties compared to adipose tissue-derived MSCs (AdSCs) [26]. AMSCs implantation also augmented blood perfusion and increased intraneural vascularity [27]. However, regarding their angiogenic potential, hAMSCs had been isolated and induced by endothelial growth medium (EBM-2). Induced hAMSCs changed their some mesenchymal phenotype and showed EC-like behavior, but they did not express the mature EC markers [28]. Thus, these findings may support hAMSCs as stromal cells to enhance the viability, sprouting of ECs and promote vessel formation indirectly. In this study, we established 3D culture system to investigate the enhancement of vessel formation by hAMSC *in vivo* and *in vitro*.

## 2. Materials and Methods

*2.1. Cell Culture.* Bone marrow-derived mesenchymal stem cells (BMSCs, passage 2) were tested by the manufacturer (Cyagen Biosciences Inc., Guangzhou, China) for purity by flow cytometry and for their ability to differentiate into osteogenic, chondrogenic, and adipogenic lineages. Cells are positive for the cell surface markers CD105, CD166, CD29, and CD44 and negative for CD14, CD34, and CD45.

*2.2. Isolation and Culture of hAMSC.* Human term placentas and umbilical cords were harvested from normal pregnancies (range 38 to 41 weeks) after spontaneous delivery or cesarean section with informed consent. Approval of the Ethical Committee of Nanjing Medical University was granted. Isolation of hAMSC was performed following a previously established protocol [22]. Briefly, the decidua parietalis was removed by careful scraping. The amnions were cut into small pieces (2 ∗ 2 cm) and then manually separated and washed extensively in phosphate-buffered saline containing 100 U/mL penicillin and 100 $\mu$g/mL streptomycin (Beyotime, China). Amnion fragments were incubated for 7 min at 37°C in PBS containing 2.4 U/mL dispase (Roche, Mannheim, Germany). The incubated fragments were transferred to $\alpha$-MEM (GIBCO, USA) supplemented with 10% heat-inactivated fetal bovine serum (FBS; GIBCO, USA) for resting 5–10 min at room temperature. After the resting period, the fragments were digested with 0.75 mg/mL collagenase (Roche) and 20 $\mu$g/mL DNAse (Roche) for approximately 3 h at 37°C. Amnion fragments were then removed and mobilized cells were passed through a 100 $\mu$m cell strainer (BD Falcon, Bedford, MA) and the cells were collected by centrifugation at 200 ×g for 10 min. The cells were cultured in $\alpha$-MEM and used before passage 10.

*2.3. Isolation and Culture of HUVEC.* Human umbilical vein endothelial cells (HUVECs) were harvested from fresh umbilical cords following a previously established protocol [14]. Fresh umbilical veins were digested with 0.1% (w/v) collagenase type 1A solution at 37°C for 15 min to release endothelial cells from the vessel walls. And then, the vessels incubated with collagenase type 1A were rinsed with ECM (ScienCell, San Diego, USA); HUVECs were collected by centrifugation at 1000 rpm for 5 min and cultured in ECM. HUVECs were used at passage 3.

*2.4. Flow Cytometry.* To evaluate cell-surface marker expression, the samples were analysed on a FACSCalibur cytometer and the resulting data were processed using CellQuest software (BD Biosciences). The cell suspensions were incubated for 20 min at 4°C with fluorescein isothiocyanate- (FITC-) or phycoerythrin- (PE-) conjugated monoclonal antibodies specific for human markers associated with mesenchymal and haematopoietic lineages. The antibodies used were CD29(FITC), CD34(FITC), CD44(FITC), CD45(FITC), CD73(PE), CD90(PE), CD105(PE), and HLA-DR(PE) (all from Miltenyi Biotec, Bergisch Gladbach, Germany).

*2.5. Tissue-Construct Implantation.* Animal procedures were performed in accordance with the guidelines for laboratory animal usage following a protocol approved by the Nanjing Medical University's Committee on Use and Care of Animals.

The course of implantation was performed following a previously established protocol [9]. Male 8-week-old BALB/c-nu mice (Jiangsu Provincial Experimental Animal Base for Medicine and Pharmacy) were used for all experiments. Chloral hydrate was delivered to each mouse via intraperitoneal injection before implant injection. In this study, a 2.5 mg/mL plasminogen-depleted human fibrinogen (Sigma-Aldrich, USA) was made in serum-free ECM and filtered through a 0.22 $\mu$m syringe filter. Cell mixtures in a 1 : 1 ratio of EC : MSCs (hAMSCs or BMMSCs) were spun down and resuspended in the previously prepared fibrinogen solution at a final concentration of 10 million cells/mL, totaling $3\times 10^6$ cells per injection sample (300 mL total volume). Immediately before injection, 12 $\mu$L of thrombin solution (25 U/mL; Sigma-Aldrich, USA) was added to 300 $\mu$L of fibrinogen-cell solution. For control samples, 3 million ECs without any stromal cell type were used. Solutions were immediately

injected subcutaneously on the dorsal flank of the mouse, with two implants per animal. Animals were kept stationary for 5 min to allow for implant polymerization and were then placed in fresh cages for recovery. Three replicates of each sample type were completed (HUVEC-hAMSC, HUVEC-BMMSC, and HUVEC-only).

*2.6. Histology and Immunohistochemistry.* For histology and immunohistochemical staining, explants were fixed in formalin overnight and then transferred to a PBS, pH 7.4, solution, all at 4°C. All samples were embedded in paraffin and then sectioned in 5 $\mu$m sections and stained with hematoxylin and eosin (H&E) and immunohistochemically (hCD31). HE staining was performed according to a standard protocol from pathology department of Nanjing Medical University. For CD31 staining, paraffin sections were rehydrated in serials of ethanol and antigen was retrieved by heating the slides in sodium citrate buffer (PH 6.0) at 97°C for 15 min. Subsequently, blocking was carried out using 5% BSA, and the primary antibody (rabbit anti-human CD31, Abcam, USA) was diluted 1 : 100 in PBS and incubated at 4°C overnight. Slides were then treated with a peroxidase-conjugated AffiniPure goat anti-rabbit IgG (ZSGB-BIO, China) at 1 : 500 for 1 h at room temperature, followed by counterstaining with hematoxylin. Negative controls using PBS instead of the primary antibody were generated in parallel to ensure that the staining was specific. Finally, the sections were dehydrated and mounted. Stained sections were photographed with a Zeiss Imager Z1 microscope equipped with the AxioCam MRc5 camera using AxioVision 4.8 software (Carl Zeiss Microimaging GmbH, Göttingen, Germany).

*2.7. Histomorphometrical Evaluation.* For *in vivo* samples, histomorphometrical analysis was performed to evaluate the angiogenic capacity of three groups (HUVEC-only, HUVEC-hAMSC, and HUVEC-BMMSC) based on hCD31 staining ($n = 3$ per sample) [29]. In brief, the sections were scored using computer-based image analysis techniques (Leica Qwin Proimage analysis system, Wetzlar, Germany), which recognize human endothelial marker (hCD31, stained as brown) within the collagen gels based on different RGB values from highly magnified (200x) digitalized images. Manual corrections were applied to ensure the precise selection of hCD31 staining positive parts within the region of interest (ROI, i.e., the total scaffold area). For the evaluation, VLS (from human origin) were defined by the presence of hCD31 positive (evidenced by hCD31 positive staining) structures with lumens and VLS density: VLS number/ROI ($mm^2$).

*2.8. 3D Fibrin Vasculogenic Assays.* Fibrin gels were prepared using plasminogen-depleted human fibrinogen in serum-free ECGM at a concentration of 2.5 mg/mL and filtered for sterility. HUVEC was labeled GFP by using lentivirus before this assay. Cells mixtures in ratios of 5 : 1 of GFP-HUVECs : MSCs (hAMSCs or BMMSCs) were resuspended in prepared fibrinogen solution [30], totaling $2 \times 10^4$ GFP-HUVECs and $0.4 \times 10^4$ stromal cells per well of 96-well plate (100 $\mu$L total volume per well). For control samples, $2.4 \times 10^4$ GFP-HUVECs were resuspended in prepared fibrinogen solution (100 $\mu$L total volume per well). 3 $\mu$L of thrombin solution (25 U/mL; Sigma-Aldrich) was added to 100 $\mu$L of fibrinogen-cell solution to catalyze the fibrinogen gel. Prior to fibrin polymerization, the plates were gently tapped on all four edges to assure that the fibrin gel is equally distributed throughout the well. After 30 minutes of incubation at 37°C, gels were fed with 100 $\mu$L ECGM. Medium (ECM, ScienCell, USA) was changed at day 3. For studies involving MMPs inhibitor, GM6001 (Calbiochem, San Diego, USA) was added to fibrin gels at final concentration 10 $\mu$M. Each group set up 3 repeats. Fluorescent images were captured using a fluorescence inverted microscope (Leica) at 0 h, 12 h, 24 h, 48 h, 72 h, and 96 h, each repeat in 3 random sights being selected to quantitate EC tube area during the morphogenic process by analysis software Image J.

*2.9. 3D Cell Cluster Formation Assay.* To examine the proteolytic function of MSCs in coculture system, we compared MMPs expression in 3D clusters of 3 groups (HUVEC-only, HUVEC-hAMSC, and HUVEC-BMMSCs) *in vitro* after culturing for three days. Fibrin gels were prepared using plasminogen-depleted human fibrinogen in serum-free $\alpha$-MEM at a concentration of 2.5 mg/mL and filtered for sterility. The cell density of seeding and the volume of fibrin gels were just like *in vivo* experiment. 12 $\mu$L of thrombin solution (25 U/mL; Sigma-Aldrich) was added to 300 $\mu$L of fibrinogen-cell solution to catalyze the fibrinogen gel. After 30 minutes of incubation at 37°C, the gels were transferred from centrifuge tube to culture dish and fed with 5 mL complete $\alpha$-MEM. For 72 h culture, the cell clusters were collected to measure diameter and extracted total protein. The corresponding control groups with 3D cell clusters were fibrin gels without cells.

*2.10. Western Blotting.* Total protein was extracted from cells using lysis buffer (Beyotime, China). Coomassie Brilliant Blue was used to quantify the protein content. The proteins (10 $\mu$g) were resolved using sodium dodecyl sulfate-polyacrylamide gel electrophoresis (SDS-PAGE) with 10% polyacrylamide gels and then transferred to polyvinylidene difluoride (PVDF) membranes (Millipore, Billerica, MA, USA), which were blocked with 5% nonfat milk in phosphate-buffered saline (PBS) containing Tween-20 (PBS-T) for 2 h at room temperature. The blots were then probed with primary antibodies specific for MMP2 (1 : 100, Boster, China), MMP9 (1 : 100, Boster, China), and $\beta$-actin (1 : 1000; Bioworld, USA) overnight at 4°C, washed twice with PBST, and incubated with horseradish peroxidase-conjugated (HRP) secondary antibodies for 1 h at room temperature. Finally, the protein bands were detected by Immobilon Western Chemiluminescent HRP Substrate (Millipore) and visualized using the ImageQuantLAS 4000 mini imaging system (General Electrics, USA). Three independent trials of each experiment were carried out.

*2.11. Statistical Analyses.* All the quantitative results were obtained from triplicate samples. Data are expressed as mean ± standard deviation. Statistical analysis was carried out by use of two-sample $t$-test for comparing two groups of

samples and one-way analysis of variance (ANOVA) for three groups. A value of $P < 0.05$ was considered to be statistically significant.

## 3. Results

*3.1. Identification of hAMSCs and HUVECs.* After 2 days in culture, hAMSCs displayed fibroblastic morphology (Figure 1(a)), which was similar to that observed in BMMSCs, and HUVEC displayed cobblestone-like morphology (Figure 1(b)). Surface markers of hAMSCs and HUVECs were evaluated by flow cytometry analysis at passage 2, respectively. It has been shown that hAMSCs were positive for MSC markers, such as CD29, CD44, CD73, CD90, and CD105, while negative for hematopoietic and vascular cell-related markers, such as CD45, CD34, and MHC class II antigen, such as HLA-DR (Figures 1(c)–1(h)). HUVECs were positive for CD34 and negative for CD45 (Figures 1(l) and 1(m)). Further identification of HUVECs was confirmed by immunofluorescence staining of vWF and CD31 (Figures 1(i) and 1(j)).

*3.2. Histomorphometry of Implants In Vivo.* The implants on the dorsal flank of the nude mice were collected at day 7 and day 14 (Figure 2). Images of the H&E-stained day-7 and day-14 implants showed differences on quantity, distribution, and morphology of the vessels formed in the various experimental groups. Stained sections from the day-7 implants contained vessel-like structures (VLS) in the outer layer, but these structures lacked in the inner one, and the implants contained obvious extravascular erythrocytes (Figures 3(g), 3(h), and 3(i)). Moreover, more vessel-like structures can be found within stained sections from the day-14 implants (Figures 3(w) and 3(x)). The vessel-like structures of HUVEC-only implants lacked consistent, circumscribed geometry, while the cells remained in the fibrin by day 14, and there were few capillary structures. By contrast, implants containing the MSCs (hAMSCs or BMMSCs) displayed clearly different tendency in images of the H&E-stained day-7 and day-14 implants. The samples in day-7 implants also contained many vessel-like structures in the outer layer and some atypical capillary structures, and many small capillaries with very well-defined lumens and circumscribed borders were investigated not only in outer layer but also in the center of the samples in day-14 implants. It was obvious that implants containing the MSCs had more capillary structures in the center compared with HUVEC-only implants. These capillaries were distributed throughout the entire implant to produce a vascularized implant containing both large and small blood vessels to effectively supply the tissue with oxygenated blood.

To verify the results from the H&E-stained sections, immunohistochemical staining for human CD31 was used to confirm the human origins of the neovascularization. In the implants of HUVECs-only group, there was a diffuse brown stain indicating an abundance of HUVECs and some lumen-like structures in the outer area of implants at days 7 and 14 (Figure 3). By contrast, the HUVEC-hAMSC and HUVEC-BMMSC implants contained many smaller, tightly sealed capillaries in the inner as well as outer layer, consistent with the observations from H&E staining. Quantification of the angiogenic capacity of three groups is presented in Figures 3(y) and 3(z). Both the comparison between the three groups and differences in angiogenesis over time (i.e., day 7 versus day 14) were evaluated. The increase of CD31-positive stained area was found in the comparison between the two types of cocultures at the two time points, but a significant decrease was found in HUVEC-only group. With regard to VLS density, VLS density of both HUVEC-hAMSC group and HUVEC-BMMSC group at day 14 was obviously higher than that at day 7. In addition, a significant decrease in VLS density was observed for HUVEC-only group between two time points.

*3.3. Development of HUVEC Tube Formation under Serum-Free 3D Fibrin Matrices.* According to the results of experiment *in vivo*, we used a system [30] in which vascular tube morphogenesis and pericyte recruitment occurred in 3D fibrin matrices under serum-free defined conditions and using 96-well plates to observe the development of capillary tubes and the function of MSCs as pericyte. In this assay, HUVECs were labeled with GFP prior to 3D culture set-up and monocultured or cocultured with MSCs in 3D fibrin gels. Cultures were established at a 4 : 1 HUVEC : MSC ratio and were imaged using inverted fluorescence microscopy at six timepoints (i.e., 0 h, 12 h, 24 h, 48 h, 72 h, and 96 h) (Figure 4). HUVECs invaded extracellular matrix as early as 12 h and formed obvious sprouting by 48 h, but the processes of HUVEC tube formation and sprouting seemed to be limited without MSCs in 3D matrices. By contrast, extensive and increasing vascular networks were observed in both coculture conditions (HUVEC-hAMSC and HUVEC-BMMSC) from 24 h to 96 h. In the light sight that was same as the fluorescent sight, networks were more intensive in coculture conditions, while no network was investigated, and just ECs-sprouting in HUVEC-monoculture during the observation. Lumen-like structures rounded by HUVECs were detected at 96 h timepoint in two coculture systems (Figures 4(l) and 4(r)). To compare fluorescence sight with light sight, there were intensive networks comprised of MSCs surrounding the lumen-like structures. The phenotype might indicate that hAMSCs had equal capacity with BMMSCs to enhance HUVEC-sprouting and vascular networks forming, and MSCs had especially important meaning to stabilize the networks.

Localized proteolytic activity is necessary to facilitate key steps of the angiogenic cascade [31, 32]. Matrix metalloproteinases (MMPs) serve a purpose in regulating capillary diameter and possibly in stabilizing the nascent vessels [17]. These proteolytic mechanisms are involved in fibroblast-mediated angiogenesis and in BMMSC-mediated angiogenesis [15]. To test the proteolytic mechanisms related to hAMSC-mediated angiogenesis, 3D culture system was treated with the broad-spectrum MMP inhibitor GM6001. As shown in Figure 5, broad scale inhibition of MMPs had significant effect on HUVECs tube formation and sprouting. In HUVEC-only with GM6001, there was no obvious HUVECs-sprouting at several time points. HUVECs-sprouting of HUVEC-MSC coculture with GM6001 increased slightly, but still significantly less than the coculture without GM6001.

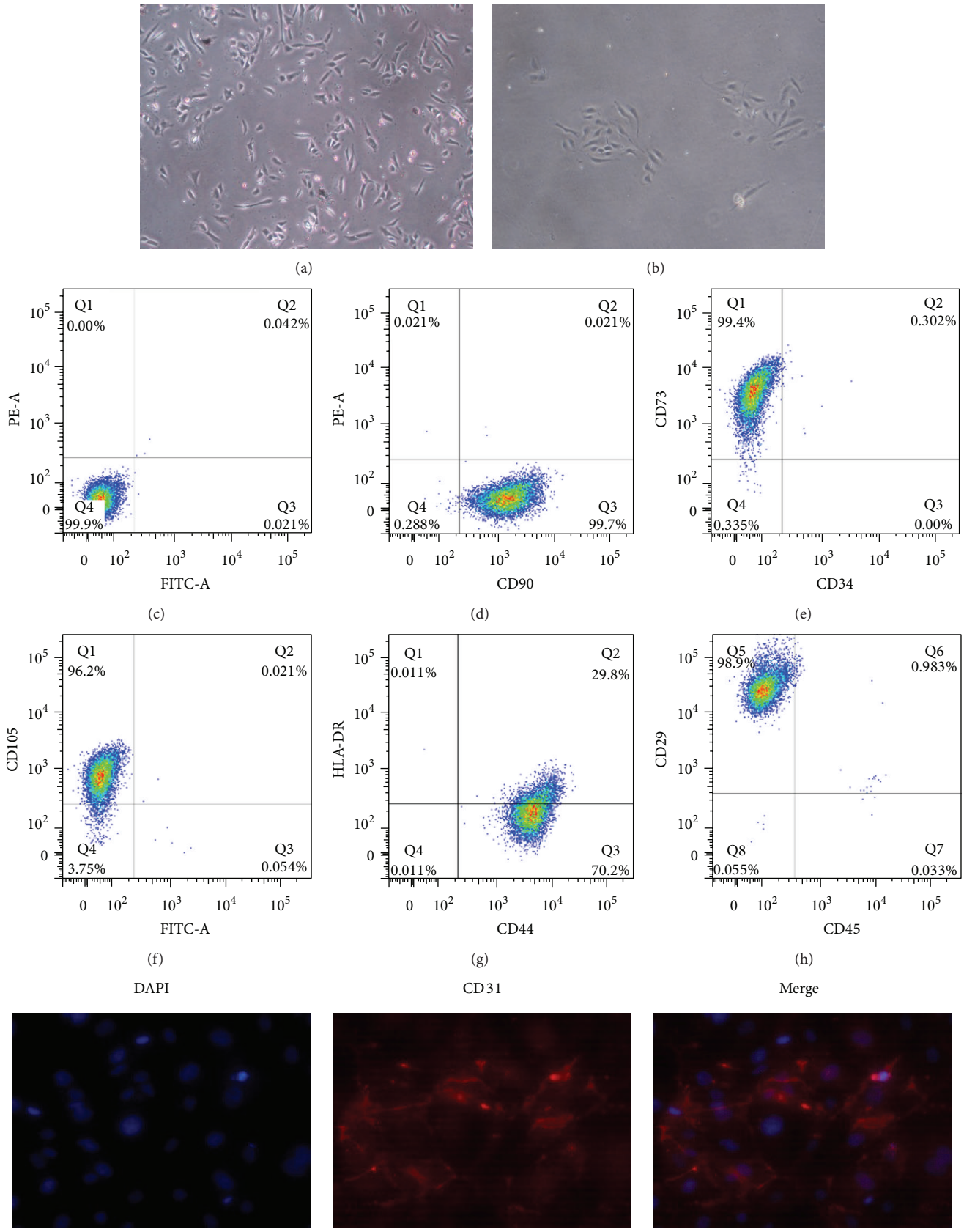


Figure 1: Continued.

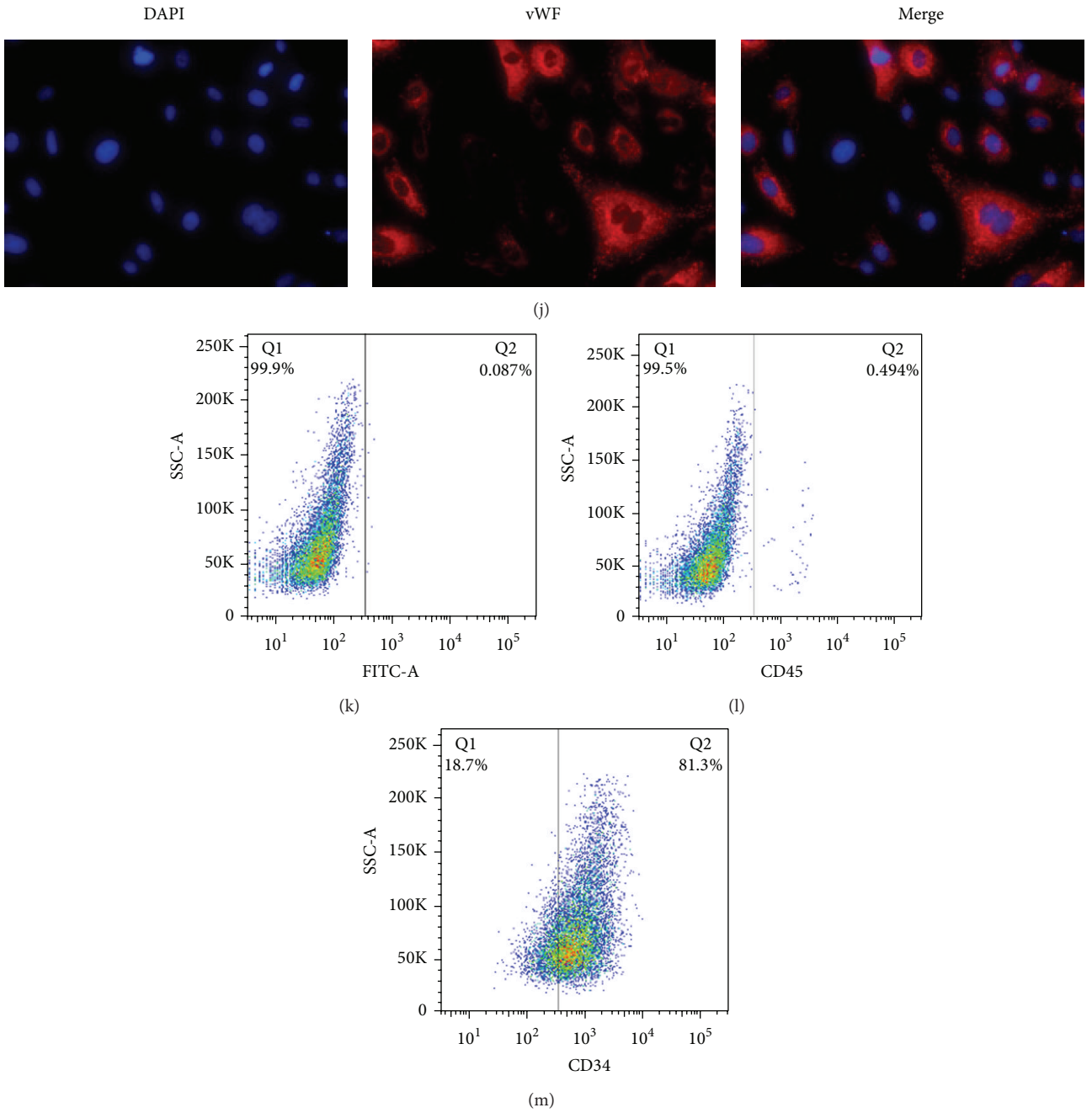


Figure 1: Identification of hAMSCs and HUVEC. Microscopic view (40*) of hAMSCs at P0 (a). Microscopic view (40*) of HUVECs at P0 (b). Surface marker analysis of freshly isolated hAMSCs by flow cytometry (c–h). The hAMSCs were positive for CD29, CD44, CD73, CD90, and CD105, while negative for CD45, CD34, and HLA-DR. Figure 1(c) acted as negative control for Figures 1(d), 1(e), 1(f), 1(g), and 1(h). The isolated HUVECs expressed CD31 on membrane surface and vWF in cytoplasm (i and j), while they were positive for CD34 and negative for CD45 (m and l). Figure 1(k) acted as negative control for Figures 1(l) and 1(m).

Interestingly, although the processes of HUVEC tube formation and sprouting were inhibited, the networks formed by MSCs still existed. These phenotypes might suggest the proteolytic mechanism related to hAMSC-mediated angiogenesis was similar to that related to BMMSC, and, on the other hand, stabilization of vascular networks supported by MSCs might be to form MSC networks.

*3.4. MMPs Expression of 3D Cell Clusters.* As shown in Figure 4, ECs cultured in the absence of MSCs do not form capillary-like structures in fibrin gels, but intensive networks and lumen-like structures were observed in both HUVEC-hAMSC and HUVEC-BMMSC cocultures. With regard to BMMSC-mediated proteolytic mechanisms, MMPs play a key role in resolving extracellular matrix and promoting

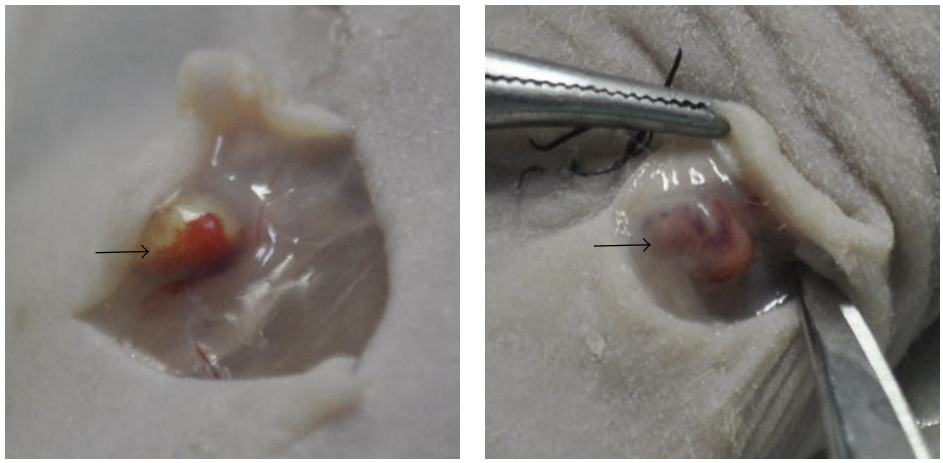

(a) (b)

Figure 2: Explantation of *in vivo* implants on day 7 and day 14. (a) Harvesting on day 7. (b) Harvesting on day 14. Arrows show the vessel surrounding or penetrating inside the implants.

HUVEC-sprouting. To study the function of MSCs in 3D coculture condition, we observed the 3D clusters of 3 groups (HUVEC-only, HUVEC-hAMSC, and HUVEC-BMMSCs) *in vitro* after culturing for three days in $\alpha$-MEM. At day 3, the samples of the gels shrunk in different degree, but the gels containing MSCs shrunk more significantly as shown in Figure 6. There was no change in gels without cells by 3-day culture. On the other hand, the results of Western blotting showed that the expression of active-MMP2 in HUVEC-hAMSC and HUVEC-BMMSC was about 4-fold more than that in HUVEC-only, while the expression of secreted MMP2 in HUVEC-hAMSC and HUVEC-BMMSC was about 5-fold more than that in HUVEC-only. The similar trend was shown in expression of MMP9 among three groups (Figure 7).

## 4. Discussion

In this study, we investigated the angiogenic capacity of hAMSC/HUVEC coculture and the function of hAMSC on proteolytic mechanisms both *in vivo* and *in vitro*. Firstly, we demonstrated that hAMSC/HUVEC coculture shared equal angiogenic capacity with BMMSC/HUVEC coculture *in vivo*. Secondly, it was similar to BMMSCs that hAMSCs could enhance the processes of HUVEC tube formation and sprouting *in vitro*. Thirdly, MMPs were found in hAMSC-mediated proteolytic mechanism shared with BMMSC-mediated proteolytic processes. Fourthly, MMPs expression levels of hAMSCs could be elevated significantly in 3D culture condition.

Mesenchymal stem cells were identified in human postnatal bone marrow (BM) and later in peripheral blood, periosteum, muscle, adipose tissue, and connective tissue of human adults [33–37]. Traditional source of MSCs for clinical investigations is BM. Extensive studies of BM-derived MSCs (BMMSCs) have proven their multipotent differentiation potential and powerful immunosuppressive qualities [38]. However, the collection of BM is associated with invasive procedures involving significant discomfort to the patient. Moreover, it results in a relatively low amount of MSCs (approximately 0.001–0.01% of all isolated nuclear cells) in adult human BM, and the number of cells decreases with donor's age [39]. Besides, ethics problems are also the important aspect of restricting its application. Because there are no ethical problems involved, using hAMSCs as an allogeneic stem cell source should be highly beneficial. They can be collected easily, have multipotential capacity, and express only low levels of the major histocompatibility complex (MHC) class I antigens and be negative for MHC class II antigens on their surface [40]. The MHC expression of BMMSCs can be induced by treating with interferon-$\gamma$, but that of hAMSCs is much lower than BMMSCs [41, 42]. For several years, BMMSCs have been considered as immune privileged cells, unable to induce alloreactivity in humans. However, more recently it has been demonstrated that donor-derived MSCs are immunogenic in an allogeneic host and stimulate graft rejection in a murine model of submyeloablative allogeneic BM transplantation [43]. Immunogenicity of hAMSCs seems to be better than that of BMMSCs. Like BMMSCs, hAMSCs can adhere and proliferate on tissue culture plastic, present fibroblast-like appearance, form clonal colonies, and express the typical range of BMMSC associated cell surface markers, such as CD29, CD44, CD49e, CD73, CD90, and CD105, while being negative for hematopoietic and vascular cell-related markers, such as CD45, CD34 [44]. Regarding HUVEC, it has been well-known that von Willebrand Factor (vWF), platelet-endothelial adhesion molecule-1 (PECAM-1; CD31), and CD34 are specific markers for endothelial cells [45, 46] and negative for human CD45, a tyrosine phosphatase also known as the leukocyte common antigen (LCA). The CD45 molecule is required for T and B cell activation and is expressed in at least five isoforms depending on the differentiation status of the cell. In the present study, identification of isolated hAMSCs and HUVECs was consistent with the conclusion published previously.

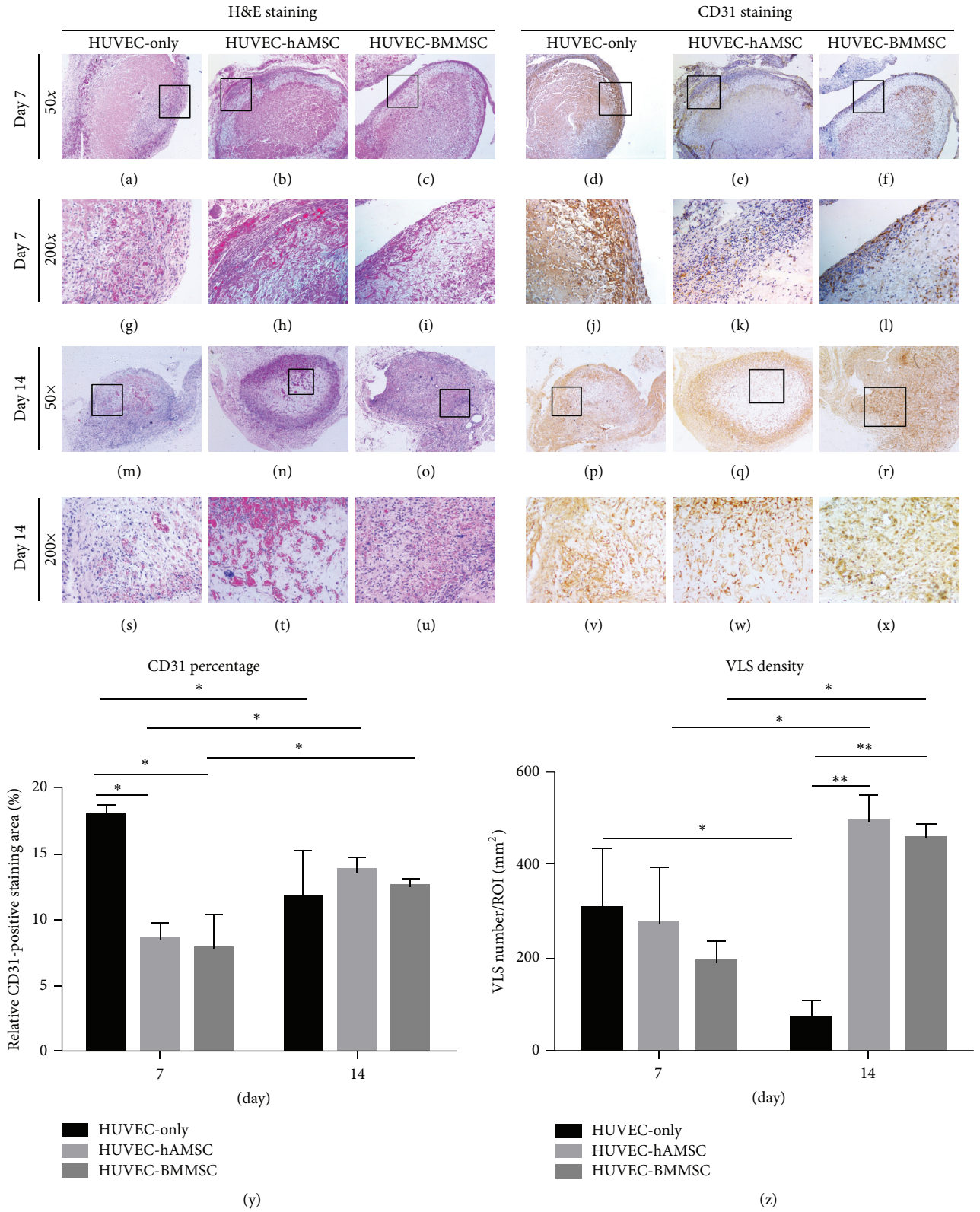


Figure 3: Histomorphometry of implants *in vivo*. H&E and CD31 staining illustrated varying blood vessel morphologies in implants in microscopic view (50* and 200*). Stained sections from the day-7 implants contained vessel-like structures (VLS) in the outer layer. Vessel-like structures (VLS) can be found within stained sections from the day-14 implants. Quantification of the angiogenic capacity of HUVEC-only, HUVEC-hAMSC, and HUVEC-BMMSC is presented by CD31 percentage and VLS density (y and z).

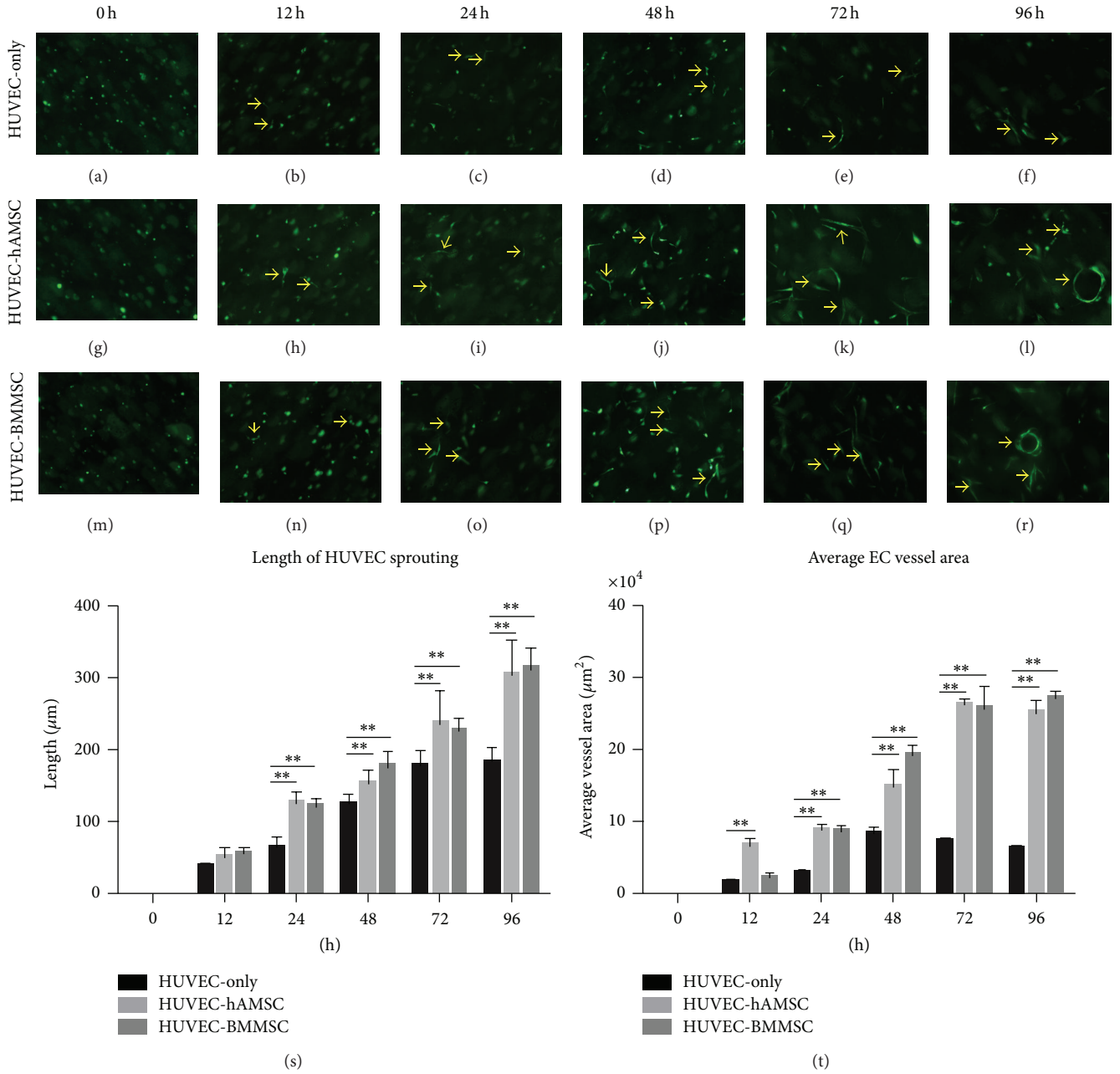


FIGURE 4: Development of HUVEC tube formation under serum-free 3D fibrin matrices. HUVECs were labeled with GFP and cocultured with MSCs (hAMSCs and BMMSCs). HUVEC-sprouting could be found as early as 12 h (indicated by arrows) and obviously at 48 h (indicated by arrows). Lumen-like structures rounded by HUVECs were indicated by arrows in (l) and (r). Microscopic view is 200*. The length of HUVEC-sprouting and average EC vessel area were showed in (s) and (t).

A number of studies have demonstrated that the direct contact and communication between ECs and pericyte-like cells are essential for vascularization [47, 48]. AdMSCs can secrete a broad range of paracrine factors that are known to be angiogenic, similar to BMMSCs [49]. Human umbilical vein endothelial cells (HUVECs) are the most commonly used type of human endothelial cells (ECs) for both *in vitro* and *in vivo* studies for bone regenerative medicine [50]. Both BMMSCs and AdMSCs can play an active role in the formation, stabilization, and maturation of newly formed VLS [51, 52] and share equal angiogenic capacity both *in vitro* and *in vivo*, and vessels from donor origin can anastomose with the host vasculature within seven days of implantation [29]. Thus, it was hypothesized that hAMSCs also had similar function like BMMSCs and AdMSCs on neovascularization. In this study, cells were cultured in direct contact according to HUVECs : MSCs as 1 : 1 ratio *in vivo* [9, 29]; the angiogenic capacities of HUVEC-only, HUVECs-hAMSCs, and HUVEC-BMMSCs were examined at two time points (i.e., day 7 and day 14) by H&E and hCD31 staining.

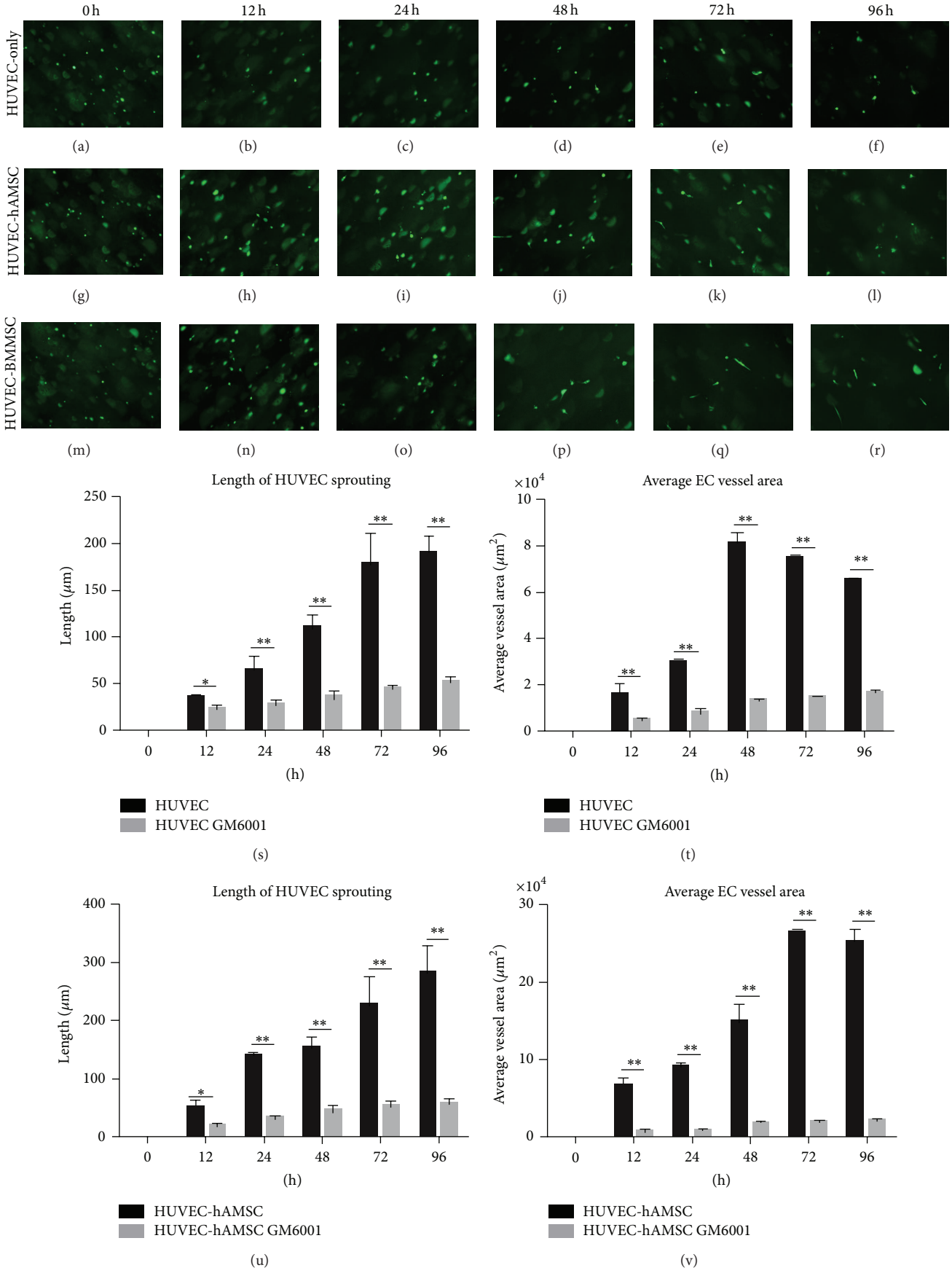


Figure 5: Continued.

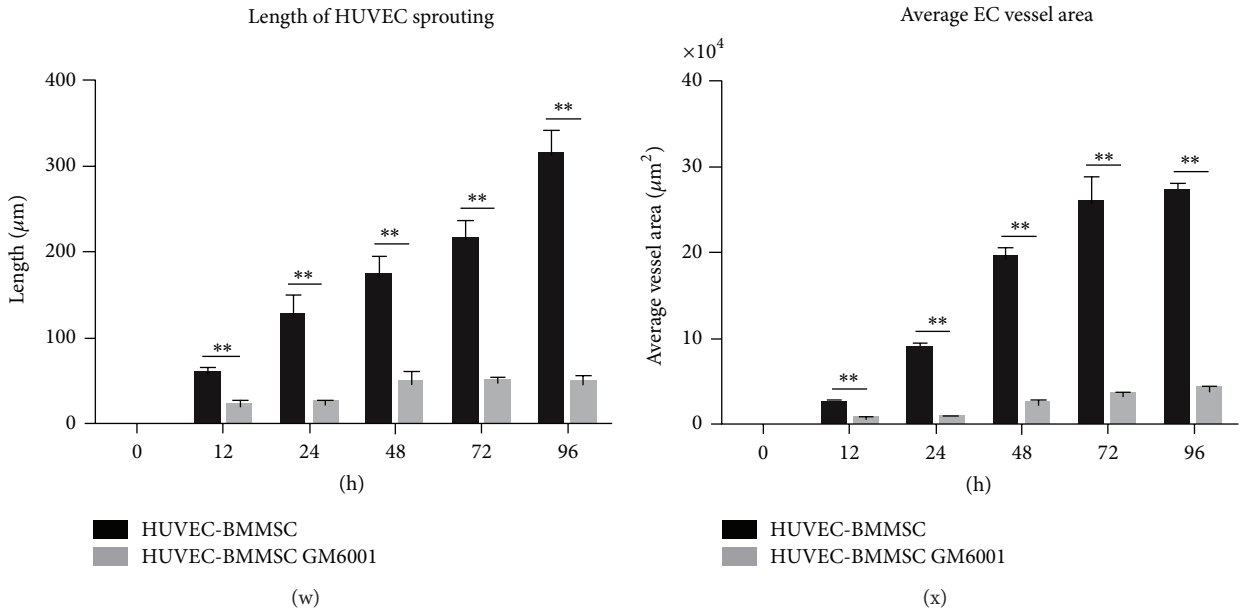


Figure 5: Inhibitory effect of MMPs in HUVEC tube formation under serum-free 3D fibrin matrices. HUVEC-sprouting had been inhibited significantly across all timepoints (a–r). Microscopic view is 200*. The length of HUVEC-sprouting and average EC vessel area were decreased remarkably (s–x). There was no significant difference among three groups.

The implants containing HUVECs alone appeared to yield greater numbers of vessel-like structures initially, but these vessels were unstable in the absence of a codelivered stromal cell. One of possible reasons was that vessels cannot be formed by HUVEC alone; pericytes provided the essential support for HUVECs to construct and stabilize newly formed vessels. Moreover, many lumen-like structures in the interior of implants of both HUVECs-hAMSCs groups and HUVEC-BMMSCs groups might reflect the function of hAMSCs on angiogenic process *in vivo* was similar to BMMSCs that MSCs as pericytes played an auxiliary role on helping HUVECs to degrade extracellular matrix and form mature capillaries.

To further detect the mechanism of hAMSC on angiogenic process, HUVEC-monoculture and HUVEC-MSCs cocultures were set up *in vitro*. hAMSCs cultured in endothelial induction conditions showed upregulation of antiangiogenic and concomitant downregulation of proangiogenic genes and proteins to protect themselves against differentiating into mature endothelial cells; however, the conditioned media of induced hAMSC had a positive effect on endothelial cells as shown by enhanced viability and stabilized network formation [28]. These results are consistent with studies showing that BMMSCs promote angiogenesis and support blood vessel formation [51, 53, 54]. In the present study, we seeded cells in the fibrin gels prepared with endothelial cell growth medium, which contained a variety of endothelial cell growth factors, and showed that hAMSC and BMMSC could constitute intensive and stable network to have a positive effect on vascular network in endothelial induction condition. On the other hand, it has been well-established that MMPs or/and the PA/plasmin axis play important roles in EC invasion during capillary morphogenesis; however, different pericyte types influence the proteolytic ways via different mechanisms. BMMSC-mediated proteolytic mechanisms had been demonstrated to be solely related to MMPs [15]. In our present work, we utilized coculture model treated or not treated with GM6001 to imitate early phrase of angiogenesis *in vitro* to demonstrate that both hAMSCs and BMMSCs stimulate capillary morphogenesis within 3D fibrin ECMs and seem to do via same proteolytic mechanism. The similar behavior of HUVEC-hAMSC and HUVEC-BMMSCs cocultures treated or not treated with GM6001 in fluorescence field and expression of MMP2 and MMP9 in coculture gels might suggest that hAMSC-mediated angiogenesis was related to MMPs, just like BMMSC-mediated angiogenesis mechanisms.

With the hope of future clinical application, there are many researches concentrating on stem cells from different sources. Stem cells are undifferentiated cells that are found in the embryonic, fetal, and adult stages of life and have become a novel hope in cell-based therapy [55, 56]. Stem cells from amniotic fluid (AF) and amniotic membrane (AM) can be used in clinical therapeutic applications without ethical limitations in the future [57]. This study demonstrated that hAMSC and BMSCs as pericytes sharing equal ability of enhancing angiogenesis via MMPs that impact the functional qualities of the capillary networks both *in vitro* and *in vivo* and stabilized new capillaries branch during the early stage. On the other hand, hAMSCs can secrete cytokines engaged in angiogenesis, osteogenesis, and anti-inflammation, such as VEGF [40], TGF-$\beta$ [58], PGE2 [58], IL-1 receptor agonist [59], and IL-10 [59]. Moreover, bone morphogenetic proteins (BMPs), the members of TGF-$\beta$ superfamily, are highly

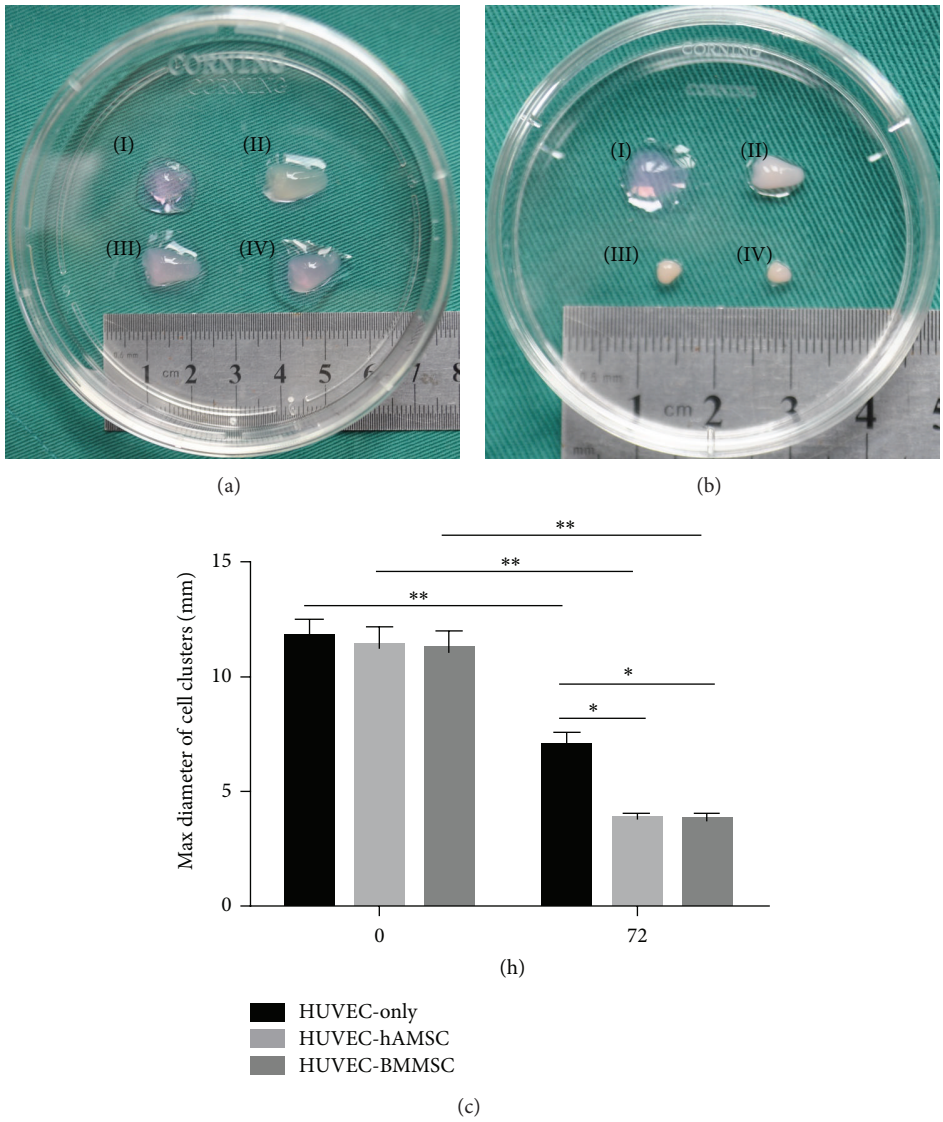


Figure 6: 3D cluster *in vitro*. (a) Prepared 3D clusters. Fibrin gel without cells (I), 3D cluster of HUVEC-only (II), 3D cluster of HUVEC-hAMSC (III), and 3D cluster of HUVEC-BMMSC (IV); (b) 3D clusters after culturing 3 days in $\alpha$-MEM. Fibrin gel without cells (I), 3D cluster of HUVEC-only (II), 3D cluster of HUVEC-hAMSC (III), and 3D cluster of HUVEC-BMMSC (IV). (c) Max diameter of cell clusters. This experiment was repeated three times and a representative sample was shown.

conserved signaling molecules that have been well-established for the function in the patterning and morphogenesis of many organs including bone regeneration [60]. It is thus conceivable that the positive effect of hAMSCs in angiogenesis should have a profound meaning in bone tissue regeneration and other clinic applications, even though many challenges should be conquered.

In conclusion, hAMSCs might be as valuable as BMMSC in a variety of cell-therapeutic and tissue engineering applications since they could promote the survival of endothelial cells and the stabilization of vascular networks. In future studies, the more effect and significance of hAMSC on tissue engineering should be investigated more comprehensively and in-depth.

## Conflict of Interests

The authors declare that there is no conflict of interests regarding the publication of this paper.

## Authors' Contribution

Fei Jiang and Jie Ma contributed equally to this work.

## Acknowledgments

This study was supported in part by the National Basic Research Program of China (2012CB966902), the National Natural Science Foundation of China (81271109), and The

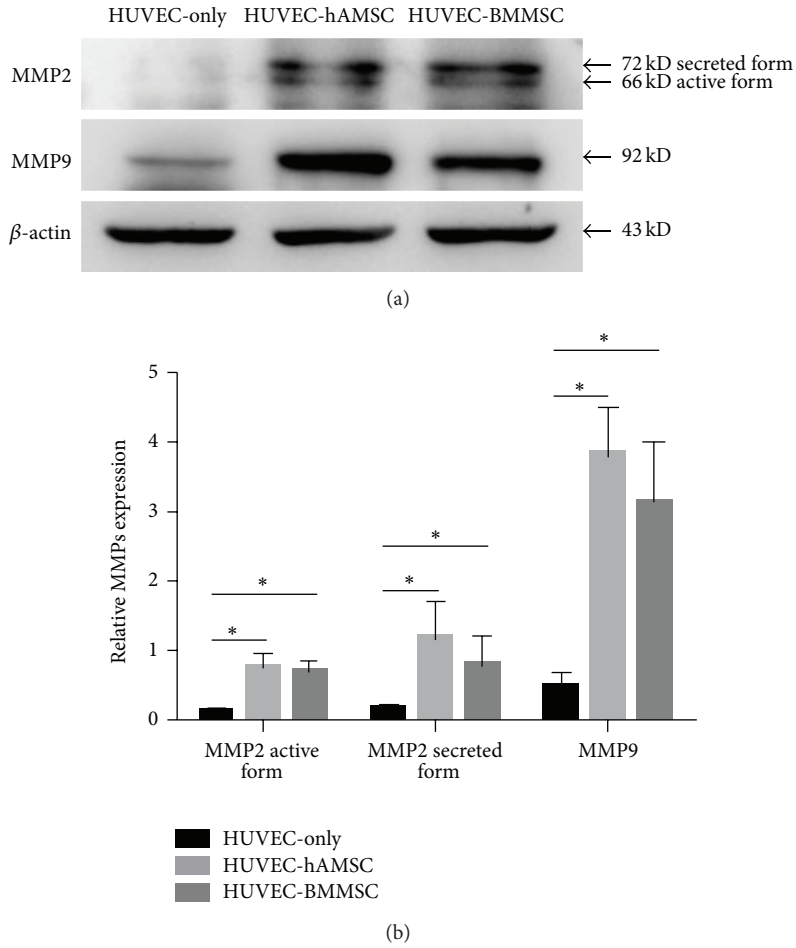


Figure 7: MMP2, MMP9 expression in 3D clusters. The MMP2, MMP9 and $\beta$-actin (internal control) expression in HUVEC-only clusters, HUVEC-hAMSC clusters, and HUVEC-BMMSC clusters were probed via Western blotting (day 3). This experiment was repeated three times and a representative sample was shown (a). The relative expression of MMPs was analyzed (b).

Project Funded by the Priority Academic Program Development of Jiangsu Higher Education Institutions (PAPD, 2014-37).

## References

[1] H. Petite, V. Viateau, W. Bensaïd et al., "Tissue-engineered bone regeneration," *Nature Biotechnology*, vol. 18, no. 9, pp. 959–963, 2000.

[2] M. I. Santos and R. L. Reis, "Vascularization in bone tissue engineering: physiology, current strategies, major hurdles and future challenges," *Macromolecular Bioscience*, vol. 10, no. 1, pp. 12–27, 2010.

[3] E. C. Novosel, C. Kleinhans, and P. J. Kluger, "Vascularization is the key challenge in tissue engineering," *Advanced Drug Delivery Reviews*, vol. 63, no. 4-5, pp. 300–311, 2011.

[4] M. Lovett, K. Lee, A. Edwards, and D. L. Kaplan, "Vascularization strategies for tissue engineering," *Tissue Engineering, Part B: Reviews*, vol. 15, no. 3, pp. 353–370, 2009.

[5] N. Ferrara and K. Alitalo, "Clinical applications of angiogenic growth factors and their inhibitors," *Nature Medicine*, vol. 5, no. 12, pp. 1359–1364, 1999.

[6] Q. Sun, R. R. Chen, Y. Shen, D. J. Mooney, S. Rajagopalan, and P. M. Grossman, "Sustained vascular endothelial growth factor delivery enhances angiogenesis and perfusion in ischemic hind limb," *Pharmaceutical Research*, vol. 22, no. 7, pp. 1110–1116, 2005.

[7] A. H. Zisch, M. P. Lutolf, M. Ehrbar et al., "Cell-demanded release of VEGF from synthetic, biointeractive cell ingrowth matrices for vascularized tissue growth," *The FASEB Journal*, vol. 17, no. 15, pp. 2260–2262, 2003.

[8] Q. Sun, E. A. Silva, A. Wang et al., "Sustained release of multiple growth factors from injectable polymeric system as a novel therapeutic approach towards angiogenesis," *Pharmaceutical Research*, vol. 27, no. 2, pp. 264–271, 2010.

[9] S. J. Grainger, B. Carrion, J. Ceccarelli, and A. J. Putnam, "Stromal cell identity influences the in vivo functionality of engineered capillary networks formed by co-delivery of endothelial cells and stromal cells," *Tissue Engineering Part A*, vol. 19, no. 9-10, pp. 1209–1222, 2013.

[10] J. Rehman, D. Traktuev, J. Li et al., "Secretion of angiogenic and antiapoptotic factors by human adipose stromal cells," *Circulation*, vol. 109, no. 10, pp. 1292–1298, 2004.

[11] T. Kinnaird, E. S. Burnett, M. Shou et al., "Local delivery of marrow-derived stromal cells augments collateral perfusion

through paracrine mechanisms," *Circulation*, vol. 109, no. 12, pp. 1543–1549, 2004.

[12] M. Pesce, A. Orlandi, M. G. Iachininoto et al., "Myoendothelial differentiation of human umbilical cord blood-derived stem cells in ischemic limb tissues," *Circulation Research*, vol. 93, no. 5, pp. e51–e62, 2003.

[13] L. Ren, D. Ma, B. Liu et al., "Preparation of three-dimensional vascularized MSC cell sheet constructs for tissue regeneration," *BioMed Research International*, vol. 2014, Article ID 301279, 10 pages, 2014.

[14] C. M. Ghajar, K. S. Blevins, C. C. W. Hughes, S. C. George, and A. J. Putnam, "Mesenchymal stem cells enhance angiogenesis in mechanically viable prevascularized tissues via early matrix metalloproteinase upregulation," *Tissue Engineering*, vol. 12, no. 10, pp. 2875–2888, 2006.

[15] C. M. Ghajar, S. Kachgal, E. Kniazeva et al., "Mesenchymal cells stimulate capillary morphogenesis via distinct proteolytic mechanisms," *Experimental Cell Research*, vol. 316, no. 5, pp. 813–825, 2010.

[16] P. Au, J. Tam, D. Fukumura, and R. K. Jain, "Bone marrow derived mesenchymal stem cells facilitate engineering of long-lasting functional vasculature," *Blood*, vol. 111, no. 9, pp. 4551–4558, 2008.

[17] S. Kachgal and A. J. Putnam, "Mesenchymal stem cells from adipose and bone marrow promote angiogenesis via distinct cytokine and protease expression mechanisms," *Angiogenesis*, vol. 14, no. 1, pp. 47–59, 2011.

[18] S. Merfeld-Clauss, N. Gollahalli, K. L. March, and D. O. Traktuev, "Adipose tissue progenitor cells directly interact with endothelial cells to induce vascular network formation," *Tissue Engineering—Part A*, vol. 16, no. 9, pp. 2953–2966, 2010.

[19] X. Chen, A. S. Aledia, S. A. Popson, L. Him, C. C. W. Hughes, and S. C. George, "Rapid anastomosis of endothelial progenitor cell-derived vessels with host vasculature is promoted by a high density of cotransplanted fibroblasts," *Tissue Engineering—Part A*, vol. 16, no. 2, pp. 585–594, 2010.

[20] B. R. Shepherd, S. M. Jay, W. M. Saltzman, G. Tellides, and J. S. Pober, "Human aortic smooth muscle cells promote arteriole formation by coengrafted endothelial cells," *Tissue Engineering Part A*, vol. 15, no. 1, pp. 165–173, 2009.

[21] G. Bergers and S. Song, "The role of pericytes in blood-vessel formation and maintenance," *Neuro-Oncology*, vol. 7, no. 4, pp. 452–464, 2005.

[22] M. Soncini, E. Vertua, L. Gibelli et al., "Isolation and characterization of mesenchymal cells from human fetal membranes," *Journal of Tissue Engineering and Regenerative Medicine*, vol. 1, no. 4, pp. 296–305, 2007.

[23] S. Ilancheran, Y. Moodley, and U. Manuelpillai, "Human fetal membranes: a source of stem cells for tissue regeneration and repair?" *Placenta*, vol. 30, no. 1, pp. 2–10, 2009.

[24] L. de Girolamo, E. Lucarelli, G. Alessandri et al., "Mesenchymal stem/stromal cells: a new "cells as drugs" paradigm. efficacy and critical aspects in cell therapy," *Current Pharmaceutical Design*, vol. 19, no. 13, pp. 2459–2473, 2013.

[25] F. Alviano, V. Fossati, C. Marchionni et al., "Term amniotic membrane is a high throughput source for multipotent mesenchymal stem cells with the ability to differentiate into endothelial cells in vitro," *BMC Developmental Biology*, vol. 7, article 11, 2007.

[26] S.-W. Kim, H.-Z. Zhang, C. E. Kim, H. S. An, J.-M. Kim, and M. H. Kim, "Amniotic mesenchymal stem cells have robust angiogenic properties and are effective in treating hindlimb ischaemia," *Cardiovascular Research*, vol. 93, no. 3, pp. 525–534, 2012.

[27] Y. Li, L. Guo, H. S. Ahn, M. H. Kim, and S.-W. Kim, "Amniotic mesenchymal stem cells display neurovascular tropism and aid in the recovery of injured peripheral nerves," *Journal of Cellular and Molecular Medicine*, vol. 18, no. 6, pp. 1028–1034, 2014.

[28] J. König, B. Huppertz, G. Desoye et al., "Amnion-derived mesenchymal stromal cells show angiogenic properties but resist differentiation into mature endothelial cells," *Stem Cells and Development*, vol. 21, no. 8, pp. 1309–1320, 2012.

[29] J. Ma, F. Yang, S. K. Both et al., "In vitro and in vivo angiogenic capacity of BM-MSCs/HUVECs and AT-MSCs/HUVECs cocultures," *Biofabrication*, vol. 6, no. 1, Article ID 015005, 2014.

[30] A. O. Smith, S. L. K. Bowers, A. N. Stratman, and G. E. Davis, "Hematopoietic stem cell cytokines and fibroblast growth factor-2 stimulate human endothelial cell-pericyte tube co-assembly in 3D fibrin matrices under serum-free defined conditions," *PLoS ONE*, vol. 8, no. 12, Article ID e85147, 2013.

[31] N. Hiraoka, E. Allen, I. J. Apel, M. R. Gyetko, and S. J. Weiss, "Matrix metalloproteinases regulate neovascularization by acting as pericellular fibrinolysins," *Cell*, vol. 95, no. 3, pp. 365–377, 1998.

[32] I. Yana, H. Sagara, S. Takaki et al., "Crosstalk between neovessels and mural cells directs the site-specific expression of MT1-MMP to endothelial tip cells," *Journal of Cell Science*, vol. 120, no. 9, pp. 1607–1614, 2007.

[33] M. F. Pittenger, A. M. Mackay, S. C. Beck et al., "Multilineage potential of adult human mesenchymal stem cells," *Science*, vol. 284, no. 5411, pp. 143–147, 1999.

[34] P. A. Zuk, M. Zhu, P. Ashjian et al., "Human adipose tissue is a source of multipotent stem cells," *Molecular Biology of the Cell*, vol. 13, no. 12, pp. 4279–4295, 2002.

[35] N. J. Zvaifler, L. Marinova-Mutafchieva, G. Adams et al., "Mesenchymal precursor cells in the blood of normal individuals," *Arthritis Research*, vol. 2, no. 6, pp. 477–488, 2000.

[36] H. Nakahara, S. P. Bruder, S. E. Haynesworth et al., "Bone and cartilage formation in diffusion chambers by subcultured cells derived from the periosteum," *Bone*, vol. 11, no. 3, pp. 181–188, 1990.

[37] H. E. Young, T. A. Steele, R. A. Bray et al., "Human reserve pluripotent mesenchymal stem cells are present in the connective tissues of skeletal muscle and dermis derived from fetal, adult, and geriatric donors," *Anatomical Record*, vol. 264, no. 1, pp. 51–62, 2001.

[38] A. Harichandan and H.-J. Bühring, "Prospective isolation of human MSC," *Best Practice and Research: Clinical Haematology*, vol. 24, no. 1, pp. 25–36, 2011.

[39] J. Isern and S. Méndez-Ferrer, "Stem cell interactions in a bone marrow niche," *Current Osteoporosis Reports*, vol. 9, no. 4, pp. 210–218, 2011.

[40] G. Kmiecik, W. Niklińska, P. Kuć et al., "Fetal membranes as a source of stem cells," *Advances in Medical Sciences*, vol. 58, no. 2, pp. 185–195, 2013.

[41] K. le Blanc, C. Tammik, K. Rosendahl, E. Zetterberg, and O. Ringdén, "HLA expression and immunologic properties of differentiated and undifferentiated mesenchymal stem cells," *Experimental Hematology*, vol. 31, no. 10, pp. 890–896, 2003.

[42] C. Götherström, O. Ringdén, C. Tammik, E. Zetterberg, M. Westgren, and K. Le Blanc, "Immunologic properties of human fetal mesenchymal stem cells," *American Journal of Obstetrics & Gynecology*, vol. 190, no. 1, pp. 239–245, 2004.

[43] A. J. Nauta, G. Westerhuis, A. B. Kruisselbrink, E. G. A. Lurvink, R. Willemze, and W. E. Fibbe, "Donor-derived mesenchymal stem cells are immunogenic in an allogeneic host and stimulate donor graft rejection in a nonmyeloablative setting," *Blood*, vol. 108, no. 6, pp. 2114–2120, 2006.

[44] Y. Zhang, C. Li, X. Jiang et al., "Human placenta-derived mesenchymal progenitor cells support culture expansion of long-term culture-initiating cells from cord blood $CD34^+$ cells," *Experimental Hematology*, vol. 32, no. 7, pp. 657–664, 2004.

[45] S. M. Albelda, W. A. Muller, C. A. Buck, and P. J. Newman, "Molecular and cellular properties of PECAM-1 (endoCAM/CD31): a novel vascular cell-cell adhesion molecule," *The Journal of Cell Biology*, vol. 114, no. 5, pp. 1059–1068, 1991.

[46] J.-P. Girma, D. Meyer, C. L. Verweij, H. Pannekoek, and J. J. Sixma, "Structure-function relationship of human von Willebrand factor," *Blood*, vol. 70, no. 3, pp. 605–611, 1987.

[47] X. Cai, Y. Lin, C. C. Friedrich et al., "Bone marrow derived pluripotent cells are pericytes which contribute to vascularization," *Stem Cell Reviews*, vol. 5, no. 4, pp. 437–445, 2009.

[48] R. R. Rao, A. W. Peterson, J. Ceccarelli, A. J. Putnam, and J. P. Stegemann, "Matrix composition regulates three-dimensional network formation by endothelial cells and mesenchymal stem cells in collagen/fibrin materials," *Angiogenesis*, vol. 15, no. 2, pp. 253–264, 2012.

[49] S. T.-F. Hsiao, A. Asgari, Z. Lokmic et al., "Comparative analysis of paracrine factor expression in human adult mesenchymal stem cells derived from bone marrow, adipose, and dermal tissue," *Stem Cells and Development*, vol. 21, no. 12, pp. 2189–2203, 2012.

[50] J.-E. Alard, M. Dueymes, R. A. Mageed, A. Saraux, P. Youinou, and C. Jamin, "Mitochondrial heat shock protein (HSP) 70 synergizes with HSP60 in transducing endothelial cell apoptosis induced by anti-HSP60 autoantibody," *The FASEB Journal*, vol. 23, no. 8, pp. 2772–2779, 2009.

[51] F. Verseijden, S. J. Posthumus-van Sluijs, P. Pavljasevic, S. O. P. Hofer, G. J. V. M. van Osch, and E. Farrell, "Adult human bone marrow-and adipose tissue-derived stromal cells support the formation of prevascular-like structures from endothelial cells in vitro," *Tissue Engineering—Part A*, vol. 16, no. 1, pp. 101–114, 2010.

[52] B. Sacchetti, A. Funari, S. Michienzi et al., "Self-renewing osteoprogenitors in bone marrow sinusoids can organize a hematopoietic microenvironment," *Cell*, vol. 131, no. 2, pp. 324–336, 2007.

[53] T. Kinnaird, E. Stabile, M. S. Burnett et al., "Marrow-derived stromal cells express genes encoding a broad spectrum of arteriogenic cytokines and promote in vitro and in vivo arteriogenesis through paracrine mechanisms," *Circulation Research*, vol. 94, no. 5, pp. 678–685, 2004.

[54] R. Gruber, B. Kandler, P. Holzmann et al., "Bone marrow stromal cells can provide a local environment that favors migration and formation of tubular structures of endothelial cells," *Tissue Engineering*, vol. 11, no. 5-6, pp. 896–903, 2005.

[55] V. Volarevic, S. Bojic, J. Nurkovic et al., "Stem cells as new agents for the treatment of infertility: current and future perspectives and challenges," *BioMed Research International*, vol. 2014, Article ID 507234, 8 pages, 2014.

[56] M. Jin, Y. Xie, Q. Li, and X. Chen, "Stem cell-based cell therapy for glomerulonephritis," *BioMed Research International*, vol. 2014, Article ID 124730, 15 pages, 2014.

[57] M. G. Roubelakis, O. Trohatou, and N. P. Anagnou, "Amniotic fluid and amniotic membrane stem cells: marker discovery," *Stem Cells International*, vol. 2012, Article ID 107836, 9 pages, 2012.

[58] D. Rossi, S. Pianta, M. Magatti, P. Sedlmayr, and O. Parolini, "Characterization of the conditioned medium from amniotic membrane cells: prostaglandins as key effectors of its immunomodulatory activity," *PLoS ONE*, vol. 7, no. 10, Article ID e46956, 2012.

[59] A. Silini, O. Parolini, B. Huppertz, and I. Lang, "Soluble factors of amnion-derived cells in treatment of inflammatory and fibrotic pathologies," *Current Stem Cell Research and Therapy*, vol. 8, no. 1, pp. 6–14, 2013.

[60] A. Hussain, K. Takahashi, J. Sonobe, Y. Tabata, and K. Bessho, "Bone regeneration of rat calvarial defect by magnesium calcium phosphate gelatin scaffolds with or without bone morphogenetic protein-2," *Journal of Maxillofacial and Oral Surgery*, vol. 13, no. 1, pp. 29–35, 2014.

Hindawi Publishing Corporation
BioMed Research International
Volume 2015, Article ID 139476, 8 pages
http://dx.doi.org/10.1155/2015/139476

*Research Article*

# Biocompatibility of Novel Type I Collagen Purified from Tilapia Fish Scale: An In Vitro Comparative Study

**Jia Tang and Takashi Saito**

*Division of Clinical Cariology and Endodontology, Department of Oral Rehabilitation, School of Dentistry, Health Sciences University of Hokkaido, 1757 Kanazawa, Ishikari-Tobetsu, Hokkaido 061-0293, Japan*

Correspondence should be addressed to Jia Tang; tangjia@hoku-iryo-u.ac.jp

Received 21 April 2015; Revised 29 May 2015; Accepted 30 May 2015

Academic Editor: Joo L. Ong



Type I collagen (COL-1) is the prevailing component of the extracellular matrix in a number of tissues including skin, ligament, cartilage, bone, and dentin. It is the most widely used tissue-derived natural polymer. Currently, mammalian animals, including pig, cow, and rat, are the three major sources for purification of COL-1. To reduce the risk of zoonotic infectious diseases transmission, minimize the possibility of immunogenic reaction, and avoid problems related to religious issues, exploration of new sources (other than mammalian animals) for the purification of type I collagen is highly desirable. Hence, the purpose of the current study was to investigate the in vitro responses of MDPC-23 to type I collagen isolated from tilapia scale in terms of cellular proliferation, differentiation, and mineralization. The results suggested that tilapia scale collagen exhibited comparable biocompatibility to porcine skin collagen, indicating it might be a potential alternative to type I collagen from mammals in the application for tissue regeneration in oral-maxillofacial area.

## 1. Introduction

Type I collagen (COL-I) is the most abundant extracellular matrix protein in mammals. It acts as not only the mechanical structural support to bone, skin, tendons, ligaments, and blood vessels, but also the extracellular cue regulating physiological processes including cell adhesion, proliferation, and differentiation [1, 2]. Biological function of COL-1 might be attributable to the following reasons. First, its amino acid sequence contains a number of motifs (i.e., DGEA, GFOGER, and RGD, etc.) that are able to bind with various integrins [3–7]; following the binding with cells, certain signal pathways are activated and specific gene transcription is initiated [8]. In addition, COL-I is able to interact with other extracellular matrix proteins and facilitate mineralization [9, 10]. The structure of COL-1 is characterized by a tripeptide repeats Gly-X-Y, where X and Y are frequently taken by proline (Pro) and hydroxyproline (Hyp), respectively. The denaturation temperature of COL-1 is correlated to the content of Hyp [11] and an overall higher content of Hyp accounts for higher thermal stability for the COL-1. Moreover, amino acid composition of COL-1 varies between species; for example, bird feet collagen contains higher glutamic acid (Glu) and aspartic acid (Asp), while shark skin collagen contains lower aspartic acid and hydroxyproline (Hyp) [12]. In general, marine collagen types contain lower amount of Hyp and consequently lower denaturation temperature ($T_m$) (25.0°C–30.0°C) [13] as compared to mammalian collagen types.

COL-1 has been used in numerous applications: drug delivery, skin substitute, soft tissue augmentation, suturing, and tissue engineering substrate [14, 15]. However, most of the COL-1 used were from mammals, namely, pig, cow, and rat. With the outbreak of zoonotic infectious diseases, such as Bovine Spongiform Encephalopathy (BSE), it becomes questionable whether to use mammalian derived-COL-1 for scientific research or food supplements purposes. Allergy is another problem; part of the population is allergic to bovine or porcine collagen [16]. Furthermore, in countries having religious restrictions, the application of certain mammalian animals-isolated products is strictly prohibited. Hence, it is highly desirable and necessary to explore alternative sources for purification of COL-I.

Ocean, where thousands of fish reside, takes up 70.9% of the earth's surface area. The vast amount of energy,

minerals, and fish in ocean made it one of the most attractive treasuries. Each year, thousands of tons of ocean fish are destined for human consumption, generating considerable amount of byproducts such as fish bones, skin, and scale, which are usually discarded as commercial waste. Processing the byproducts into other substances (fish oil, fish collagen, etc.) is cost effective for large fish processing plants and ecofriendly. Fish collagen is easier for digestion and adsorption than bovine and porcine collagen thanks to its low Hyp content and $T_m$ and has already gained popularity in cosmetic industry. However, exactly due to the lower thermal stability of fish collagen, initial attempts to employ fish-derived COL-1 in tissue engineering field were met with limited success. For instance, the $T_m$ of salmon skin collagen is only 19°C [17], suggesting that it is impossible to be adopted as scaffold material for in vitro cell culture. Recently, a new COL-I with higher $T_m$ (37°C) [18] was purified from tilapia fish scale. This COL-I is superior to porcine skin COL-I in inducing human mesenchymal stem cells differentiation [17]; importantly, it is safe and causes no skin reaction following intracutaneous and topical application [18].

To confirm its applicability in the dental field, we compared the in vitro effects of COL-I derived from tilapia scale and porcine skin on a rat odontoblast-like cell line, MDPC-23. This neural crest originating cell line was isolated from 18-19-day-old fetal mouse molar dental papillae and has been described to be capable of expressing and secreting dentin matrix proteins [19]; a recent species specific RT-PCR study confirmed that it is indeed of rat origin [20]. Moreover, MDPC-23 retains the ability to differentiate along odontoblast lineage and can bind with COL-1 via integrin $\alpha 1$ $\alpha 2$ and CD44 in a concentration-dependent manner [21]. Hence, MDPC-23, as a representative of cell from dental tissue, was used in this experiment.

## 2. Materials and Methods

*2.1. Materials.* Tissue culture polystyrene dishes (TCPS, 35 mm) were purchased from Iwaki, Japan. Type I collagen derived from tilapia (*Oreochromis niloticus*) scale and porcine skin were generated from Taki chemical, Japan, and Nitta gelatin, Japan, respectively. Dulbecco's modified eagle medium (DMEM) and Triton-X-100 were bought from Sigma-Aldrich, USA. Fetal bovine serum (FBS), TypLE express, and 1x phosphate buffered saline (PBS, pH of 7.4) were all from Gibco, USA. Glycerol-2-phosphate disodium salt n-hydrate ($\beta$-GP), L-Ascorbic acid phosphate magnesium salt n-hydrate, 10% formalin neutral buffer solution, Alizarin red S powder, and LabAssay ALP kit were purchased from Wako, Japan. Pierce BCA protein assay kit was from Thermo scientific, USA. TRIzol was purchased from Invitrogen, USA. Chloroform, 2-propanol, and ethanol were from Nacalai Tesque, Japan. FastStart Essential DNA Green Master for real time PCR reaction was purchased from Roche, Switzerland.

*2.2. Coating of Type I Collagen to TCPS.* COL-I (0.3%, w/v) was diluted by tenfold in sterilized acidic water (pH of 3.0) and coated to TCPS (1.5 mL/dish) for 2 hours at room temperature. Afterwards, the coating solution was aspirated and the dishes were air dried up. Immediately before cell inoculation, COL-I-coated dishes were rinsed with PBS to remove excess acidic water. TCPS without exposure to COL-1 was taken to be the control throughout the whole experiment. For convenience, in the following experiments, tilapia scale derived type I collage-coated dishes were denoted as T-COL, while porcine skin derived type I collagen-coated dishes were presented as P-COL.

*2.3. Cell Culture.* MDPC-23 was generously provided by Professor Jacques Nör at University of Michigan, Ann Arbor. Cells were grown in DMEM supplemented with 10% FBS, in a humidified atmosphere of 5% $CO_2$ and 95% air at 37°C. For each experiment, cells were detached using TrypLE express and seeded into a COL-I-treated or control 35 mm TCPS at the initial number of $5 \times 10^4$ cells per dish. Cells were maintained in serum-free DMEM for the first day prior to addition of FBS. After six days of culture, 10 mM $\beta$-GP and 50 $\mu$g/mL ascorbic acid were supplemented to the culture medium (i.e., odontogenic medium: OM) for induction of odontogenic differentiation. The medium was changed every second day. Cell passages from 20 to 30 were used in this experiment.

*2.4. Cell Morphology Observation and Cell Number Determination.* Cell morphology on 19 hours, 44 hours, and day 3 was observed using phase contrast microscopy (Olympus, Shinjuku, Tokyo, Japan). The number of cells on each plate was counted on days 2, 3, and 4 to quantitatively evaluate the initial effect of COL-I on cell growth. Briefly, the cells were detached using 200 $\mu$L TrypLE express per plate and diluted with 800 $\mu$L PBS; the cell suspension was centrifuged at 500 g, 4°C for 5 minutes (Kubota 2800, Tokyo, Japan). After aspirating the supernatant, the cell pellet was reconstituted in PBS; the number of cells per dish was counted manually by a hemocytometer.

*2.5. ALP Activity.* Cells were harvested and lysed with 0.1% (v/v) Triton-X-100 in distilled water and the lysates were sonicated on ice (Bioruptor, Diagenode, Seraing, Belgium) for 10 minutes and then centrifuged at 12,000 rpm, 4°C for 15 minutes (Hitachi Koki, Chiyoda, Tokyo, Japan). The supernatant was analyzed with a LabAssay ALP kit (Wako) according to the manufacturer's instruction. Total protein was quantified with a BCA protein assay kit (Pierce). ALP production was normalized to total protein amount. Absorbance was read using iMark microplate reader (BIO-RAD, Hercules, California, USA) at 405 nm and 570 nm for ALP assay and protein quantification assay respectively.

*2.6. Real Time RT-PCR.* Cell differentiation was quantified in terms of odontogenic gene expression by collecting total RNA using TRIzol reagent at prescribed times. Isolated RNA was pelleted, washed in 75% ethanol, and resuspended in nuclease-free water. RNA concentration of each sample was measured spectroscopically by GeneQuant (GE Healthcare

Table 1: Real time RT-PCR primer.

| Gene name | Sense | Antisense | Fragment size |
|---|---|---|---|
| Rat *DMP-1* | cgttcctctgggggctgtcc | ccgggatcatcgctctgcatc | 577 bp |
| Rat *ALP* | ggaaggaggcaggattgaccac | gggcctggtagttgttgtgagc | 338 bp |
| Rat *BSP* | ctgctttaatcttgctctg | ccatctccattttcttcc | 211 bp |
| Rat *OCN* | agctcaaccccaattgtgac | agctgtgccgtccatacttt | 190 bp |
| Rat *Runx-2* | ccacagagctattaaagtgacagtg | aacaaactaggtttagagtcatcaagc | 87 bp |
| Rat *β-actin* | aaccctaaggccaacagtgaaaag | tcatgaggtagtctgtgaggt | 240 bp |

Table 2: Real time RT-PCR reaction condition.

| | Initialization | Denaturation | Annealing | Elongation | Cycle |
|---|---|---|---|---|---|
| *DMP-1* | 95°C 10 min | 95°C 15 sec | 60°C 30 sec | 72°C 30 sec | 50 |
| *ALP* | 95°C 10 min | 95°C 15 sec | 55°C 30 sec | 72°C 30 sec | 45 |
| *BSP* | 95°C 10 min | 95°C 15 sec | 55°C 15 sec | 72°C 30 sec | 50 |
| *OCN* | 94°C 10 min | 95°C 15 sec | 55°C 30 sec | 68°C 30 sec | 50 |
| *Runx-2* | 95°C 10 min | 95°C 15 sec | 55°C 30 sec | 72°C 40 sec | 45 |
| *β-actin* | 95°C 10 min | 95°C 15 sec | 53°C 30 sec | 72°C 40 sec | 40 |

Life Sciences, Little Chalfont, UK), and one microgram of isolated RNA was then reverse-transcribed into complementary DNA (cDNA) using M-MLV reverse transcriptase in a 20 $\mu$L reaction system according to manufacturer's instruction. The resulting complementary DNA (cDNA) was used for real time RT-PCR. Real time RT-PCR was carried out using a LightCycler Nano (Roche Diagnostics, Basel, Switzerland) according to the manufacturer's instruction. The comparative $2^{-\Delta\Delta Ct}$ method was employed to calculate relative gene expression. The gene expression levels were normalized to the $\beta$-actin mRNA level. Primer sequences and reaction condition are described in Tables 1 and 2, respectively.

*2.7. Alizarin Red Staining.* Matrix calcification was observed using alizarin red staining. Culture medium was aspirated and cell monolayer was washed twice with PBS. Cell was fixed with 10% formalin neutral buffer solution for twenty minutes; afterwards the cell monolayer was washed again by PBS. Alizarin red solution (ARS) (1% w/v, pH 4.1) was added gently not to disrupt the cell monolayer. After five minutes, the staining solution was removed and the cell monolayer was firstly washed by distilled water and subsequently washed thoroughly with PBS to remove the nonspecific background stain. Photographs were taken using a digital imaging system (Funakoshi, Tokyo, Japan) incorporating an inverted digital camera (Canon, Tokyo, Japan). The quantification of staining was conducted using Cetylpyridinium Chloride (CPC) extraction method. Briefly, after staining with ARS, CPC (10%, w/v, in distilled water) was added to each dish (2 mL/dish) and incubated for one hour at 37°C. Following incubation, the transparent CPC solution, which turned into purple, was diluted by fivefold in original CPC solution and transferred to a 96-well plate (200 $\mu$L/well) for absorbance reading (BIO-RAD) at 570 nm.

*2.8. Statistical Analysis.* All the experiments were conducted in triplicate. Results were expressed as mean ± standard deviation (SD). Data was subjected to Tukey Kramer test. Statistical significance level was set at $p < 0.05$.

## 3. Results

*3.1. Cell Morphology.* On 19 hours (serum-free medium) (Figure 1(a)), the morphology of cells did not differ in each group, whereas it is evident that more cells attached to P-COL and T-COL substrates. On 44 hours (after addition of serum) (Figure 1(b)), the cell started to proliferate and spread; cells cultured on P-COL substrate adopted elongated morphology, while those cultured on T-COL exhibited a more polygonal shape; in comparison, much less cells adhered to TCPS, and cells cultured on TCPS were poorly spread, implying immature cellular cytoskeleton assembly. On day 3 (Figure 1(c)), cells number in each group increased markedly; nonetheless, attached cell number in T-COL and P-COL was much higher than that on control dish; cells cultured on T-COL and P-COL substrates presented elongated, fibroblast-like shape, while those on control dish were polygonal and less spread.

*3.2. Cell Proliferation.* To estimate the effect of COL-1 on proliferation of MDPC-23, cell number on 2, 3, and 4 days was determined using a hemocytometer (Figure 2). As depicted by the bars in Figure 2, the total number of cells in all the groups increased progressively with time. Upon exposure to COL-1, total number of cells in T-COL and P-COL significantly increased to $9.83 \pm 0.76 \times 10^4$ ($p < 0.05$) and $8.83 \pm 0.72 \times 10^4$ ($p < 0.05$), respectively, by day 2 and continued to increase to $25.63 \pm 3.01 \times 10^4$ ($p < 0.05$) and $22.5 \pm 3.90 \times 10^4$ ($p > 0.05$) by day 3; in comparison, the number of cells in TCPS was merely $6.53 \pm 0.23 \times 10^4$ on day 2 and $16.5 \pm 1.80 \times 10^4$ on day 3. However, cell number in T-COL ($44.33 \pm 4.54 \times 10^4$), P-COL ($44.33 \pm 2.08 \times 10^4$), and TCPS ($45.5 \pm 2.29 \times 10^4$) leveled off after 4-day incubation.

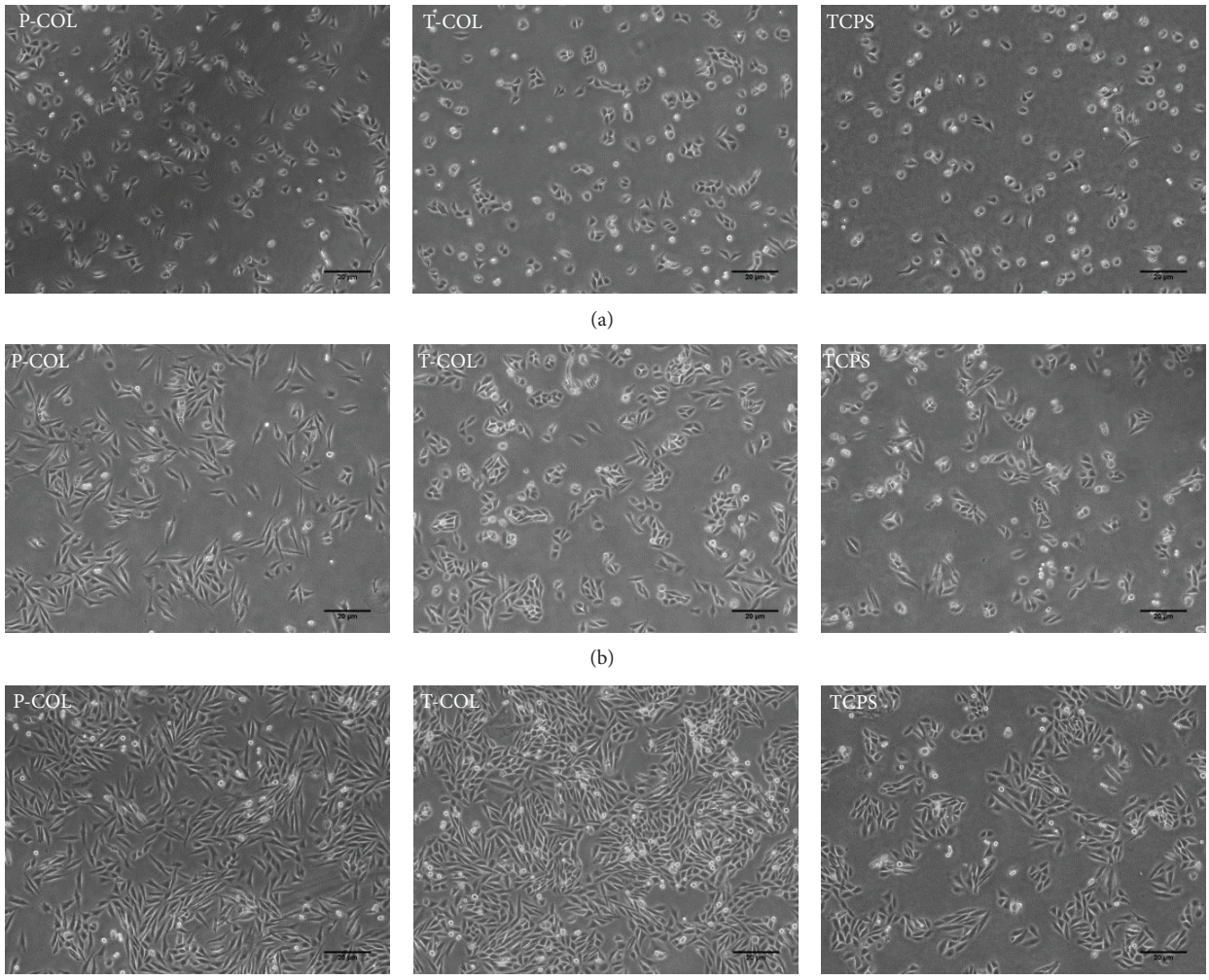


Figure 1: No evident difference in terms of cell morphology and number was observed on 19 hours in each group. On 44 hours, more cells attached to T-COL and P-COL substrates as compared to TCPS; cells cultured in P-COL and T-COL adopted well spread, extended shape, whereas those cultured in TCPS were scarcely scattered and poorly spread. On day 3, cell number in each group increased progressively with time; however, the number of cells in T-COL and P-COL was significantly higher than that in TCPS. Scale bar equals 20 $\mu$m.

*3.3. ALP Activity.* To evaluate the initial effect of COL-1 on MDPC-23 differentiation, ALP activity at 6, 8, and 10 days was quantified using a LabAssay ALP kit (Wako) (Figure 3). By day 6, a time point representative of the onset of differentiation, the normalized ALP activity found in MDPC-23 seeded on T-COL and P-COL, was $1.27 \pm 0.04$ U/$\mu$g protein ($p < 0.05$) and $1.31 \pm 0.07$ U/$\mu$g protein ($p < 0.05$), which was nearly two times more than that of TCPS ($0.59 \pm 0.25$ U/$\mu$g protein); the ALP activity remained almost unchanged in T-COL (day 8: $1.26 \pm 0.11$ U/$\mu$g protein; day 10: $1.23 \pm 0.11$ U/$\mu$g protein) and P-COL (day 8: $1.33 \pm 0.05$ U/$\mu$g protein; day 10: $1.26 \pm 0.14$ U/$\mu$g protein) until day 10, significantly surpassing ALP activity of cells cultured on TCPS (day 8: $0.79 \pm 0.11$ U/$\mu$g protein; day 10: $0.90 \pm 0.06$ U/$\mu$g protein).

*3.4. Real Time RT-PCR.* To examine the effect of COL-1 on the differentiation of MDPC-23, mRNA expression level of *ALP BSP OCN DMP-1* and *Runx-2* was investigated by real time RT-PCR (Figure 4). On day 7, T-COL and P-COL enhanced $1.21 \pm 0.05$ ($p < 0.05$) and $1.25 \pm 0.11$ ($p < 0.05$) fold the mRNA expression of *BSP*; *ALP* mRNA expression was upregulated in the two experimental groups; however, no statistical significances were detected between them and control. Interestingly, *DMP-1* mRNA expression was downregulated by P-COL ($0.59 \pm 0.11$ fold) ($p < 0.05$) and T-COL ($0.74 \pm 0.25$ fold) ($p > 0.05$) on day 10. As for *OCN* and *Runx-2* mRNA expression on the two days, no statistical significances were detected between groups.

*3.5. Alizarin Red Staining.* To investigate the effect of COL-1 on mineralization of MDPC-23, cells were stained with Alizarin Red S and quantified by CPC extraction (Figure 5). After culturing the cells on T-COL and P-COL substrates, the formation of mineralized nodules was apparently increased

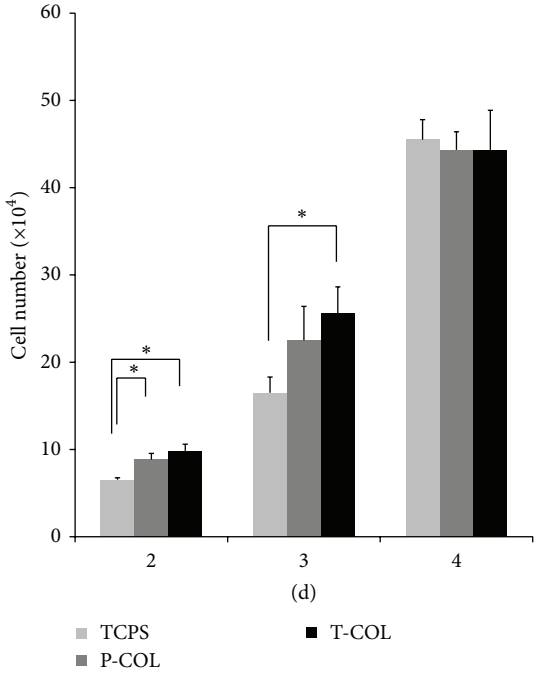


Figure 2: Cell number determination. Cell number was counted manually using a hemocytometer on days 2, 3, and 4. All the experiments were conducted in triplicate. ($^*p < 0.05$).

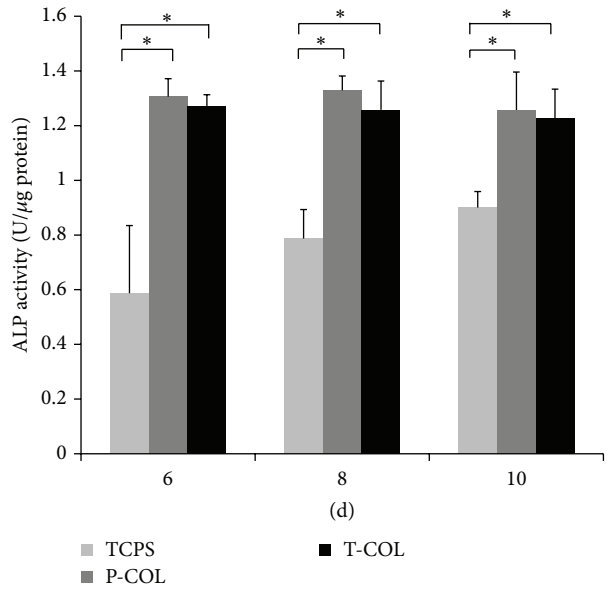


Figure 3: ALP activity: ALP activity of MDPC-23 on T-COL and P-COL maintained at a significant higher level as compared to that of TCPS on the three days tested. Experiments were carried out in triplicate for each group. ($^*p < 0.05$).

on day 10. CPC quantification further lends support to the observation and showed an approximately two times increase in the cells cultured on T-COL and P-COL compared with the control cells ($p < 0.05$). However, no significant difference in mineralization was noted between cells cultured on T-COL and P-COL substrates.

## 4. Discussion

Cells, factors, and scaffolds are of fundamental importance to successful tissue regeneration; the regeneration of dentin-pulp complex is no exception. The cells can detect the surrounding signals from scaffolds and soluble factors, initiating odontogenesis, which is important in the repair process of dentin matrix. Tissue specificity is determined by its own extracellular matrix proteins. Therefore, mimicking the natural ECM has considered a promising approach in the design of artificial scaffold for dentin. Because of its abundance and ubiquity, COL-1 is frequently used as scaffold material in the study of dentin regeneration. Some have reported the use of COL-I decorated with nanobioactive glass promoted the regeneration of dentin [22]. Previously, mammalian derived collagen types are the mainstream products used in scientific researches. However, the recent outbreak of zoonotic infectious diseases threatens people's health and made it no longer safe to use those mammalian collagen types; attempts have since been made to explore collagen alternatives from the ocean.

Recently, a novel COL-1 was purified from tilapia scale and was reported to possess similar $T_m$ with porcine skin derived COL-1 [18]. In the present work, a comparative study was carried out between tilapia scale COL-I and porcine skin COL-I. Given that odontoblast is responsible for production of primary and reparative dentin during one's life time, MDPC-23, a rat odontoblast-like cell line was used as a model tissue cell to address the efficacy of the two COL-I. The COL-I was noted to be able to bind with the cell surface integrin and activate a series of intracellular signal pathways, for example, COL-I can bind with $\alpha 2\beta 1$ via its GFOGER motif to direct cellular behavior [23]. Moreover, induction of $\alpha 1$ expression in human skeletal muscle stem cells was sufficient to promote odontoblast differentiation [24]. MDPC-23 expresses $\alpha v\beta 3$ [25], $\alpha 1$, $\alpha 2$ [21], and $\beta 1$ [26]. As a result, it is conceivable that, in the current study, MDPC-23 interacts with COL-I via those integrins; however, this hypothesis awaits further investigation.

Initial cell adhesion and proliferation are critical for subsequent cellular functions. MDPC-23 showed favorable growth on T-COL and P-COL substrates, especially on 44 hours (Figure 1(b)) and day 3 (Figure 1(c)). Cells cultured on P-COL substrate adopted bipolar, elongated shape after culturing for 44 hours, whereas those cultured on T-COL were polygonal in shape, with more regular dimensions, similar with the shape of cells cultured in control dish (Figure 1(b)). Ongoing work on the cell number determination further demonstrated that MDPC-23 grew preferentially on COL-I groups, rather than on the control dish.

The odontoblastic capacity of MDPC-23 was subsequently investigated by measuring their ALP activity, mRNA expression level of differentiation markers, and Alizarin red staining intensity. Alkaline phosphatase (ALP) is a cell membrane-associated phosphatase that is involved in

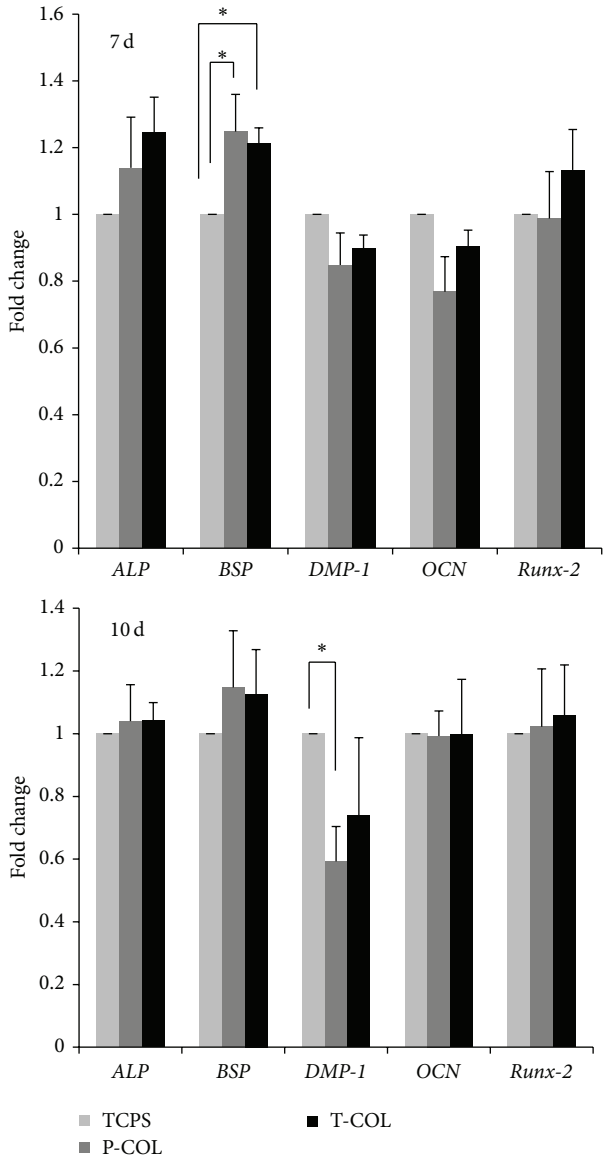


Figure 4: Real time RT-PCR. RNA was isolated on days 7 and 10, respectively, to quantify the mRNA expression level of *ALP*, *BSP*, *DMP-1*, *OCN*, and *Runx-2*. T-COL and P-COL enhanced the *BSP* mRNA expression on day 7; P-COL downregulated *DMP-1* mRNA expression on day 10. Experiments were carried out in triplicate for each group. ($^*p < 0.05$).

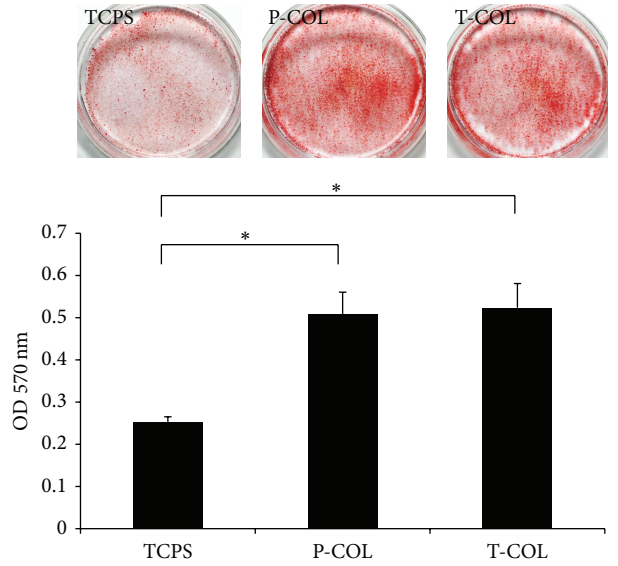


Figure 5: Alizarin red staining. On day 10, the calcific deposition of MDPC-23 in each dish was stained by alizarin red. The T-COL and P-COL markedly accelerated mineralization of cells as demonstrated by enhanced staining intensity and CPC quantification method. Experiments were carried out in triplicate for each group. ($^*p < 0.05$).

the onset of matrix mineralization and perceived as a relatively early marker in the cascade of osteo/odontoblast differentiation. Data revealed that ALP activity was significantly enhanced during the three days of test (days 6, 8, and 10) on P-COL and T-COL substrates. Similar results elicited by COL-I were also observed in the culture of MC3T3-E1 cells [27]. Biomineralization is widespread phenomenon, which refers to a process of deposition of extracellular matrix calcium and phosphate by cells. Alizarin red stains the calcific deposition red. In comparison to the negligible stain in control dish, cells cultured in T-COL and P-COL displayed much intensive staining, and CPC quantification data further demonstrated that T-COL and P-COL significantly accelerated the mineralization phase.

Gene expression analysis was conducted to further examine the influence of the COL-I on the odontogenesis of MDPC-23. *ALP* is used as a marker for the early differentiation of cells; *OCN* is a late stage marker for osteoblast, odontoblast, since they all secret *OCN* after maturation [28]. *BSP* is an acidic, noncollagenous glycoprotein expressed in mineralized tissues [29], which is considered a differentiation marker in the experiment. *Runx-2* is an important transcription factor for bone and tooth development, its overexpression induced DSPP protein expression in preodontoblast [30]. Overexpression of *DMP-1* in C3H10T1/2, MC3T3-E1, and RPC-2A induced differentiation of those cells toward odontoblast-like cells [16]; therefore, *DMP-1* was used as an odontoblast cell marker here. Whereas the former four genes are also considered osteogenic markers, the later gene is specific markers for odontogenesis. Real time RT-PCR data noted that MDPC-23 cultured on the COL-I-coated substrates had stimulated mRNA levels of *BSP* on day 7; surprisingly, the mRNA expression level of *DMP-1* was suppressed by P-COL ($0.59 \pm 0.11$ fold) ($p < 0.05$) and T-COL ($0.74 \pm 0.25$ fold) ($p > 0.05$) on day 10; this is in agreement with a previous study from Mizuno et al. [31]. DMP-1 and BSP were distinctively distributed during teeth development [32]. Further, Transforming growth factor-beta 1 (TGF-$\beta$1), a multifunctional growth factor that is positively involved in the repair process of dentin, induces *COL-1* expression [33] while it suppresses the expression of *DMP-1* [34]. It is therefore proposed that different mechanisms might exist in the regulation of *DMP-1* and *BSP* gene expression.

Studies are warranted to elucidate the observed downregulation phenomena. The upregulation of ALP activity, *BSP* gene, acceleration of mineralization, and downregulation of *DMP-1* gene indicated that COL-1 is effective in directing the differentiation of cells toward osteoblastic lineage rather than odontoblastic lineage. Interestingly, this might provide an important implication for future research; since COL-1 alone is not sufficient to elicit odontoblast differentiation, it is suggested that, to achieve the induction of odontoblast differentiation, COL-1 should be used in combination with other bioactive growth factors or proteins; for example, Ozeki and colleagues successfully induced the mouse-induced pluripotent stem (iPS) cells differentiation into odontoblast using COL-1 scaffold decorated by bone morphogenetic protein-4 (BMP-4) [35].

During the experiment course, no significant differences were detected between the T-COL and P-COL in terms of cell proliferation, differentiation, and mineralization. This is different from the results obtained by Matsumoto et al. [17]. In their work, the T-COL enhanced nearly twofold greater ALP activity in comparison to P-COL in the preculture period. The basis for this difference is unclear at present but may be related to the different cell types and/or experimental conditions used. Yamada and colleagues have reported the induction effect of fish (Gadiformes and Pleuronectidae) collagen peptide on MC3T3-E1 mineralization [36]. To the best of our knowledge, the current work is the first one to report the comparative study of tilapia scale COL-I and porcine skin COL-I in MDPC-23.

## 5. Conclusion

In summary, our findings indicated that adsorption of COL-I (including T-COL and P-COL) to TCPS led to a better biocompatibility, as evidenced by increased initial cell attachment, enhanced ALP activity, and upregulated gene expression of *BSP*, as well as accelerated matrix mineralization. For the whole experiments, T-COL exhibited comparable effect to P-COL. As the use of kinds of mammalian collagen may be restricted in future due to BSE, foot and mouth disease, it is suggested by the current work that the COL-I derived from tilapia scale, an usually underutilized material, offers promise to be an alternative for the mammalian collagen and might be useful for dentin-pulp regeneration.

## Disclosure

The authors declare that this paper is original, has not been published before, and is not currently being considered for publication elsewhere. They confirmed that the paper has been approved by all named authors. They further confirm that the order of authors listed in the paper has been approved by all of them.

## Conflict of Interests

The authors declare that there is no conflict of interests regarding the publication of this paper.

## Acknowledgment

The work was supported by a grant-in-aid for scientific research from the Japanese Society for the Promotion of Science (Grants no. 23390436 and no. 15H05024).

## References

[1] W. Li, B. Zhu, Z. Strakova, and R. Wang, "Two-way regulation between cells and aligned collagen fibrils: local 3D matrix formation and accelerated neural differentiation of human decidua parietalis placental stem cells," *Biochemical and Biophysical Research Communications*, vol. 450, no. 4, pp. 1377–1382, 2014.

[2] S.-W. Tsai, H.-M. Liou, C.-J. Lin et al., "MG63 osteoblast-like cells exhibit different behavior when grown on electrospun collagen matrix versus electrospun gelatin matrix," *PLoS ONE*, vol. 7, no. 2, Article ID e31200, 2012.

[3] J. Jokinen, E. Dadu, P. Nykvist et al., "Integrin-mediated cell adhesion to type I collagen fibrils," *The Journal of Biological Chemistry*, vol. 279, no. 30, pp. 31956–31963, 2004.

[4] C.-W. Huang, Z. Li, and P. S. Conti, "In vivo near-infrared fluorescence imaging of integrin $\alpha_2\beta_1$ in prostate cancer with cell-penetrating-peptide- conjugated DGEA probe," *Journal of Nuclear Medicine*, vol. 52, no. 12, pp. 1979–1986, 2011.

[5] M. M. Mizuno, R. Fujisawa, and Y. N. Kuboki, "Type I collagen-induced osteoblastic differentiation of bone-marrow cells mediated by collagen-$\alpha 2\beta 1$ integrin interaction," *Journal of Cellular Physiology*, vol. 184, no. 2, pp. 207–213, 2000.

[6] A. Shekaran, J. R. García, A. Y. Clark et al., "Bone regeneration using an alpha 2 beta 1 integrin-specific hydrogel as a BMP-2 delivery vehicle," *Biomaterials*, vol. 35, no. 21, pp. 5453–5461, 2014.

[7] A. V. Taubenberger, M. A. Woodruff, H. Bai, D. J. Muller, and D. W. Hutmacher, "The effect of unlocking RGD-motifs in collagen I on pre-osteoblast adhesion and differentiation," *Biomaterials*, vol. 31, no. 10, pp. 2827–2835, 2010.

[8] J. Green, S. Schotland, D. J. Stauber, C. R. Kleeman, and T. L. Clemens, "Cell-matrix interaction in bone: type I collagen modulates signal transduction in osteoblast-like cells," *American Journal of Physiology—Cell Physiology*, vol. 268, no. 5, pp. C1090–C1103, 1995.

[9] T. Saito, M. Yamauchi, Y. Abiko, K. Matsuda, and M. A. Crenshaw, "In vitro apatite induction by phosphophoryn immobilized on modified collagen fibrils," *Journal of Bone and Mineral Research*, vol. 15, no. 8, pp. 1615–1619, 2000.

[10] A. K. Yadav, A. Tyagi, J. K. Kaushik, A. C. Saklani, S. Grover, and V. K. Batish, "Role of surface layer collagen binding protein from indigenous Lactobacillus plantarum 91 in adhesion and its anti-adhesion potential against gut pathogen," *Microbiological Research*, vol. 168, no. 10, pp. 639–645, 2013.

[11] T. D. Sutherland, Y. Y. Peng, H. E. Trueman et al., "A new class of animal collagen masquerading as an insect silk," *Scientific Reports*, vol. 3, article 2864, 2013.

[12] Y. K. Lin and D. C. Liu, "Comparison of physical-chemical properties of type I collagen from different species," *Food Chemistry*, vol. 99, no. 2, pp. 244–251, 2006.

[13] T. Nagai and N. Suzuki, "Isolation of collagen from fish waste material—skin, bone and fins," *Food Chemistry*, vol. 68, no. 3, pp. 277–281, 2000.

[14] E. E. Antoine, P. P. Vlachos, and M. N. Rylander, "Review of collagen I hydrogels for bioengineered tissue microenvironments: characterization of mechanics, structure, and transport," *Tissue Engineering Part B: Reviews*, vol. 20, no. 6, pp. 683–696, 2014.

[15] S. M. Oliveira, R. A. Ringshia, R. Z. Legeros et al., "An improved collagen scaffold for skeletal regeneration," *Journal of Biomedical Materials Research, Part A*, vol. 94, no. 2, pp. 371–379, 2010.

[16] E. A. Berg, T. A. E. Platts-Mills, and S. P. Commins, "Drug allergens and food—the cetuximab and galactose-$\alpha$-1,3-galactose story," *Annals of Allergy, Asthma and Immunology*, vol. 112, no. 2, pp. 97–101, 2014.

[17] R. Matsumoto, T. Uemura, Z. Xu, I. Yamaguchi, T. Ikoma, and J. Tanaka, "Rapid oriented fibril formation of fish scale collagen facilitates early osteoblastic differentiation of human mesenchymal stem cells," *Journal of Biomedical Materials Research Part A*, 2014.

[18] K. Yamamoto, K. Igawa, K. Sugimoto et al., "Biological safety of fish (Tilapia) collagen," *BioMed Research International*, vol. 2014, Article ID 630757, 9 pages, 2014.

[19] C. T. Hanks, D. Fang, Z. Sun, C. A. Edwards, and W. T. Butler, "Dentin-specific proteins in MDPC-23 cell line," *European Journal of Oral Sciences*, vol. 106, supplement 1, pp. 260–266, 1998.

[20] T. Botero, V. Otero-Corchon, and J. Nor, "MDPC-23: a rat odontoblast-like cell line," in *Proceedings of the IADR Poster Session*, June 2012.

[21] M. K. Ahn, T. S. Jeong, and S. Kim, "The adhesion of odontoblast to type I collagen," *Journal of the Korean Academy of Pediatric Dentistry*, vol. 37, no. 3, pp. 308–316, 2010.

[22] W.-J. Bae, K.-S. Min, J.-J. Kim, J.-J. Kim, H.-W. Kim, and E.-C. Kim, "Odontogenic responses of human dental pulp cells to collagen/nanobioactive glass nanocomposites," *Dental Materials*, vol. 28, no. 12, pp. 1271–1279, 2012.

[23] C. G. Knight, L. F. Morton, A. R. Peachey, D. S. Tuckwell, R. W. Farndale, and M. J. Barnes, "The collagen-binding a-domains of integrins $\alpha_1/\beta_1$ and $\alpha_2/\beta_1$ recognize the same specific amino acid sequence, GFOGER, in native (triple-helical) collagens," *The Journal of Biological Chemistry*, vol. 275, no. 1, pp. 35–40, 2000.

[24] N. Ozeki, M. Mogi, H. Yamaguchi et al., "Differentiation of human skeletal muscle stem cells into odontoblasts is dependent on induction of $\alpha$1 integrin expression," *The Journal of Biological Chemistry*, vol. 289, no. 20, pp. 14380–14391, 2014.

[25] H. Wu, P. N. Teng, J. H. Li et al., "DMP-1 signals through MAPK in hMSC, MDPC-23 and MC3T3 cells," in *Proceedings of the IADR Poster Session, Metro Toronto Convention Centre Room*, July 2008.

[26] J.-H. Park, J.-H. Yoon, Y.-S. Lim, H.-K. Hwang, S.-A. Kim, and S.-G. Ahn, "TAT-Hsp27 promotes adhesion and migration of murine dental papilla-derived MDPC-23 cells through $\beta$1 integrin-mediated signaling," *International Journal of Molecular Medicine*, vol. 26, no. 3, pp. 373–378, 2010.

[27] D. Mushahary, C. Wen, J. M. Kumar et al., "Strontium content and collagen-I coating of Magnesium-Zirconia-Strontium implants influence osteogenesis and bone resorption," *Clinical Oral Implants Research*, 2014.

[28] K. Narayanan, R. Srinivas, A. Ramachandran, J. J. Hao, B. Quinn, and A. George, "Differentiation of embryonic mesenchymal cells to odontoblast-like cells by overexpression of dentin matrix protein 1," *Proceedings of the National Academy of Sciences of the United States of America*, vol. 98, no. 8, pp. 4516–4521, 2001.

[29] J. A. R. Gordon, C. E. Tye, A. V. Sampaio, T. M. Underhill, G. K. Hunter, and H. A. Goldberg, "Bone sialoprotein expression enhances osteoblast differentiation and matrix mineralization in vitro," *Bone*, vol. 41, no. 3, pp. 462–473, 2007.

[30] S. Chen, S. Rani, Y. Wu et al., "Differential regulation of dentin sialophosphoprotein expression by *Runx2* during odontoblast cytodifferentiation," *The Journal of Biological Chemistry*, vol. 280, no. 33, pp. 29717–29727, 2005.

[31] M. Mizuno, T. Miyamoto, K. Wada, S. Watatani, and G. X. Zhang, "Type I collagen regulated dentin matrix protein-1 (Dmp-1) and osteocalcin (OCN) gene expression of rat dental pulp cells," *Journal of Cellular Biochemistry*, vol. 88, no. 6, pp. 1112–1119, 2003.

[32] O. Baba, C. Qin, J. C. Brunn, J. N. Wygant, B. W. McIntyre, and W. T. Butler, "Colocalization of dentin matrix protein 1 and dentin sialoprotein at late stages of rat molar development," *Matrix Biology*, vol. 23, no. 6, pp. 371–379, 2004.

[33] X. Pan, Z. Chen, R. Huang, Y. Yao, and G. Ma, "Transforming growth factor $\beta$1 induces the expression of collagen type I by DNA methylation in cardiac fibroblasts," *PLoS ONE*, vol. 8, no. 4, Article ID e60335, 2013.

[34] A. Unterbrink, M. O'Sullivan, S. Chen, and M. MacDougall, "TGF$\beta$-1 downregulates DMP-1 and DSPP in odontoblasts," *Connective Tissue Research*, vol. 43, no. 2-3, pp. 354–358, 2002.

[35] N. Ozeki, M. Mogi, R. Kawai et al., "Mouse-induced pluripotent stem cells differentiate into odontoblast-like cells with induction of altered adhesive and migratory phenotype of integrin," *PLoS ONE*, vol. 8, no. 11, Article ID e80026, 2013.

[36] S. Yamada, H. Nagaoka, M. Terajima, N. Tsuda, Y. Hayashi, and M. Yamauchi, "Effects of fish collagen peptides on collagen post-translational modifications and mineralization in an osteoblastic cell culture system," *Dental Materials Journal*, vol. 32, no. 1, pp. 88–95, 2013.

Hindawi Publishing Corporation
BioMed Research International
Volume 2015, Article ID 926291, 9 pages
http://dx.doi.org/10.1155/2015/926291

*Research Article*

# Repair of Cranial Bone Defects Using rhBMP2 and Submicron Particle of Biphasic Calcium Phosphate Ceramics with Through-Hole

**Byung-Chul Jeong,[1] Hyuck Choi,[1] Sung-Woong Hur,[1] Jung-Woo Kim,[1] Sin-Hye Oh,[1] Hyun-Seung Kim,[2] Soo-Chang Song,[3] Keun-Bae Lee,[4] Kwang-Bum Park,[5] and Jeong-Tae Koh[1]**

[1]*Research Center for Biomineralization Disorders and Department of Pharmacology and Dental Therapeutics, School of Dentistry, Chonnam National University, Gwangju 500-757, Republic of Korea*
[2]*RIS Foundation for Advanced Biomaterials, Chonnam National University, Gwangju 500-757, Republic of Korea*
[3]*Center for Biomaterials, Korea Institute of Science & Technology, Seoul 130-650, Republic of Korea*
[4]*Department of Orthopedic Surgery, Chonnam National University Medical School and Hospital, Gwangju 501-757, Republic of Korea*
[5]*Megagen Implant, Gyeongsan, Gyeongbuk 712-850, Republic of Korea*

Correspondence should be addressed to Jeong-Tae Koh; jtkoh@chonnam.ac.kr

Received 22 April 2015; Accepted 24 June 2015

Academic Editor: Norbert R. Kuebler



Recently a submicron particle of biphasic calcium phosphate ceramic (BCP) with through-hole (donut-shaped BCP (d-BCP)) was developed for improving the osteoconductivity. This study was performed to examine the usefulness of d-BCP for the delivery of osteoinductive rhBMP2 and the effectiveness on cranial bone regeneration. The d-BCP was soaked in rhBMP2 solution and then freeze-dried. Scanning electron microscope (SEM), energy dispersive spectroscopy (EDS), and Raman spectroscopy analyses confirmed that rhBMP2 was well delivered onto the d-BCP surface and the through-hole. The bioactivity of the rhBMP2/d-BCP composite was validated in MC3T3-E1 cells as an *in vitro* model and in critical-sized cranial defects in C57BL/6 mice. When freeze-dried d-BCPs with rhBMP2 were placed in transwell inserts and suspended above MC3T3-E1, alkaline phosphatase activity and osteoblast-specific gene expression were increased compared to non-rhBMP2-containing d-BCPs. For evaluating *in vivo* effectiveness, freeze-dried d-BCPs with or without rhBMP2 were implanted into critical-sized cranial defects. Microcomputed tomography and histologic analysis showed that rhBMP2-containing d-BCPs significantly enhanced cranial bone regeneration compared to non-rhBMP2-containing control. These results suggest that a combination of d-BCP and rhBMP2 can accelerate bone regeneration, and this could be used to develop therapeutic strategies in hard tissue healing.

## 1. Introduction

Bone defects caused by accidents, trauma, or delayed recovery from diseases can result in major clinical skeletal problems that require reconstruction to restore bone function [1, 2]. Autologous bone grafting is a widely used approach, especially in the regeneration of craniofacial bone defects [3]. However, autologous bone grafts have significant limitations, including often painful and limited access to the graft site, as well as morbidity to the donor site. Therefore, various synthetic biomaterials have been developed as bone substitutes to bone grafts, including bioactive ceramic, bioactive glasses, reinforced natural materials, and synthetic polymers [4].

Biphasic calcium phosphate ceramics (BCPs) are composed of two calcium phosphate phases: hydroxyapatite (HA) and beta-tricalcium phosphate ($\beta$-TCP) at a specific ratio, and they exhibit good biocompatibility and bone conduction performance [5]. However, pure BCP mainly acts as an osteoconductive substance with limited bone formation and relatively long regeneration time. Therefore, it is necessary to provide it with macro-/microporous structures for enhancing osteoconductivity or to combine the bioactive molecules such

as bone morphogenetic proteins (BMPs) for improving osteoinductive properties.

Chemical composition, geometry, and macrostructural properties of BCP have been shown to play an important role in osteoconductivity. Porosity and pore size at both the macro- and microlevels are important morphological properties. Both influence bone healing and regeneration by allowing blood vessels to invade the material, supplying nutrients and oxygen and, thus, sustaining the cell metabolism inside the scaffold [6, 7]. Recently, a submicron particle of BCP ceramics (60 : 40 HA/$\beta$-TCP) with through-hole (donut-shaped BCP; d-BCP) was developed for improving the osteoconductivity, and their effectiveness on bone regeneration was determined in rabbit calvarial bone defects [6].

The recombinant human BMP 2 (rhBMP2) has been well characterized as a strong inducer of bone formation in a variety of conditions [8, 9]. A few animal and human studies have shown efficacious bone regeneration and healing with functional restoration after the implantation of rhBMP2 [10–13]. Therefore, combinations of bone substitutes and osteoinductive agents such as rhBMP2 have received increasing attention as potential bone graft substitutes [14]. Moreover, it has been reported that BMP-loaded HA/$\beta$-TCP ceramics greatly increase bone formation [15]. However, only a few studies have investigated the osteoinductivity of BMP-loaded BCP ceramics with porosity [13]. In the present study, we aimed to determine the usefulness of d-BCP for delivering rhBMP2 and the effectiveness on cranial bone regeneration in a well-documented animal model. We provide *in vitro* and *in vivo* evidence that a combination of rhBMP2 and d-BCP offered higher osteogenic and bone healing activities than that by d-BCP alone. Thus, the implantation of rhBMP2/d-BCP could provide a significant approach to clinical bone regeneration and reconstruction.

## 2. Materials and Methods

*2.1. Recombinant Proteins and Materials.* rhBMP2 was purchased from Cowellmedi (Seoul, Korea). Submicroporous biphasic calcium phosphate ceramics with through-hole (d-BCP; Bone Plus), a mixture of HA/$\beta$-TCP (60 : 40), was kindly supplied by Megagen Implant Co. (Gyeongsan, Korea).

*2.2. Delivery of rhBMP2 onto the d-BCP.* Ten mg of d-BCP was soaked into 1 mL of rhBMP2 solution (5 $\mu$g/mL) and then freeze-dried. Successful delivery of rhBMP2 onto the d-BCP surface or through-hole was verified by morphological and compositional analyses. The surface morphology of the freeze-dried d-BCP with rhBMP2 was observed using field emission scanning electron microscopy (FE-SEM, Hitachi, Tokyo, Japan; Korea Basic Science Institute, Gwangju Center). The surfaces were sputter-coated with platinum and voltages ranging from 5 to 15 kV were used. In addition, compositional analysis using energy dispersive spectroscopy (EDS, Bruker AXS, Karlsruhe, Germany; Korea Basic Science Institute) attached to SEM was carried out. Micro-Raman spectrum was also recorded for d-BCP with rhBMP2 (rhBMP2/d-BCP) in the spectral range of 100–4000 $cm^{-1}$ by using a micro-Raman spectrometer (InVia Reflex UV Raman microscope, Renishaw, UK; Korea Basic Science Institute). A He–Ne laser at 15 mW was used with an excitation wavelength of 633 nm and a resolution of 1.2 $cm^{-1}$.

*2.3. Cell Culture.* MC3T3-E1 preosteoblasts were seeded at a density of $2.5 \times 10^4$ cells/$cm^2$ in 6-well Transwell plates (SPL Inc., Seoul, Korea) and grown with $\alpha$-minimal essential medium ($\alpha$-MEM; Invitrogen, Carlsbad, CA, USA), supplemented with 10% fetal bovine serum (FBS; Gibco, BRL, USA) and 1% penicillin/streptomycin (Invitrogen, Carlsbad, CA, USA), in a humidified atmosphere of 5% CO2 at 37°C. For the transwell cultivation, freeze-dried d-BCPs with or without rhBMP2 were placed in transwell inserts and suspended above the cell cultures using three wells per sample group, allowing for release of the factor from the matrix without direct cell contact. After 72 h, the lower cells were harvested for further analysis.

*2.4. Total RNA Extraction and RT-PCR.* Total RNA was isolated from the cultured cells using TRIzol reagent (Invitrogen) according to the manufacturer's instructions. To amplify the transcripts of osteoblast-specific genes, cDNA was synthesized from 1 $\mu$g of total RNA using random primers and SuperScript II reverse transcriptase (200 units; Invitrogen), and then polymerase chain reaction was performed. The reaction consisted of an initial denaturation step at 94°C for 1 min, followed by a three-stage cycle: denaturation at 94°C for 30 s, annealing at a temperature optimized for each primer pair for 30 s, and extension at 72°C for 30 s. After the requisite number of cycles, the reactions underwent a final extension at 72°C for 5 min. Annealing temperatures, number of cycles, and primer sequences for alkaline phosphatase (ALP), osteocalcin (OC), osterix (Osx), and $\beta$-actin are as follows: ALP (55°C, 25 cycles), (F) 5′-TACATTCCCCATGTGATGGC-3′ and (R) 5′-ACCTCTCCCTTGAGTGTGGG-3′; OC (55°C, 25 cycles), (F) 5′-CTCCTGAGTCTGACAAAGCCTT-3′ and (R) 5′-GCTGTGACATCCATTACTTGC-3′; Osx (55°C, 25 cycles), (F) 5′-TGAGGAAGAAGCCCATTCAC-3′ and (R) 5′-ACTTCTTCTCCCGGGTGTG-3′; $\beta$-actin (55°C, 25 cycles), (F) 5′-TGGATGGCTACGTACATGGCTGGG-3′ and (R) 5′-TTCTTTGCAGCTCCTTCGTTGCCG-3′. The amplified PCR products were electrophoresed on a 1.5% agarose gel and visualized by RedSafe Nucleic Acid Staining solution (Intron Biotechnology, Sungnam, Korea) using the i-MAX gel image analysis system (CoreBioSystem, Seoul, Korea).

*2.5. Alkaline Phosphatase (ALP) Staining.* To examine effects of rhBMP2/d-BCP on bioactivity of bone-forming osteoblasts, ALP staining was performed in MC3T3-E1. Cells were fixed with 70% ethanol, rinsed three times with deionized water, and then treated for 15 min with a 5-bromo-4-chloro-3-indolyl phosphate/nitro blue tetrazolium solution (Sigma Aldrich, St. Louis, MO, USA). For quantitative analysis, the stains were extracted with 10% (w/v) cetylpyridinium chloride in 10 mM sodium phosphate (pH 7.0) for 15 min, and absorbance was measured with microplate reader (Multiskan GO; Thermo Scientific, Waltham, USA) at 540 nm.

*2.6. Animal Preparations.* All animal studies were reviewed and approved by the Animal Ethics Committee of Chonnam National University (number CNU-IACUC-YB-2014-35). Six-week-aged male C57BL/6 mice were obtained from Daehan Biolink (Chungbuk, Korea), and 10 mice per group were randomly assigned. Animals were anesthetized by intraperitoneal injection of a mixture of Zoletil (30 mg/kg; Virbac Lab, Carros, France) and Rompun (10 mg/kg; Bayer Korea Ltd., Seoul, Korea). A sagittal incision was made on the scalp and the calvarium was exposed. A critical-sized bone defect was created by using a 5 mm inner diameter trephine bur (Fine Science Tools, Foster City, CA, USA) under low speed drilling and cool saline irrigation. The defects were filled with d-BCP (10 mg) or rhBMP2/d-BCP composites (5 or 10 $\mu$g of rhBMP2 with 10 mg of d-BCP) according to group. In the control group, the defects were unfilled. The animals were sacrificed 2 and 8 weeks after surgery by CO2 asphyxiation. The crania were carefully removed and fixed for 24 h in 10% neutral buffered formalin solution and then transferred into 70% ethyl alcohol for storage.

*2.7. Soft X-Ray and Microcomputed Tomography (Micro-CT) Scanning.* The whole body and the isolated crania from each mouse were radiographed by 2-dimensional radiographic apparatus (Hitex Ltd., Osaka, Japan) using diagnostic X-ray film (X-OMAT V, Kodak, Rochester, NY, USA) under the following conditions 35 kVp and 400 $\mu$A for 45 s. For a 3-dimensional analysis, each specimen was scanned by micro-CT (Skyscan 1172; Skyscan, Aartselaar, Belgium) in cone-beam acquisition mode. The X-ray source was set at 50 kV and 200 $\mu$A with a 0.5 mm aluminum filter at 17.09 $\mu$m resolution. The exposure time was 1.2 s. 449 projections were acquired over an angular range of 180° (angular step; 0.4°). The image slices were reconstructed by using the NRecon program (version 1.6.2.0, Skyscan, Aartselaar, Belgium) and bone volume and thickness were measured using the CT-Analyzer program (version 1.10.0.5, Skyscan, Aartselaar, Belgium). 3D surface rendering images were obtained by using the Mimics software 14.0 (Materialise NV, Leuven, Belgium).

*2.8. Histological Analysis.* All specimens were decalcified in a rapid decalcifying solution (Calci-Clear Rapid, National Diagnostics, Atlanta, USA) for 10 days and then embedded in paraffin and cut into 7 $\mu$m thick serial slices. The sections were deparaffinized in xylene at room temperature for 20 min and then rehydrated through a graded series of alcohols. The sections were then stained with hematoxylin and eosin (H&E). The H&E-stained sections from each group were then examined under a light microscope (Leica, Wetzlar, Germany) to evaluate new bone formation.

*2.9. Statistical Analysis.* Statistical analysis was performed using one-way analysis of variance (ANOVA) and Duncan's multiple comparisons using the Graph Pad Prism 4 for Windows statistical software package (Graph Pad Software Inc., La Jolla, CA, USA). All the data presented are expressed as the mean ± SEM from three independent measurements. A $p < 0.05$ was considered statistically significant.

## 3. Results

*3.1. Surface Morphology and Compositional Analyses of rhBMP2/d-BCP.* The osteoconductive d-BCP was soaked into the osteoinductive rhBMP2 solution and then freeze-dried. Morphological analysis with FE-SEM showed that the d-BCPs were 500 and 700 $\mu$m size of spherical particles with macro-/microinterconnected pore structures and a central through-hole (Figures 1(a) and 1(b)). The freeze-dried d-BCP with rhBMP2 solution (rhBMP2/d-BCP) had an irregular or closed spherical morphology with a relatively rough surface compared to d-BCP, indicating good packaging of rhBMP2 in the central through-hole of d-BCP (Figures 1(c) and 1(d)).

In the compositional analysis of EDS, an N and Mg layer was observed on the surface of the rhBMP2/d-BCP but not on that of d-BCP itself (Figure 2(a)). Raman spectroscopy analysis revealed that lots of peaks of rhBMP2/d-BCP are accorded with those of rhBMP2 itself, indicating that rhBMP2 can be transferred on the surface or through-hole of d-BCP (Figure 2(b)).

*3.2. In Vitro Osteogenic Differentiation by the rhBMP2/d-BCP.* ALP activity is widely used as a marker for the early differentiation of osteoblasts [16]. To examine the effects of the rhBMP2/d-BCP on osteogenic differentiation *in vitro*, preosteoblast MC3T3-E1 cells were maintained for 3 days in a transwell system, containing either d-BCP or rhBMP2/d-BCP, and then ALP staining was performed. ALP activity significantly increased in models with the rhBMP2/d-BCP compared to those with the control d-BCP group (Figure 3(a)). The expression levels of osteoblast-specific genes (such as ALP, OC) and Osx were also significantly higher in models with the rhBMP2/d-BCP than in the control models with only d-BCP (Figure 3(b)).

*3.3. In Vivo Bone Formation by the rhBMP2/d-BCP.* To evaluate bone formation by the rhBMP2/d-BCP *in vivo*, we implanted either d-BCP or rhBMP2/d-BCP (5 or 10 $\mu$g) into a 5 mm inner diameter cranial defect, which was created in the central part of the mouse cranial bone. To visualize the regions of bone healing, soft X-ray and micro-CT analysis were performed 2 and 8 weeks after surgery. X-ray analysis revealed that the control group without the scaffold showed round and radiolucent cranial defects for up to 8 weeks. In the group with d-BCP implant, both d-BCP particles and a radio-opaque shadow around the defects were detected at 2 weeks. After 8 weeks, the radio-opaque shadow decreased and new bone was detected in the spaces between the particles. However, the cranial defect had not completely healed (Figures 4(a) and 4(b)). In the groups with rhBMP2/d-BCP implants, d-BCP particles and a rounded radio-opaque shadow were also shown. However, the cranial defect had healed more effectively in this group. The 3-dimensional analyses of defects using micro-CT scanning showed that the group with rhBMP2/d-BCP implants had substantial platelike bone structure, which was visible in the center of the cranial defect, and that this group had a higher capacity for healing in the peripheral area surrounding the defect, compared to

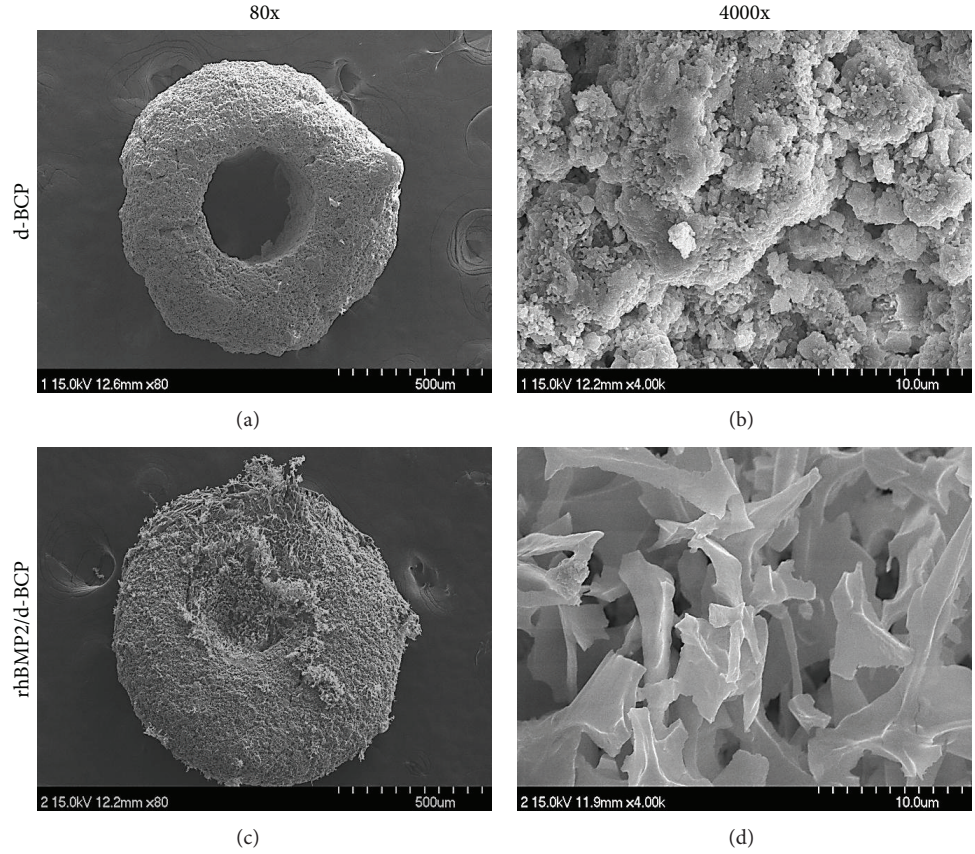


Figure 1: Morphology of the donut shape of microporous biphasic calcium phosphate ceramics (d-BCP) in the presence or absence of rhBMP2 (recombinant human bone morphogenetic proteins 2) was analyzed with SEM. d-BCP (10 mg) was soaked into rhBMP2 solution (5 $\mu$g/mL) and then freeze-dried. (a, b) d-BCP, (c, d) rhBMP2/d-BCP, and (b, d) high magnification image of the d-BCP with and without rhBMP2.

the group with d-BCP implants (Figures 4(c) and 4(d)). Volumetric analysis using micro-CT also demonstrated that bone volume in the defects with rhBMP2/d-BCP implant is greater than that with d-BCP implant alone. The thickness of newly regenerated bone was also significantly higher in the rhBMP2/d-BCP groups than in the d-BCP group. When compared to the negative control, the group with d-BCP implants alone also exhibited a significant increase in both bone volume and bone thickness (Figures 4(e) and 4(f)).

*3.4. Histological Analysis.* Histological analysis was performed using H&E stained sections at 2 and 8 weeks after implantation, in order to qualitatively evaluate new bone formation. In the control group, no mineralized bone was observed in the empty cranial defect and instead the thin fibrous tissue coverage was seen. In the group with d-BCP implants, only a small amount of newly formed bone was found in the limited peripheral region of d-BCP particles at 8 weeks (Figure 5). However, the group with the rhBMP2/d-BCP implants showed greater amounts of bone regeneration with normal bone-like structure compared to the group with the d-BCP implants. In the rhBMP2/d-BCP group, the newly regenerated bone almost covered the outer surface as well as inner through-hole surface of d-BCP particles and was observed in the interparticular space (Figures 5(a) and 5(b)), suggesting that the regeneration may be affected by BMP2 adsorption on d-BCP.

## 4. Discussion

In this study, we investigated whether donut shape of BCP is useful for delivering osteogenic rhBMP2 and the delivery can synergically enhance bone regeneration in cranial defects of mice. Our results showed that BMP2 can be adsorbed on the microspore surface of BCP and plugged the central through-hole by freeze-drying and that the rhBMP2-adsorbed d-BCP (rhBMP2/d-BCP) enhanced *in vitro* osteoblast differentiation and *in vivo* bone formation, compared to d-BCP alone.

BCP integrates the excellent mechanical properties of less resorbable HA with faster resorbable $\beta$-TCP, and a HA/$\beta$-TCP ratio of 60 : 40 has been reported as the optimal composition for synthetic bone in previous animal studies [17, 18]. Previously the donut shape of BCP (d-BCP; HA/$\beta$-TCP ratio of 60 : 40), which is made of submicron-sized grains with 300–400 $\mu$m central pore and 20–60 $\mu$m micropores on surface, was developed as a bone substitute and characterized to have osteoconductivity [6]. In the present study, we consistently observed that implantation of d-BCP alone partly induced cranial bone regeneration in mice. We still consider that the response might come from the increase of

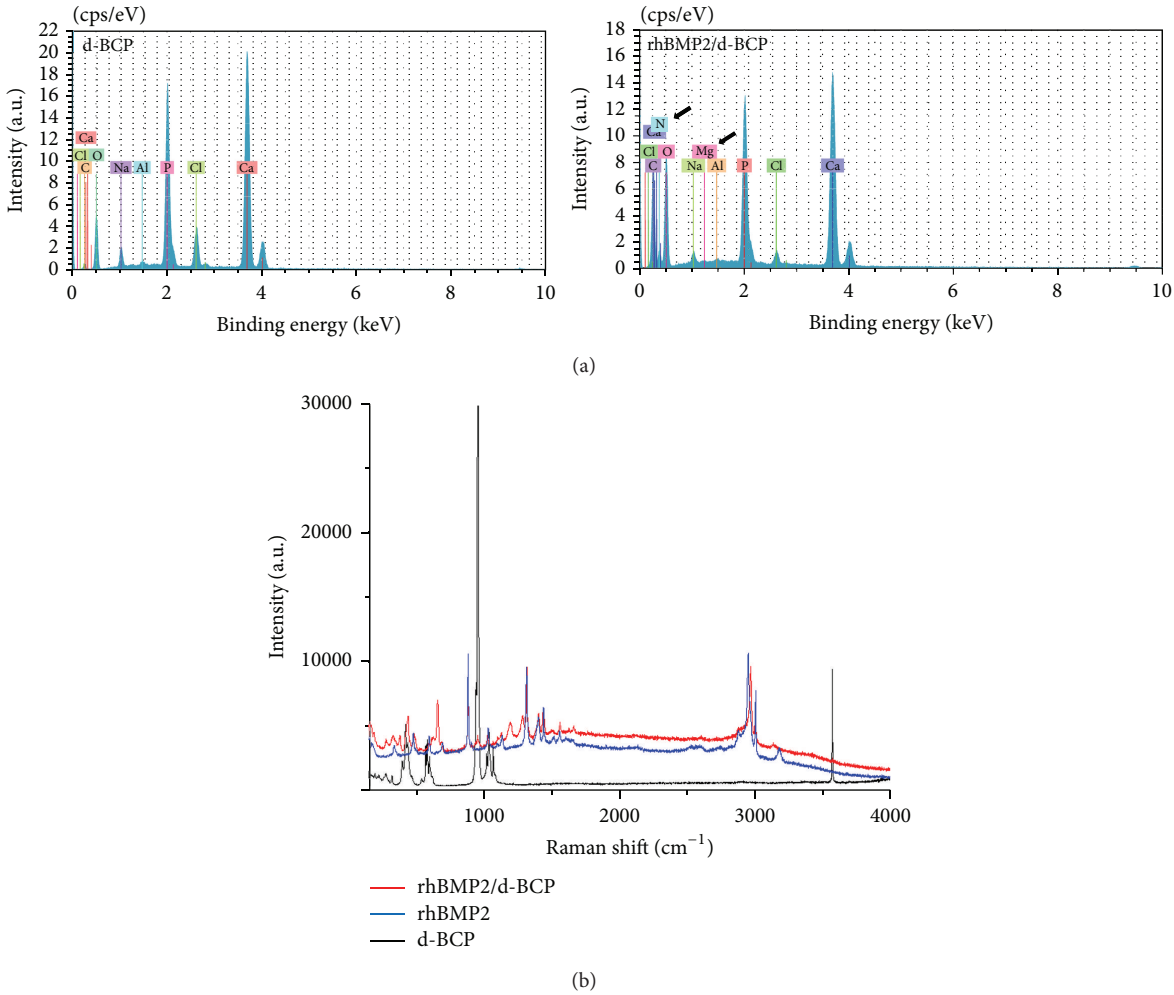


Figure 2: Energy dispersive spectra (EDS) and Raman spectroscopy were used to identify the chemical composition of the d-BCP with or without rhBMP2. (a) EDS profiles of d-BCP with and without rhBMP2, (b) Raman spectra of d-BCP (bottom), rhBMP2 protein (center), and rhBMP2/d-BCP (top) samples in the range of 100–4000 cm$^{-1}$.

osteoconductivity of d-BCP due to the surface characteristics with interconnected microporosity and through-hole, allowing some space for migrating osteoblasts and endothelial cells and contributing to vascularization and bone ingrowth.

So far, there are lots of trials to deliver osteoinductive BMP2 onto BCP particles and the enhancement of bone regeneration by them has been introduced with the limited functional evaluation [1]. This study was also undertaken with a hypothesis that d-BCP will be a more powerful bone substitute if osteoinductive substances are delivered into the macro-/micropore structures and the central through-hole of d-BCP. When d-BCP was soaked with rhBMP2 solution and freeze-dried in the present study, adsorption of rhBMP2 on the surface of d-BCP and through-hole was identified by morphological and compositional analyses such as SEM, EDS, and Raman spectrum. SEM images showed that the postlyophilized remnants roughly covered the outer surface of d-BCP particles and also plugged a central through-hole. In the EDS results, nitrogen and magnesium layers were observed in the surface of rhBMP2/d-BCP, not in that of d-BCP only [19]. Because nitrogen is a component of amino acid and magnesium is one of the protein binding inorganics [20], we can assume that postlyophilized remnants on the surface of rhBMP2/d-BCP might be BMP2 protein. Raman spectra analysis showed that lots of peaks of rhBMP2/d-BCP are accorded with those of rhBMP2 itself, indicating that rhBMP2 can be transferred on the surface or through-hole of d-BCP. Because d-BCP has a 300–400 $\mu$m of central through-hole unlike previous plain particle type of BCPs, it has an advantage to deliver more rhBMP2 and to enhance bone regeneration.

BMP2 is the most potent osteoinductive growth factor to stimulate the development of endogenous bones or repair of damaged bones [21, 22]. In addition, BMP2 stimulates osteoblastic differentiation from mesenchymal stem cells or progenitor cells with the increases in osteoblast-specific gene expressions, including alkaline phosphatase enzyme, bone matrix proteins, and transcription factors [23, 24].

In this study, we further examined whether the adsorbed rhBMP2 on d-BCP surface still has such a stimulatory effect

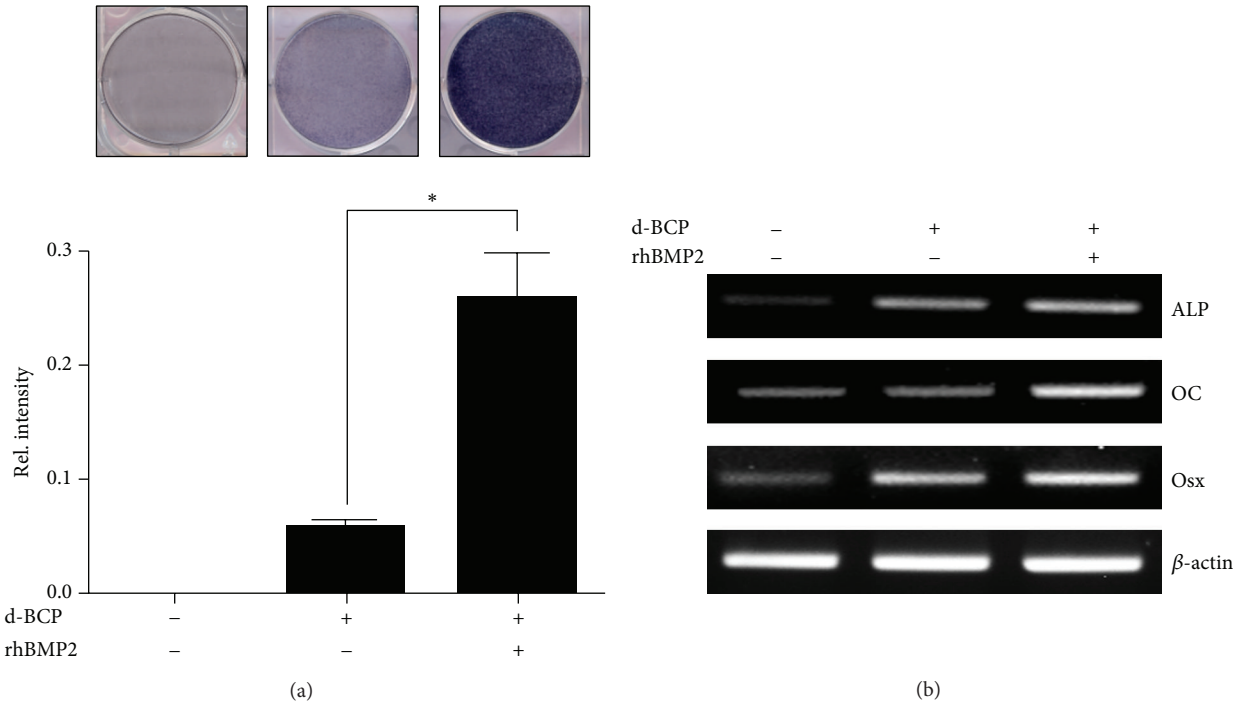


Figure 3: The effect of rhBMP2/d-BCP on osteogenic differentiation in MC3T3-E1 cells. Cells were maintained for 3 days in growth medium with d-BCP (1 mg) or rhBMP2 (0.5 $\mu$g)/d-BCP (1 mg). (a) The cells were subjected to ALP staining. (b) Total RNA was isolated and expression of osteoblast-specific genes was analyzed by RT-PCR. $\beta$-actin was used as a loading control. ALP: alkaline phosphatase. OC: osteocalcin. Osx: osterix. $^{*}p < 0.05$ compared to the indicated group. Representative data are shown. $n = 3$.

on osteoblast differentiation and bone regeneration. Our results of *in vitro* culture experiments showed that MC3T3E1 preosteoblasts with rhBMP2/d-BCP produced more increases in ALP enzyme activity, gene expression of ALP, bone matrix protein osteocalcin, and transcription factor osterix, compared with d-BCP alone. The results indicate that the rhBMP2 on d-BCP surface still has biological activity regardless of lyophilized process and adsorption on d-BCP surface.

Our *in vivo* study confirmed the rhBMP2/d-BCP effects on bone regeneration; rhBMP2/d-BCP implants induced greater bone regeneration, compared to d-BCP alone, in the critical-sized calvarial defects in mice. In the radiographic analysis, d-BCP alone also induced bone repair of calvarial defects as in a previous report [6]; however, the defects were not completely covered with new bones even at 8 weeks after implantation. On the other hand, rhBMP2/d-BCP implant significantly enhanced the bone repair with increases in bone volume and thickness in the defects, and the d-BCP with 10 $\mu$g of rhBMP2 produced the completed healing even at 2 weeks after implantation; the defect was fully covered with new regenerated bone. However, the volume of new bone by the combination at 8 weeks was not increased, compared to that at 2 weeks. These indicate that rhBMP2 can initially burst from the rhBMP2/d-BCP complex to be inactive after 8 weeks or d-BCP itself may be improper to slowly release rhBMP2. For more efficient regeneration for long time, a sustained releasing system for rhBMP2 has to be added to the combination.

Histology results consistently revealed that d-BCP alone also produced new bone formation; however, that new bone was observed in the limited surface of d-BCP. On the other hand, the rhBMP2/d-BCP implant elicited to greater amounts of bone regeneration than the d-BCP implants; the newly regenerated bones almost covered the outer surface as well as inner through-hole surface of d-BCP particles and even were observed in interspace between d-BCP particles. The bone-forming pattern appears to be closely related to the rhBMP2 adsorption on d-BCP particles, when we consider the putative localization of rhBMP2 and osteoinductive activity. These consistently suggest that the adsorbed rhBMP2 has a stimulatory effect on *in vivo* bone regeneration. However, the different concentrations (5 $\mu$g or 10 $\mu$g) of rhBMP2 appear to have no effect on the maturity of new bone, indicating that the doses of rhBMP2 might not be enough to produce the matured bone in the presence of d-BCP in mice. To develop an optimal combination system using rhBMP2 and d-BCP for cranial bone regeneration, further studies are still needed including a sustained release strategy for long-term effects of rhBMP2, degradation behavior of d-BCP, appropriate concentration of rhBMP2, and so forth.

## 5. Conclusions

This study showed that donut shape of BCP (d-BCP) can deliver rhBMP2 through the hole with freeze-drying and that the rhBMP2/d-BCP can stimulate *in vivo* bone regeneration as well as *in vitro* osteogenic differentiation and

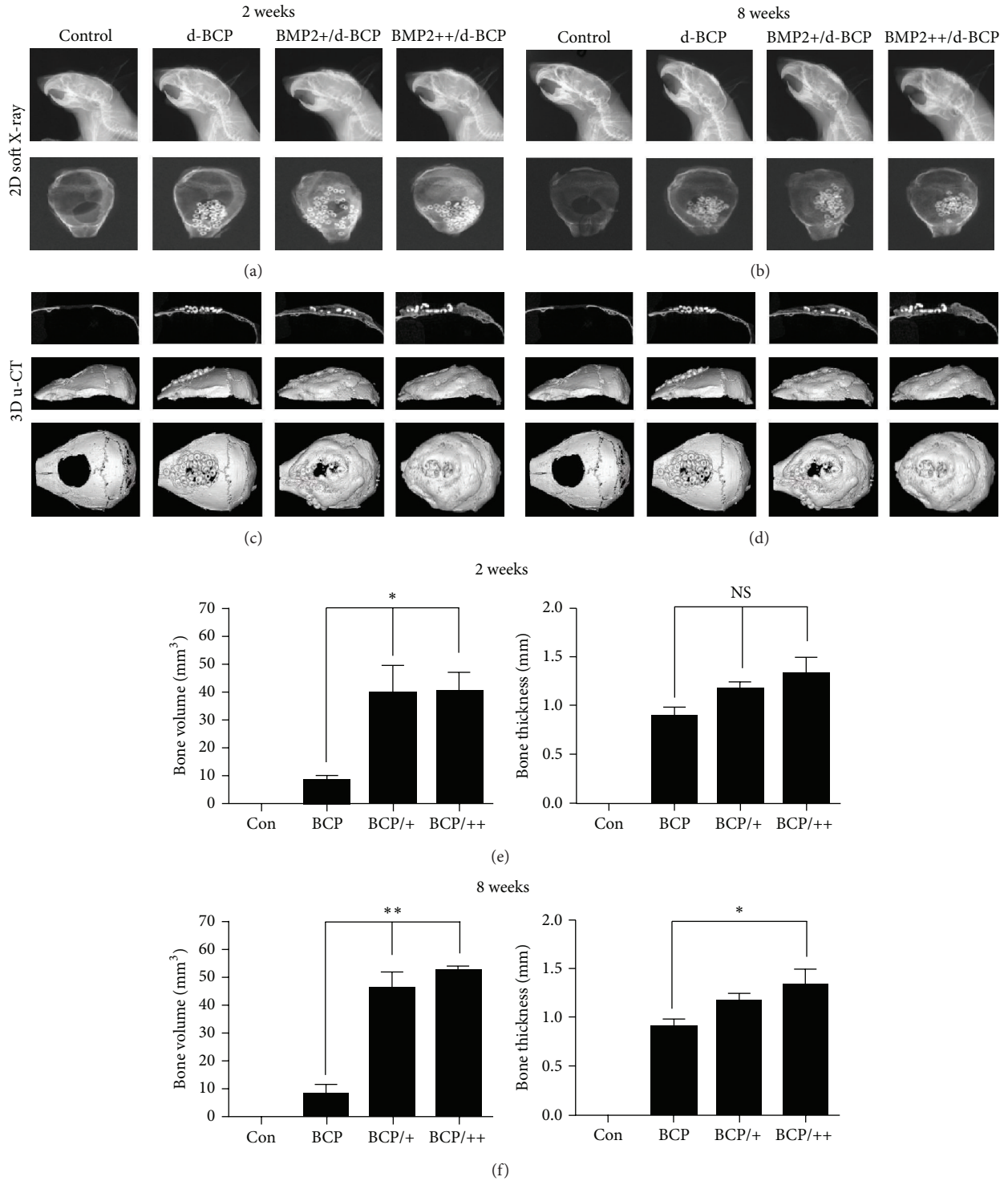


Figure 4: Effects of rhBMP2/d-BCP on bone repair of calvarial defects in mice. d-BCP (10 mg) or rhBMP2 (5 or 10 $\mu$g)/d-BCP (10 mg) were implanted into a 5 mm inner diameter cranial defect. Control group was left without any implantation. The mice were harvested at 2 and 8 weeks after implantation, and 2D soft X-ray (a, b) and 3D microcomputed tomography (c, d) analyses were performed. Volume and thickness of regenerative bone were measured using micro-CT apparatus and micro-CT-Analyzer program (e, f). $^{*}P < 0.05$ and $^{**}P < 0.01$ compared to the indicated group. Representative data are shown. $n = 5$.

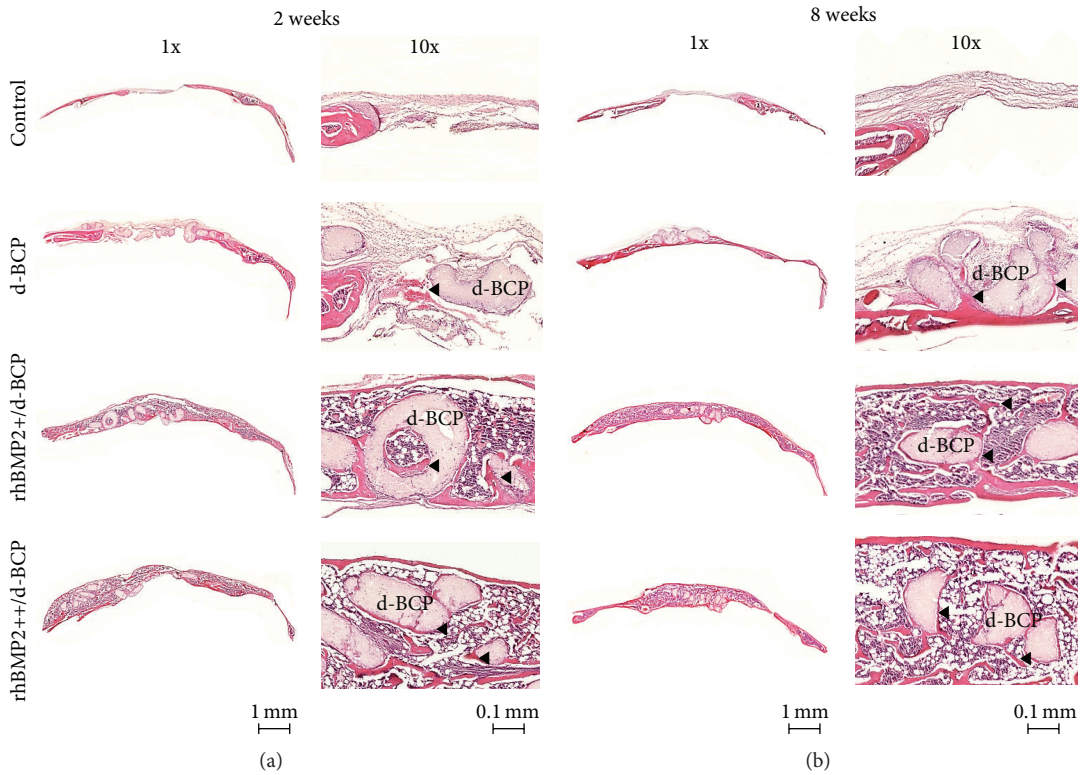


FIGURE 5: Histological analysis of rhBMP2/d-BCP induced bone regeneration in calvarial defects of mice. All specimens used for radiographic analyses (Figure 4) were formalin-fixed, paraffin-embedded, and then cut into 7 $\mu$m thick sections. The sections were then stained with hematoxylin and eosin (H&E). Micrographs are shown at ×1 and ×10 magnifications.

mineralization. This rhBMP2 delivery system can be used to develop therapeutic strategies in bone regeneration and defect healing.

## Disclosure

The authors declare that this paper is original, has not been published before, and is not currently being considered for publication elsewhere. They confirm that the paper has been read and approved by all named authors and there are no other persons who met the criteria for authorship that are not listed. The authors further confirm that the order of authors listed in the paper has been approved by all of them.

## Conflict of Interests

The authors declare that there is no conflict of interests regarding the publication of this paper.

## Authors' Contribution

Byung-Chul Jeong and Hyuck Choi contributed equally to this work.

## Acknowledgments

This study was supported by the National Research Foundation of Korea (NRF) Grants funded by the Korea Government (MSIP) (nos. 2011-0030121 and 2012K001392) and Chonnam National University Hospital Research Institute of Clinical Medicine (CRI 11-078-21, 22).

## References

[1] K. Yoshida, Y. Sumita, E. Marukawa, M. Harashima, and I. Asahina, "Effect of platelet-rich plasma on bone engineering with an alloplastic substitute containing BMP2," *Bio-Medical Materials and Engineering*, vol. 23, no. 3, pp. 163–172, 2013.

[2] R. Tavakoli-Darestani, A. Manafi-Rasi, and A. Kamrani-Rad, "Dexamethasone-loaded hydroxyapatite enhances bone regeneration in rat calvarial defects," *Molecular Biology Reports*, vol. 41, no. 1, pp. 423–428, 2014.

[3] J. E. Hausamen and F. W. Neukam, "Transplantation of bones," *European Archives of Oto-Rhino-Laryngology. Supplement*, vol. 1, pp. 163–177, 1992.

[4] W. G. De Long Jr., T. A. Einhorn, K. Koval et al., "Bone grafts and bone graft substitutes in orthopaedic trauma surgery—a critical analysis," *The Journal of Bone and Joint Surgery—American Volume*, vol. 89, no. 3, pp. 649–658, 2007.

[5] L. Cheng, F. Ye, R. Yang et al., "Osteoinduction of hydroxyapatite/$\beta$-tricalcium phosphate bioceramics in mice with a fractured fibula," *Acta Biomaterialia*, vol. 6, no. 4, pp. 1569–1574, 2010.

[6] J.-W. Park, E.-S. Kim, J.-H. Jang, J.-Y. Suh, K.-B. Park, and T. Hanawa, "Healing of rabbit calvarial bone defects using biphasic calcium phosphate ceramics made of submicron-sized

grains with a hierarchical pore structure," *Clinical Oral Implants Research*, vol. 21, no. 3, pp. 268–276, 2010.

[7] G. F. Muschler, C. Nakamoto, and L. G. Griffith, "Engineering principles of clinical cell-based tissue engineering," *The Journal of Bone & Joint Surgery—American Volume*, vol. 86, no. 7, pp. 1541–1558, 2004.

[8] R. E. Jung, R. Glauser, P. Schärer, C. H. F. Hàmmerle, H. F. Sailer, and F. E. Weber, "Effect of rhBMP-2 on guided bone regeneration in humans: a randomized, controlled clinical and histomorphometric study," *Clinical Oral Implants Research*, vol. 14, no. 5, pp. 556–568, 2003.

[9] F. Schwarz, D. Ferrari, M. Sager, M. Herten, B. Hartig, and J. Becker, "Guided bone regeneration using rhGDF-5- and rhBMP-2-coated natural bone mineral in rat calvarial defects," *Clinical Oral Implants Research*, vol. 20, no. 11, pp. 1219–1230, 2009.

[10] H. D. Zegzula, D. C. Buck, J. Brekke, J. M. Wozney, and J. O. Hollinger, "Bone formation with use of rhBMP-2 (recombinant human bone morphogenetic protein-2)," *The Journal of Bone & Joint Surgery—American Volume*, vol. 79, no. 12, pp. 1778–1790, 1997.

[11] D. Wulsten, V. Glatt, A. Ellinghaus et al., "Time kinetics of bone defect healing in response to BMP-2 and GDF-5 characterised by in vivo biomechanics," *European Cells & Materials*, vol. 21, pp. 177–192, 2011.

[12] T. J. Sigurdsson, S. Nguyen, and U. M. E. Wikesjö, "Alveolar ridge augmentation with rhBMP-2 and bone-to-implant contact in induced bone," *International Journal of Periodontics and Restorative Dentistry*, vol. 21, no. 5, pp. 461–473, 2001.

[13] N. Murakami, N. Saito, H. Horiuchi, T. Okada, K. Nozaki, and K. Takaoka, "Repair of segmental defects in rabbit humeri with titanium fiber mesh cylinders containing recombinant human bone morphogenetic protein-2 (rhBMP-2) and a synthetic polymer," *Journal of Biomedical Materials Research*, vol. 62, no. 2, pp. 169–174, 2002.

[14] S.-H. Jun, E.-J. Lee, T.-S. Jang, H.-E. Kim, J.-H. Jang, and Y.-H. Koh, "Bone morphogenic protein-2 (BMP-2) loaded hybrid coating on porous hydroxyapatite scaffolds for bone tissue engineering," *Journal of Materials Science: Materials in Medicine*, vol. 24, no. 3, pp. 773–782, 2013.

[15] I. Ono, H. Gunji, F. Kaneko, T. Saito, and Y. Kuboki, "Efficacy of hydroxyapatite ceramic as a carrier for recombinant human bone morphogenetic protein," *Journal of Craniofacial Surgery*, vol. 6, no. 3, pp. 238–244, 1995.

[16] B. G. Keselowsky, L. Wang, Z. Schwartz, A. J. Garcia, and B. D. Boyan, "Integrin $\alpha 5$ controls osteoblastic proliferation and differentiation responses to titanium substrates presenting different roughness characteristics in a roughness independent manner," *Journal of Biomedical Materials Research A*, vol. 80, no. 3, pp. 700–710, 2007.

[17] J. L. Rouvillain, F. Lavallé, H. Pascal-Mousselard, Y. Catonné, and G. Daculsi, "Clinical, radiological and histological evaluation of biphasic calcium phosphate bioceramic wedges filling medial high tibial valgisation osteotomies," *Knee*, vol. 16, no. 5, pp. 392–397, 2009.

[18] O. Gauthier, J.-M. Bouler, E. Aguado, P. Pilet, and G. Daculsi, "Macroporous biphasic calcium phosphate ceramics: influence of macropore diameter and macroporosity percentage on bone ingrowth," *Biomaterials*, vol. 19, no. 1–3, pp. 133–139, 1998.

[19] D. Steinmüller-Nethl, F. R. M. Kloss, M. Najam-Ul-Haq et al., "Strong binding of bioactive BMP-2 to nanocrystalline diamond by physisorption," *Biomaterials*, vol. 27, no. 26, pp. 4547–4556, 2006.

[20] B. T. Björnsson and C. Haux, "Distribution of calcium, magnesium and inorganic phosphate in plasma of estradiol-17$\beta$ treated rainbow trout," *Journal of Comparative Physiology B*, vol. 155, no. 3, pp. 347–352, 1985.

[21] S. S. Zhu, D. H. Song, X. W. Jiang, H. Zhou, and J. Hu, "Combined effects of recombinant human BMP-2 and Nell-1 on bone regeneration in rapid distraction osteogenesis of rabbit tibia," *Injury*, vol. 42, no. 12, pp. 1467–1473, 2011.

[22] N. Duguy, H. Petite, and E. Arnaud, "Biomaterials and osseous regeneration," *Annales de Chirurgie Plastique et Esthetique*, vol. 45, no. 3, pp. 364–376, 2000.

[23] A. Hari Reddi, "Role of morphogenetic proteins in skeletal tissue engineering and regeneration," *Nature Biotechnology*, vol. 16, no. 3, pp. 247–252, 1998.

[24] B.-C. Jeong, H.-J. Kim, I.-H. Bae et al., "COMP-Ang1, a chimeric form of Angiopoietin 1, enhances BMP2-induced osteoblast differentiation and bone formation," *Bone*, vol. 46, no. 2, pp. 479–486, 2010.